UiO : Department of Mathematics
University of Oslo

Freak waves over nonuniform depth with different slopes

Shirin Fallahi

Master's Thesis, Spring 2016

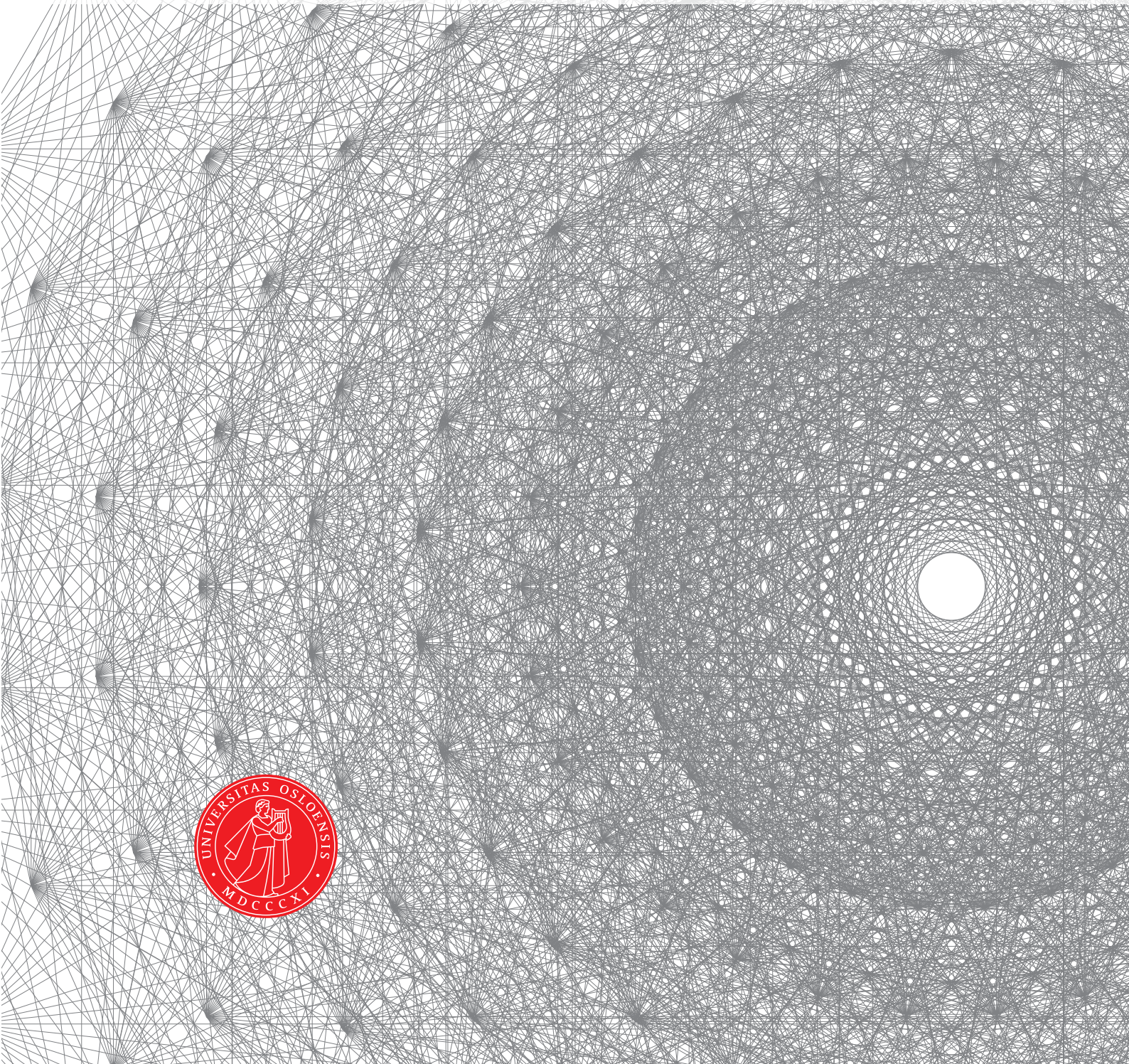

Cover design by Martin Helsø

The front page depicts a section of the root system of the exceptional Lie group E_8, projected into the plane. Lie groups were invented by the Norwegian mathematician Sophus Lie (1842–1899) to express symmetries in differential equations and today they play a central role in various parts of mathematics.

Abstract

Both previous experimental and numerical studies revealed that there are two different regimes when waves propagate from deep water over a slope to shallow water. For shallow water and/or abrupt depth transition there can be a local maximum of extreme waves near the shallow edge of the bottom slope, while for deep water and/or mild depth transition no such local maximum of extreme waves is found. Standard simplified wave models, in particular nonlinear Schrödinger equations for nonuniform depth, have not been able to account for the transition between these two regimes. With this background, in this thesis we derive a modified NLS equation for nonuniform depth in order to better represent abrupt bathymetry of arbitrary depth, in the hope that this may allow NLS models to account for previous experimental observations. The NLS equation derived in this thesis is expressed in space and time evolution forms which can be used for both finite and infinite depth. In the limit of finite depth, the stability analysis for both space and time evolution equations indicates that wave trains on water of uniform depth, h, are unstable if the wavenumber, k, satisfies $kh > 1.363$, but they are otherwise stable. Furthermore, our investigation in stability analysis shows that the asymptotic behavior of the finite-depth results reproduce the deep-water results.

Acknowledgement

I would like to thank the Department of Mathematics at the University of Oslo, for all of the opportunities I was given as an international student to carry out this master thesis.

I would like to express my very profound gratitude to my supervisor, Professor Karsten Trulsen, for his patience, motivation, endless enthusiasm, and immense knowledge. I truly grateful for all the help I have gotten from all discussions which helped me both with this thesis and further academical prospects.

I would like to thank my mother, Roya Panjeyany, and my husband, Pouya Rahmani, for providing me with unfailing moral support and their wise counsel. This accomplishment would not have been possible without their invaluable help.

Shirin Fallahi

Oslo, May 2016

Contents

List of Figures

List of Tables

Chapter 1

Introduction

1.1 Previous works

Understanding of ocean waves is a key factor for ship navigation, offshore platforms, renewable energy devices, offshore wind turbine foundations, etc. For instance, considerable forces on offshore structures are produced when waves occur often, and become extreme. Therefore, an estimate of extreme wave condition and the statistics of waves have been a topic of interest in the scientific community for several decades.

The term *rogue* or *freak* has been used by the researchers and engineers for waves that are surprisingly large amplitude waves in comparison with the other waves in the sea state. Some classic criteria for freak waves are $\eta_c > 1.25H_s$ or $H > 2H_s$ where η_c is the crest height, H is the wave height and H_s is the significant wave height (Dysthe et al., 2008). The significant wave height is defined as four times the standard deviation of the surface elevation.

The importance of freak waves has led many scientists devote their attention to the study of the formation and dynamics of these waves in open ocean domains with deep water condition [e.g. (Dysthe et al., 2008) ,(Kharif et al., 2009)]. It is known that the probability of occurrence of freak waves can be indicated by the value of the kurtosis parameter (normalized fourth-order moment of free surface elevation). For instance, an expression for the probability density function (PDF) of the maximum wave height was derived in Mori and Janssen (2006) based on the value of the Benjamin-Feir Index (BFI). Although, the effect of finite water depth or variable water depth assumptions on freak waves have been a topic of interest for researchers and engineers, there are few experimental, theoretical and numerical studies of freak waves in finite depth or considering the effect of variable water depth in coastal areas, as discussed hereafter.

1.1.1 Experimental investigations

Experimental investigations of freak wave occurrence are rare. In recent years, some experiments have been carried out to investigate if the change of depth can provoke increased likelihood of freak waves. Some of these experimental studies are discussed in the following text.

A set of experiments was performed at Marin in the Netherlands by Bunnik (2010) with long-crested wave conditions over a sloping bottom. In these experiments, three cases of long-crested irregular waves were investigated by considering three different wave fields. They defined small parameter $\epsilon = k_p a_c$ as the steepness of the waves where k_p and a_c showed the peak wavenumber and the characteristic amplitude, respectively. The three wave fields had a steepness respectively $k_p a_c = 0.057$, 0.038 and 0.028, and a depth of respectively $k_p h = 1.6, 1.1$ and 0.81 on the deep side, and $k_p h = 0.99, 0.70$ and 0.54 at the shallow side with a steepness $k_p a_c = 0.070$, 0.049 and 0.038, respectively. A JONSWAP spectrum with peak enhancement factor $\gamma = 3.3$ was used to simulate these irregular waves. All these three irregular long-crested waves were propagated over a 1:20 slope from water of constant depth 0.60 m to shallower side with constant depth 0.30 m. This set of experiments was recently analyzed by Trulsen et al. (2012), and they concluded that as the waves propagate over the slope, from deeper to the shallower side, a local maximum of kurtosis and skewness can be attained near the shallower part of the slope. In addition, they have anticipated that in this region, which kurtosis and skewness gain their local maximum, there can also be a corresponding local maximum of freak waves probability.

Recently a set of experiments was carried out in a random wave flume by Kashima et al. (2013) and Kashima et al. (2014) in Japan. In these studies, various bottom profiles were considered, and a series of physical experiments was performed to examine the behavior of unidirectional random waves from deep water propagating to shallow water region. They selected four different types of bathymetry configurations: (1) flat bottom, (2) slope bottom with fixed impermeable 1:20 slope, (3) the complex bathymetries composed of a skewed portion with slope 1:30 and a horizontal portion, (4) the bottom topography consisted of two skewed portions with different slopes 1:30 and 1:10. We are interested only in type (3), since it is the only type which can be relevant to our investigation. For bathymetry type (3), they examined a case of random waves simulated based on the JONSWAP spectrum with peak enhancement factor $\gamma = 10.0$. A two-dimensional wave tank with 0.6 m width, 1.5 m height and 35.0 m length, was used to conduct this experiment. They have investigated the behavior of the kurtosis and, their results also illustrated a significant increase of the kurtosis in the region around the end of the sloping part of the bottom profile.

A series of experiments was conducted in China by Ma et al. (2014) to study variations of statistics in random waves passing over a submerged symmetrical bar. They used a wave flume which was 50.0 m long, 3.0 m wide and 1.0 m deep. A submerged isosceles trapezoidal bar was employed as a bottom topography with slope 1:20 and a 3 m horizontal crest. They examined 4 cases of random waves simulated based on the JONSWAP spectrum by considering constant significant wave heights H_s and constant peak frequencies f_p, but various peak enhancement factors γ. They concluded that the

remarkable increase of the kurtosis can occur in the region around the end of the sloping part of the bottom profile. Additionally, some freak waves can appear in the shoaling region near the top of the bar.

In the master thesis of Raustøl (2014), a set of experiments was conducted recently to investigate the freak waves on variable depth. A wave tank with 24.6 m length and 0.5 m width was used to perform these experiments. The bottom profile was formed of two skewed portions with slope 0.2625 and a horizontal portion, each having length 1.6 m, and the height of construction was 0.42 m. Furthermore, they carried out these experiments by considering two water depths 0.5 m and 0.6 m. Various cases for deep-water regime and the transition between the far- and shallow water regime were examined by changing the period of random waves simulated by the JONSWAP spectrum. In this study, a local maximum of kurtosis over the shoal has been found for small shallow-water depth. In addition, the experimental results revealed that as the shallow-water depth is increased, the maximum of kurtosis is suppressed, and eventually vanishes.

Based on this review of previous experimental studies on uneven bottom, we can categorize the applied bottom topographies in these works to two types of bathymetry. These bottom profiles are described by figures 1.1 and 1.2. Furthermore, table 1.1 indicates the type of bottom and parameter values employed in theses experimental studies.

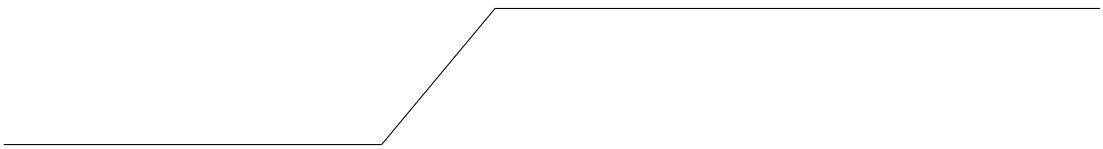

Figure 1.1: Bottom topography type 1.

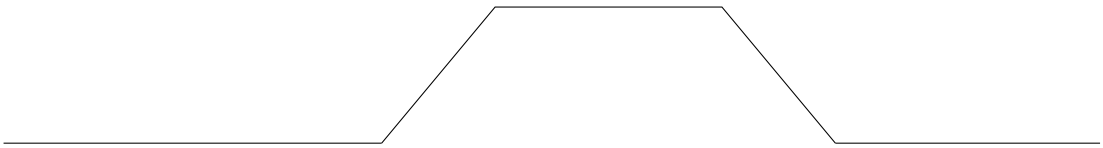

Figure 1.2: Bottom topography type 2.

Study	Type of bottom	Case	$\frac{\partial h}{\partial x}$	Order	$k_0 h_{max}$	Order	k_0[1/m]	ϵ	γ	Ske_{max}	Kur_{max}
Trulsen et al. (2012)	1	1	0.05	ϵ	1.59	$\epsilon^{0.1}$	2.66	0.05	3.3	0.2	3.25
”	”	2	”	$\epsilon^{0.9}$	0.32	$\epsilon^{0.02}$	1.83	0.03	”	0.32	3.10
”	”	3	”	$\epsilon^{0.8}$	0.81	$\epsilon^{0.05}$	1.35	0.02	”	0.48	3.25
Kashima et al. (2014)	1	6	0.03	ϵ	2.022	$\epsilon^{0.2}$	4.044	0.04	10	$\diamond$	$\diamond$
Raustøl (2014)	2	1	0.2625	$\epsilon^{0.4}$	4.11	$\epsilon^{0.4}$	8.22	0.0489	3.3	0.9	4.00
”	”	”	”	$\epsilon^{0.4}$	3.16	$\epsilon^{0.3}$	6.32	0.0378	”	1.00	4.5
”	”	”	”	$\epsilon^{0.3}$	2.52	$\epsilon^{0.2}$	5.04	0.0306	”	0.75	3.85
”	”	”	”	$\epsilon^{0.3}$	2.08	$\epsilon^{0.1}$	4.16	0.0241	”	0.5	3.38
”	”	”	”	$\epsilon^{0.3}$	1.76	$\epsilon^{0.0.1}$	3.52	0.0180	”	0.42	3.45
”	”	2	”	$\epsilon^{0.5}$	4.93	$\epsilon^{0.5}$	8.216	0.0617	”	0.35	3.32
”	”	”	”	$\epsilon^{0.5}$	4.29	$\epsilon^{0.5}$	7.15	0.0598	”	0.23	3.32
”	”	”	”	$\epsilon^{0.5}$	3.78	$\epsilon^{0.4}$	6.30	0.0577	”	0.21	3.30
”	”	”	”	$\epsilon^{0.4}$	3.35	$\epsilon^{0.4}$	5.58	0.0541	”	0.20	3.25
”	”	”	”	$\epsilon^{0.4}$	3.00	$\epsilon^{0.3}$	5.00	0.0559	”	0.19	3.24
”	”	”	”	$\epsilon^{0.4}$	2.45	$\epsilon^{0.2}$	4.08	0.0487	”	0.19	3.24
Ma et al. (2014)	2	1	0.05	$\epsilon^{1.1}$	1.89	$\epsilon^{0.2}$	4.2141	0.0729	1.5	*	*
”	”	”	”	$\epsilon^{1.1}$	”	$\epsilon^{0.2}$	”	”	3.3	*	*
”	”	”	”	$\epsilon^{1.1}$	”	$\epsilon^{0.2}$	”	”	5.0	*	*
”	”	”	”	$\epsilon^{1.1}$	”	$\epsilon^{0.2}$	”	”	7.0	*	*

Table 1.1: Experimental quantities: $\frac{\partial h}{\partial x}$, $k_0 h_{max}$, k_0, ϵ, γ, Ske_{max} and Kur_{max} indicate bottom slope, largest dimensionless depth, characteristic wavenumber applies to maximum depth, steepness of the waves, peak enhancement factor, maximum amount of skewness and maximum amount of kurtosis, respectively. $\diamond$: The results were not reported. $*$: Skewness and kurtosis were not reported in the proper scales comparable to the other works.

1.1.2 Theoretical and numerical studies

In recent years, wave models have been developed in order to improve understanding of waves, and to be able to interpret results reported by different experimental studies with theory. One of the simplest nonlinear models for water waves on finite depth is the nonlinear Schrödinger equation with variable coefficients and a shoaling term for slowly varying depth derived by Djordjević and Redekopp (1978). They assumed small wave steepness $\epsilon = ka \ll 1$, and the depth varied on the scale of ϵ so that $h = h(\epsilon^2 x)$ with mild slope $\frac{\partial h}{\partial x} = O(\epsilon^2)$. Their model was appropriate to describe the behavior of waves propagate over a nonuniform bathymetry with a bottom variation of order ϵ^2. By employing the multiple scale method, the NLS equation was derived, and in this derivation the induced mean flow $\bar{\phi}_0$ and the set-down $\bar{\eta}_0$ were expanded in power series of ϵ. The expansions employed for $\bar{\phi}_0$ and $\bar{\eta}_0$ are justified only for sufficiently small depth, limited from above and $kh = O(1)$. This restricted assumption causes that their results can not be valid for greater depth.

In the study by Iusim and Stiassnie (1985), the NLS equation derived by Djordjevic & Redekopp was refined by investigating the evolution during the shoaling of a modulated wave train. By considering the small wave steepness $\epsilon = ka \ll 1$, slow variation for depth was assumed, $\frac{\partial h}{\partial x} = O(\epsilon^2)$, and it was in agreement with the assumption for bottom variation considered by Djordjević and Redekopp (1978). To derive the NLS equation, the same method of derivation used by Djordjević and Redekopp (1978) was applied, but they considered different strategy to treat with the induced mean flow $\bar{\phi}_0$ and the set-down $\bar{\eta}_0$. They presented a rather general model which consisted of a coupled system of equations for the complex wave envelope and the induced mean flow potential.

A more sophisticated model was investigated in the theoretical study of Liu and Dingemans (1989) who relaxed the assumption for slowly varying depth to $\frac{\partial h}{\partial x} = O(\epsilon)$, where ϵ was defined as steepness of waves. The bathymetry consisted of two components h_0 and h_1 varied on the scale of ϵ so that $h_0 = h_0(\epsilon x)$ and $h_1 = h_1(\epsilon^0 x)$. Furthermore, h_1 was assumed to be small, $O(kh_1) = O(\epsilon^2)$, where k was the characteristic wavenumber. These assumptions led to express depth by $h = h_0(x_1) + \epsilon h_1(x_1)$ where $x_1 = \epsilon x$. By expanding the velocity potential and the free surface displacement in terms of small parameter ϵ, they derived a third-order evolution equation for the envelope of a modulated wave train propagating over uneven bottom and the associated long-wave equation. By expanding $\bar{\phi}_0$ and $\bar{\eta}_0$ in the power series of ϵ, their model is also restricted to shallow water assumption, $kh = O(1)$, and it is not valid for greater depth.

Recent numerical studies have investigated variations of statistics in random waves propagating over variable depths with different profiles, and the probability of occurrence of freak waves for these cases. Numerical modeling of the formation and dynamics of freak waves in uneven bottom cases is challenging since it requires an accurate numerical code based on a mathematical model able to properly represent both nonlinear effects and dispersive effects. The Korteweg de Vries (KdV) frameworks, nonlinear Schrödinger-type equations (NLSE) and Boussinesq-type models can be mentioned as the approximation models to investigate the transformation of a random wave field in variable water depth. In several studies for shallow water, Boussinesq-type models have been applied, with different orders of approximation for dispersive and nonlinear effects [(Kashima et al., 2014),

(Gramstad et al., 2013)]. However the standard Boussinesq equations can not be applied to deep water due to increasing error with increment of depth from the linear dispersion relation (Zhao et al., 2004), and they are valid when the water depth is small $kh < 0.75$ (Madsen et al., 2002), where k is the wavenumber that corresponds to the depth h. Due to this, several teams have considered an extension of NLS-type models instead of Boussinesq equations to describe waves propagating over variable bathymetry.

A Korteweg de Vries equation has been employed by Sergeeva et al. (2011) to study the transformation of a random wave field in variable shallow water depth. They reported that the kurtosis increases as the water depth decrease, and the kurtosis can attain a local maximum around the shallower side.

Recently the Boussinesq model with improved linear dispersion was employed by Gramstad et al. (2013) as an approximation model for shallow water. In their study, random long-crested wave fields were investigated when they propagated over uneven bottom with bottom variation $\frac{\partial h}{\partial x} = O(\epsilon)$, both from deeper to shallower and from shallower to deeper region. They have used a bottom consisting of a step with an upward slope, then a horizontal portion followed by a downward slope which is shown in figure 1.2. The studied cases were $kh = 1.06$ in the deep part of the domain, and three cases of depth at the shallow part $kh = 0.55$, 0.70 and 0.82. In addition, similar cases studied experimentally in Trulsen et al. (2012) were simulated. This investigation has shown that significantly increased skewness, kurtosis and probability of freak waves, both at the shallow end of the slope and for some distance after the slope, can occur when long-crested waves propagate over a slope. They found good agreement with the experiments described by Trulsen et al. (2012) which is reported in table 1.1.

In the study of Zeng and Trulsen (2012), the development of freak waves in a wave field with long-crested waves propagated from deeper to shallower water, was studied. The depth was assumed finite but not too small, $(k_0 h)^{-1} = O(1)$, that the depth $h(x)$ was slowly varying, $\frac{\partial h}{\partial x} = O(\epsilon^2)$ where ϵ defined as steepness of waves. The bottom topography applied in their study can be demonstrated by figure 1.1. The velocity potential ϕ and the surface displacement η were expanded in terms of the small parameter ϵ. By employing power series of ϵ to expand the induced mean flow $\bar{\phi}_0$ and the set-down $\bar{\eta}_0$, they derived the nonlinear Schrödinger equation in terms of surface displacement valid only for shallow water. The nonlinear Schrödinger equation with variable coefficients and a shoaling term for slowly varying depths were implemented. The previous findings have shown that the critical depth for narrowband long-crested waves may be subjected to modulational instability, is given by $kh \approx 1.363$. By motivating from this fact, simulations were performed at depths approximately equal to this critical depth or deeper. Three different wave trains were simulated with different Benjamin-Feir Index ($BFI = \epsilon/\delta$, where ϵ defines steepness of waves and δ shows bandwidth) that propagated across five different slopes. The depth at the front of the slope was $kh = 10$ for all simulations, while depths at the shallow part of the slope were $kh = 1.2$, 1.363, 2.065, 3.015 and 4.003. The results showed that the kurtosis and skewness decrease for decreasing deep and get a local minimum where the shallow part of the slope begin. Furthermore, they anticipated that the probability of freak waves on or near the edge of the continental shelf may exhibit a rather complicated spatial structure for wave fields entering from deep sea (Zeng and Trulsen, 2012).

Instead of using an approximate model like KdV, Boussinesq and NLS, a full numerical implementation of the potential flow equations can be used to investigate wave dynamic over variable depth. Viotti and Dias (2014) have employed this framework to study wave dynamic over a plateau-like bathymetry profile. This fully nonlinear method applied by them was valid for any depth. They reported the freak wave activities close to the shallower region.

Figure 1.3 shows an overview of the cases studied experimentally and numerically in previous works.

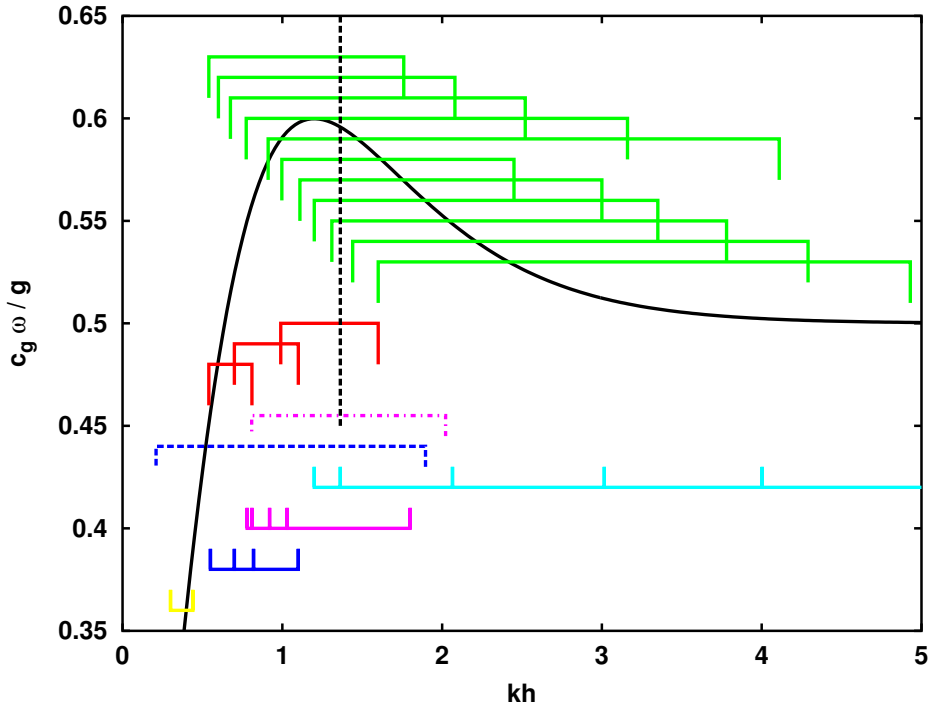

Figure 1.3: Group velocity as a function of kh (−), the depth $kh = 1.363$ (−−). Experimental study by Trulsen et al. (2012): three cases, red solid line (−). Experimental study by Kashima et al. (2014): blue dashed (−−). Experimental study by Raustøl (2014): eleven cases, green solid line(−). Experimental study by Ma et al. (2014): magenta dash-dot(−.). Numerical study by Sergeeva et al. (2011): yellow solid line (−). Numerical study by Zeng and Trulsen (2012): the waves come from the deep side, $kh = 10$, which is not shown in this figure, shallow side is shown by cyan solid line (−). Numerical study by Gramstad et al. (2013): three cases, blue solid line (−). Numerical study by Viotti and Dias (2014): magenta solid line (−).

1.2 Motivation

The experimental and numerical results found by Trulsen et al. (2012), Raustøl (2014) and Gramstad et al. (2013) are in good agreement with each other, as they reported there can be a local maximum of kurtosis after the slope. However, the behavior of kurtosis after the slope according to the nonlinear Schrödinger equation employed by Zeng and Trulsen (2012), which was there can be a local minimum of kurtosis after the slope, is opposite from the experiments presented by Trulsen et al. (2012) and Raustøl (2014) and the numerical results by Gramstad et al. (2013). Zeng and Trulsen (2012) used a numerical implementation of the nonlinear Schrödinger equation valid only for slowly varying depth with $\frac{\partial h}{\partial x} = O(\epsilon^2)$, whereas the assumption for the bottom variation in both studies by Trulsen et al. (2012) and Gramstad et al. (2013) was relaxed to $\frac{\partial h}{\partial x} = O(\epsilon)$, and in the experiments associated with thesis of Raustøl (2014) bottom was varying rapidly with $\frac{\partial h}{\partial x} = O(\epsilon^{\frac{1}{2}})$. These are important systematic differences between the work by Zeng and Trulsen (2012) and the studies of Trulsen et al. (2012), Raustøl (2014) and Gramstad et al. (2013).

Based on previous experimental and theoretical works, it appears that there are two different regimes when waves propagate from deep water over a slope to shallow water, a shallower regime with a possible local maximum of extreme waves near the shallow edge of the bottom slope, and a deeper regime with no such local maximum of extreme waves. Standard simplified wave models, in particular NLS equations for nonuniform depth employed by Djordjević and Redekopp (1978), Iusim and Stiassnie (1985) and Zeng and Trulsen (2012), have not been able to account for the transition between these two regimes. This is because a nonlinear Schrödinger equation enhanced with shoaling terms and depth–dependent coefficients should be employed for investigating wave dynamics over arbitrary depth and arbitrary nonuniform bathymetry. Furthermore, the NLS equation derived by Liu and Dingemans (1989) could not capture the qualitative change between these two regimes since it is valid only for shallow water. Therefore, it seems that there is not a proper model which is capable to bridge the gap between the works of Trulsen et al. (2012), Raustøl (2014) and Gramstad et al. (2013) and the study by Zeng and Trulsen (2012). The main focus in this thesis is to improve previous NLS equations for nonuniform depth in order to better represent abrupt bathymetry of arbitrary depth, in the hope that this may allow NLS models to account for the experimental observations by Raustøl (2014), and investigate if there is a qualitative difference behavior depending on bottom slope. In comparison with the full nonlinear model used by Viotti and Dias (2014), we hope our analytical approach will give further insight into the problem, and we hope that our final equations will be significantly faster for numerical simulation. Moreover, modulational instability of Stokes wave as one of the mechanisms responsible for the formation of freak waves is studied for the flat bottom case.

1.3 Outline

In chapter 2, the experiments performed by Raustøl (2014) and results reported by her are presented in detail. In addition, appropriate modulation scales, assumptions for steepness, bottom amplitude and bottom slope are described based on her experimental work.

Chapter 3 describes the derivation of the Nonlinear Schrödinger equation for uneven bottom. Starting from the governing equations which describe propagation of a water-wave train over a variable depth, and approximating the velocity potential function and the surface displacement by using WKB expansions. Finding the equations for the zeroth, first and second harmonics leads to find the space and time evolution equations valid for arbitrary depth with variable coefficients and enhanced with shoaling terms. These equations are presented in terms of the surface displacement.

Chapter 4 is dedicated to investigate some special cases. The Green's law is recovered for space evolution equations. By considering flat bottom topography, both space and time evolution equations are studied, and analytical solutions of the induced mean flow and the set-down are found.

Chapter 5 contains the modulational instability for space and time evolution equations. Instability for each of these equations is studied by considering two different cases deep water and finite depth in the limit of flat bottom.

In chapter 6, we present a discussion how the results achieved in chapters 3, 4, 5 are connected with previous researches and whether these can be compared. Some possible future works are also suggested in this chapter.

Finally, in chapter 7 a concluding remark is presented to explain what is found in this study.

Chapter 2

Experiments of Raustøl

Based on previous works, it seems that there are two opposite regimes, a "shallower" regime where kurtosis and skewness get a local maximum at the shallow part of the slope, and a "deeper" regime with the reduction of kurtosis and skewness toward the shallower side. An experimental study has been carried out by Raustøl (2014), in order to find the transition between these two regimes. The aim of her thesis was to carry out experiments that could say something about the transition between deeper regime and shallower regime for long-crested waves propagating over a sloping bottom. Since the main focus in this thesis is to derive a theory that could explain the experiment of Raustøl (2014), in this chapter a summary of her work will be presented. Finally, specified assumptions for mathematical model in this thesis will be introduced based on the experimental study of Raustøl (2014).

2.1 Experimental setup

Variations of statistics such as variance, skewness and kurtosis of irregular wave trains that propagating over uneven bottom were studied experimentally in her thesis. An isosceles trapezoidal bar was considered as an inhomogeneous profile for the bottom. Since the nonuniform bottom profile was assumed, the significant wave height has been investigated locally, which means that the freak wave criterion has been viewed locally.

Bottom profile, shown in figure 2.1, was considered in her thesis, where the bottom topography consisted of two skewed portions and a horizontal portion, each having the same length L. The height of the bottom and the water depth outside the slope were shown by H and h_1 respectively. Therefore, water depth of shallow side could be given by $h_2 = h_1 - H$.

The experiments were performed in a wave tank in the Hydrodynamic Laboratory at the University of Oslo. The length and width of the wave tank were 24.6 m and 0.5 m, respectively. Surface displacement was measured by locating 16 equispaced probes placed $\Delta x = 0.3$ m apart. These probes were used in four different positions along the tank and they could be moved along the tank. For the experiments, irregular waves were generated by the JONSWAP spectrum with the peak enhancement factor $\gamma = 3.3$, and their prop-

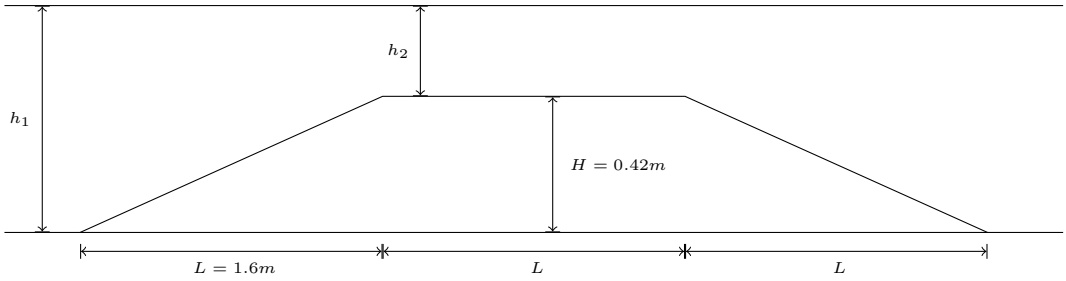

Figure 2.1: Sketch of ramp placed at the bottom of the wave tank. H is the height of ramp, h_1 is the depth of the deep side, h_2 is the depth of the shallow side, $\frac{\partial h}{\partial x} = 0.2625$.

agation along the wave tank was studied. Since she was interested in modeling realistic ocean waves in the wave tank, the waves generated by JONSWAP spectrum were the best choice.

Different experiments were performed by changing the period of the waves propagating over nonuniform bottom in the tank. Different cases for the deep water regime, and the transition between the deep- and the shallow water regime were examined. Tables 2.1 and 2.2 demonstrate various experiments which have been carried out for two different water depth $h_1 = 0.5$ m and 0.6 m.

$T_p[s]$	$\lambda_1[m]$	k_1h_1	$\frac{c_{g1}\omega}{g}$	k_2h_2	$\frac{c_{g2}\omega}{g}$	$\frac{L}{\lambda_1}$
0.4	0.25	12.6	0.5	2.08	0.548	6.61
0.5	0.39	8.05	0.5	1.44	0.592	4.59
0.6	0.562	5.59	0.5	1.11	0.598	3.54
0.7	0.765	4.11	0.502	0.911	0.579	2.9
0.8	0.996	3.16	0.51	0.774	0.549	2.47
0.9	1.25	2.52	0.526	0.675	0.515	2.15
1.0	1.51	2.08	0.548	0.6	0.482	1.91
1.1	1.78	1.76	0.569	0.54	0.451	1.72

Table 2.1: $L = 1.6$ m, $H = 0.42$ m, $h_1 = 0.5$ m. Index 1 indicates deep water, index 2 indicates shallow water.

$T_p[s]$	$\lambda_1[m]$	k_1h_1	$\frac{c_{g1}\omega}{g}$	k_2h_2	$\frac{c_{g2}\omega}{g}$	$\frac{L}{\lambda_1}$
0.4	0.25	15.1	0.5	4.53	0.501	6.41
0.5	0.39	9.66	0.5	2.91	0.514	4.12
0.6	0.562	6.71	0.5	2.08	0.548	2.94
0.7	0.765	4.93	0.5	1.6	0.581	2.27
0.8	0.998	3.78	0.503	1.31	0.598	1.85
0.9	1.26	3	0.512	1.11	0.598	1.57
1.0	1.54	2.45	0.529	0.968	0.587	1.37
1.1	1.83	2.06	0.549	0.86	0.57	1.22
0.75	0.88	4.29	0.501	1.44	0.591	1.82
0.85	1.13	3.35	0.507	1.20	0.599	1.42

Table 2.2: $L = 1.6$ m, $H = 0.42$ m, $h_1 = 0.6$ m. Index 1 indicates deep water, index 2 indicates shallow water.

2.2 Result

By performing experiments, different time series have been measured which described the surface displacement of waves propagating over uneven bathymetry. Changes of variance, skewness and kurtosis of the surface displacement, have been investigated. The results of variance for all time series indicated a systematic decline along wave tank, and this indicated the dissipation of wave field. Moreover, it was recognized that there are local maxima for skewness and kurtosis close to the shallower part of the bottom as long-crested waves propagating over a sloping bathymetry, from a deeper to shallower side. These results are consistent with the results of Trulsen et al. (2012) and Gramstad et al. (2013). In addition, the results demonstrated that the local maximum for kurtosis disappears for k_ph between 1.31 and 1.44 at the shallow side of the bottom, while the local maximum of skewness disappears for k_ph between 1.44 and 1.60.

2.3 Characteristic lengths and scaling assumptions

In this section, the appropriate scaling assumptions, assumptions for steepness, bottom amplitude and bottom slope have been introduced in such a way that it can describe a model for the experimental study by Raustøl (2014).

Steepness:

A characteristic wave amplitude, a_0, is applied to characterize surface displacement. It is assumed to be small in comparison with a wavelength $\lambda = \frac{2\pi}{k}$. We define a small parameter to characterize steepness of the waves

$$\epsilon = ka_0 \ll 1 \tag{2.1}$$

Modulation scale:

This part is dedicated to discuss the natural scale for slow modulation of the wave field. The standard assumption for classical nonlinear Schrödinger equations has been the slow modulation scales $x_1 = \epsilon x$ and $t_1 = \epsilon t$, thus assuming the steepness is the natural parameter to describe bandwidth and slow modulation. According to Trulsen and Dysthe (1997), a typical ocean wave spectrum has wider bandwidth, and thus faster modulation, better described by $x_{1/2} = \epsilon^{1/2} x$ and $t_{1/2} = \epsilon^{1/2} t$. However, since our intention is to use a JONSWAP spectrum, and that we anticipate such a spectrum can reasonably be accounted for by x_1 and t_1, even though some previous works have suggested a realistic ocean wave spectrum is actually more broadbanded.

Bottom:

The characteristic frequency of the central wave denoted by ω_0, and the acceleration of gravity g are applied for normalization. The characteristic wavenumber k_0 for infinitely deep water can be estimated from the following linear dispersion relation

$$k_0 = \frac{\omega_0^2}{g} \tag{2.2}$$

It is natural to distinguish between different regimes with respect to the water depth. If the depth satisfies $(k_0 h)^{-1} = O(\epsilon)$, the waves can be considered deep-water waves. In the shallower case, i.e. $(k_0 h)^{-1} = O(1)$, the waves can feel the bottom, and additional effects must be taken into account. In this thesis the depth is assumed to be finite but not too small. Therefore, appropriate scaling assumption is given by

$$(k_0 h)^{-1} = O(1)$$

Since in the experiments of Raustøl (2014) the bottom variations could be large, we assume $h_{max} \geq h(x) > 0$, and the following appropriate scale for bottom variation is assumed

$$\frac{dh}{dx} = O(\epsilon) \tag{2.3}$$

Furthermore, it is considered that the bottom varies over the long horizontal coordinate $x_1 = \epsilon x$ which is assumed for horizontal modulation of the waves. This means our theory allows a bathymetry of the "faster" rate of variation than Djordjević and Redekopp (1978) and Zeng and Trulsen (2012), but the similar rate of variation as Liu and Dingemans (1989). This also means that our theory allows a bathymetry of greater variation than most of these previous works.

Chapter 3

The space and time evolution equations for variable depth

In this chapter, we aim to derive a modified nonlinear Schrödinger equation which describes gravity waves propagating on the surface of a liquid of finite and varying depth. The governing equations of a uni-directional gravity waves are considered, and perturbation expansions in the style of WKB are employed to approximate the velocity potential function $\phi(x, z, t)$ and surface displacement $\eta(x, t)$. By considering the equations for the different harmonics at different orders, space evolution and time evolution equations in terms of surface elevation have been derived.

3.1 Governing equations

We consider irrotational flow of an inviscid and incompressible fluid over a nonuniform bottom. A coordinate system is defined by x as horizontal axis along the quiescent water level and z as the vertical coordinate. We denote the bottom as $z = -h(x)$ and the free surface is located at $z = \eta(x, t)$. A velocity potential function is $\phi(x, z, t)$ such that

$$\boldsymbol{v} = \nabla\phi(x, z, t)$$

where ∇ is the gradient operator.

Governing equation to satisfy continuity is the Laplace equation

$$\nabla^2\phi = 0 \qquad \text{at} \quad -h(x) < z < \eta \tag{3.1}$$

where ∇^2 is the Laplacian operator.

The boundary conditions on the free surface are the kinematic and dynamic boundary

conditions which can be written respectively as

$$\frac{\partial \eta}{\partial t} + \frac{\partial \phi}{\partial x}\frac{\partial \eta}{\partial x} = \frac{\partial \phi}{\partial z} \qquad \text{at} \quad z = \eta \tag{3.2}$$

$$\frac{\partial \phi}{\partial t} + g\eta + \frac{1}{2}(\nabla \phi)^2 = 0 \qquad \text{at} \quad z = \eta \tag{3.3}$$

The boundary condition along the bottom requires

$$\frac{\partial \phi}{\partial z} + \frac{\partial h}{\partial x}\frac{\partial \phi}{\partial x} = 0 \qquad \text{at} \quad z = -h(x) \tag{3.4}$$

3.2 Normalization

In the following, all variables become dimensionless by using the characteristic wavenumber k_0 and the characteristic frequency w_0 which are defined by the dispersion relation (2.2). The magnitude of each term is shown by ordering parameter ϵ which is defined by (2.1). New dimensionless variables and parameters in terms of a_0 , k_0 and ω_0 are given by

$$t^* = \omega_0 t$$

$$x^* = k_0 x$$

$$z^* = k_0 z$$

$$h^* = k_0 h$$

$$\eta^* = \frac{\eta}{a_0}$$

$$\phi^* = \frac{k_0 \phi}{\omega_0 a_0}$$

$$\frac{\partial}{\partial x^*} = \frac{1}{k_0}\frac{\partial}{\partial x}$$

$$\frac{\partial}{\partial z^*} = \frac{1}{k_0}\frac{\partial}{\partial z}$$

$$\frac{\partial}{\partial t^*} = \frac{1}{\omega_0}\frac{\partial}{\partial t}$$

By scaling according to these assumptions and dropping the stars, governing equations then become

Laplace equation

$$\nabla^2\phi = 0 \qquad \text{at} \quad -h < z < \epsilon\eta \tag{3.5}$$

Kinematic surface condition

$$\frac{\partial\eta}{\partial t} + \epsilon\frac{\partial\phi}{\partial x}\frac{\partial\eta}{\partial x} = \frac{\partial\phi}{\partial z} \qquad \text{at} \quad z = \epsilon\eta \tag{3.6}$$

Dynamic surface condition

$$\frac{\partial\phi}{\partial t} + \eta + \frac{1}{2}\epsilon(\nabla\phi)^2 = 0 \qquad \text{at} \quad z = \epsilon\eta \tag{3.7}$$

Boundary condition along the bottom

$$\frac{\partial\phi}{\partial z} + \epsilon\frac{\partial h}{\partial x_1}\frac{\partial\phi}{\partial x} = 0 \qquad \text{at} \quad z = -h \tag{3.8}$$

where $\phi = \phi(x, z, t)$, $\eta = \eta(x, t)$ and $h = h(x_1)$. Note that our assumption regarding to the bottom variation (2.3), has been considered in equation (3.8).

The free surface boundary conditions (3.6) and (3.7) are nonlinear. We may expand both kinematic and dynamic surface conditions in a Taylor's series around $z = 0$ by applying

$$\left.\frac{\partial\phi}{\partial t}\right|_{z=\epsilon\eta} = \left.\frac{\partial\phi}{\partial t}\right|_{z=0} + \epsilon\eta\left.\frac{\partial^2\phi}{\partial z\partial t}\right|_{z=0} + \frac{1}{2}(\epsilon\eta)^2\left.\frac{\partial^3\phi}{\partial z^2\partial t}\right|_{z=0} + O(\epsilon^3)$$

$$\left.\frac{\partial\phi}{\partial x}\right|_{z=\epsilon\eta} = \left.\frac{\partial\phi}{\partial x}\right|_{z=0} + \epsilon\eta\left.\frac{\partial^2\phi}{\partial z\partial x}\right|_{z=0} + \frac{1}{2}(\epsilon\eta)^2\left.\frac{\partial^3\phi}{\partial z^2\partial x}\right|_{z=0} + O(\epsilon^3)$$

$$\left.\frac{\partial\phi}{\partial z}\right|_{z=\epsilon\eta} = \left.\frac{\partial\phi}{\partial z}\right|_{z=0} + \epsilon\eta\left.\frac{\partial^2\phi}{\partial z^2}\right|_{z=0} + \frac{1}{2}(\epsilon\eta)^2\left.\frac{\partial^3\phi}{\partial z^3}\right|_{z=0} + O(\epsilon^3)$$

Taylor expansion of kinematic surface condition about $z = 0$ yields

$$\frac{\partial\eta}{\partial t} + \epsilon[\frac{\partial\phi}{\partial x} + \epsilon\eta\frac{\partial^2\phi}{\partial z\partial x}]\frac{\partial\eta}{\partial x} + O(\epsilon^3) = \frac{\partial\phi}{\partial z} + \epsilon\eta\frac{\partial^2\phi}{\partial z^2} + \frac{1}{2}\epsilon^2\eta^2\frac{\partial^3\phi}{\partial z^3} + O(\epsilon^3) \qquad \text{at} \quad z = 0 \tag{3.9}$$

Similarly, Taylor expansion of dynamic surface condition about $z = 0$ can be written

as

$$
\begin{aligned}
&[\frac{\partial\phi}{\partial t}+\epsilon\eta\frac{\partial^2\phi}{\partial z\partial t}+\frac{1}{2}\epsilon^2\eta^2\frac{\partial^3\phi}{\partial z^2\partial t}]+O(\epsilon^3)+\eta+\frac{1}{2}\epsilon[(\frac{\partial\phi}{\partial x})^2+\epsilon\eta\frac{\partial}{\partial z}((\frac{\partial\phi}{\partial x})^2)]+O(\epsilon^3)\\
&+\frac{1}{2}\epsilon[(\frac{\partial\phi}{\partial z})^2+\epsilon\eta\frac{\partial}{\partial z}((\frac{\partial\phi}{\partial z})^2)]+O(\epsilon^3)=0 \qquad \text{at} \quad z=0
\end{aligned}
\tag{3.10}
$$

3.2.1 Representing solution in WKB style

Instead of applying full multiple scales, we use only the slow scales. Accordingly, all variables and parameters are scaled in term of new coordinates $x_1=\epsilon x$ and $t_1=\epsilon t$, and we consider

$$\frac{\partial}{\partial x}=\epsilon\frac{\partial}{\partial x_1} \quad , \quad \frac{\partial}{\partial t}=\epsilon\frac{\partial}{\partial t_1}$$

Governing equations in terms of new coordinates x_1 and t_1 can be presented as

Laplace equation

$$\epsilon^2\frac{\partial^2\phi}{\partial x_1^2}+\frac{\partial^2\phi}{\partial z^2}=0 \qquad \text{at} \quad -h<z<0 \tag{3.11}$$

Kinematic surface condition

$$\epsilon\frac{\partial\eta}{\partial t_1}+\epsilon^3\frac{\partial\phi}{\partial x_1}\frac{\partial\eta}{\partial x_1}+\epsilon^4\eta\frac{\partial^2\phi}{\partial z\partial x_1}\frac{\partial\eta}{\partial x_1}=\frac{\partial\phi}{\partial z}+\epsilon\eta\frac{\partial^2\phi}{\partial z^2}+\frac{1}{2}\epsilon^2\eta^2\frac{\partial^3\phi}{\partial z^3} \qquad \text{at} \quad z=0 \tag{3.12}$$

Dynamic surface condition

$$
\begin{aligned}
&\epsilon\frac{\partial\phi}{\partial t_1}+\epsilon^2\eta\frac{\partial^2\phi}{\partial z\partial t_1}+\frac{1}{2}\epsilon^3\eta^2\frac{\partial^3\phi}{\partial z^2\partial t_1}+\eta+\frac{1}{2}[\epsilon^3(\frac{\partial\phi}{\partial x_1})^2+\epsilon^4\eta\frac{\partial}{\partial z}((\frac{\partial\phi}{\partial x_1})^2)]\\
&+\frac{1}{2}[\epsilon(\frac{\partial\phi}{\partial z})^2+\epsilon^2\eta\frac{\partial}{\partial z}((\frac{\partial\phi}{\partial z})^2)]=0 \qquad \text{at} \quad z=0
\end{aligned}
\tag{3.13}
$$

Boundary condition along the bottom

$$\frac{\partial\phi}{\partial z}+\epsilon^2\frac{\partial h}{\partial x_1}\frac{\partial\phi}{\partial x_1}=0 \qquad \text{at} \quad z=-h \tag{3.14}$$

where $\phi=\phi(x_1,z,t_1)$, $\eta=\eta(x_1,t_1)$ and $h=h(x_1)$.

Solutions for the surface displacement η and the velocity potential ϕ can be represented in harmonic expansions in WKB style

$$\eta(x_1,t_1) = \epsilon\bar{\eta}_0 + \sum_{m=1}^{\infty} \epsilon^{m-1}(\bar{\eta}_m E^m + \bar{\eta}_{-m}E^{-m}) \tag{3.15}$$

$$\phi(x_1,z,t_1) = \bar{\phi}_0 + \sum_{m=1}^{\infty} \epsilon^{m-1}(\bar{\phi}_m E^m + \bar{\phi}_{-m}E^{-m}) \tag{3.16}$$

where the harmonics are identified by

$$E = e^{i\epsilon^{-1}\chi(x_1,t_1)} \tag{3.17}$$

and $\bar{\eta}_{-m} = \overset{*}{\bar{\eta}}_m$, $\bar{\phi}_{-m} = \overset{*}{\bar{\phi}}_m$.

$\chi(x_1,t_1)$ is the phase function defined by

$$k(x_1) = \frac{\partial\chi}{\partial x_1} \qquad \text{and} \qquad \omega = -\frac{\partial\chi}{\partial t_1} \tag{3.18}$$

where ω and k are related by the dispersion relation

$$\omega^2 = gk(x_1)\tanh(k(x_1)h(x_1)) \tag{3.19}$$

Notice that since our depth depends on the long spatial coordinate and the wavenumber k depends on the depth, the wavenumber is also considered as a function of this coordinate. Furthermore, our medium has no temporal variation, thus we fix ω to be a constant when we compute the corresponding $k(x_1)$.

Since we are interested in dimensionless equations, ω and $k(x_1)$ are made dimensionless in the following way

$$\omega^* = \frac{\omega}{\omega_0} \qquad \text{and} \qquad k^*(x_1) = \frac{k(x_1)}{k_0} \tag{3.20}$$

where characteristic wavenumber k_0 and characteristic frequency ω_0 are related to each other according to the equation (2.2). By applying new variables, following dimensionless dispersion relation is achieved

$$(\omega^*)^2 = k^*(x_1)\tanh(k^*(x_1)h^*(x_1)) \tag{3.21}$$

Since medium has no temporal variation, characteristic frequency ω_0 will be the same everywhere. Therefore, we assume ω_0 as our reference frequency, such as $\omega = \omega_0$, and this implies $\omega^* = 1$. After normalization and dropping the stars, the normalized frequency is 1, and the normalized wavenumber is the solution of

$$k\tanh(kh) = 1 \tag{3.22}$$

Consequently, we get the dimensionless phase function

$$\chi(x_1, t_1) = \int^{x_1} k(\xi)\, d\xi - t_1. \tag{3.23}$$

Furthermore, the dimensionless phase speed c and the group velocity c_g can be expressed by

$$c = \frac{\omega^*}{k^*} = \frac{1}{k} \tag{3.24}$$

$$c_g = \frac{\partial \omega^*}{\partial k^*} = \frac{1}{2k}[1 + h(k^2 - 1)] \tag{3.25}$$

where k and h are dimensionless. Following figures describe the wavenumber k, phase speed c, group velocity c_g and their asymptotes as dimensionless functions of h and kh.

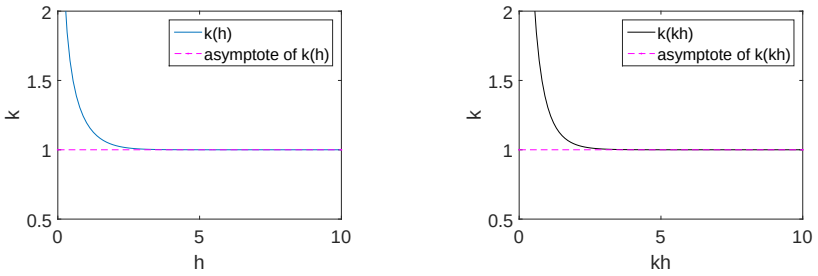

Figure 3.1: Dimensionless wavenumber k and its asymptote.

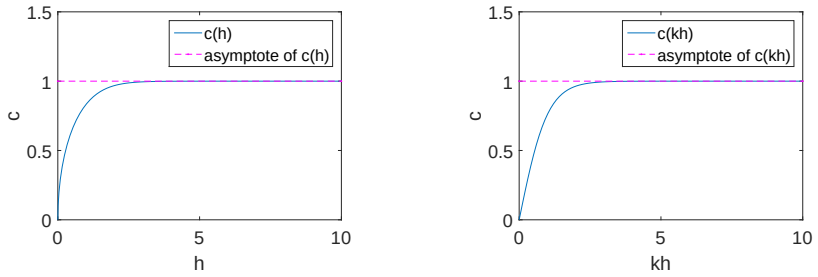

Figure 3.2: Dimensionless phase speed c and its asymptote.

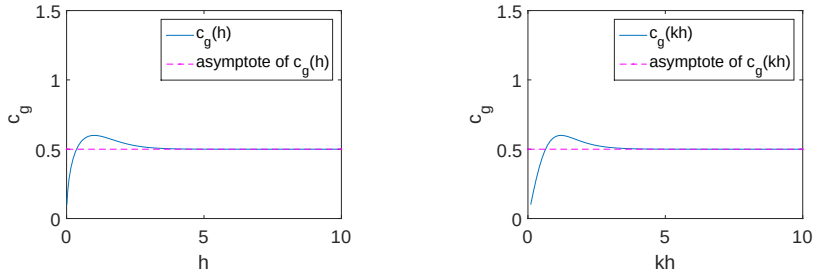

Figure 3.3: Dimensionless group velocity c_g and its asymptote.

The induced-current potential $\bar{\phi}_0$ and the set-down $\bar{\eta}_0$ as well as the complex harmonic amplitudes $\bar{\phi}_1, \bar{\phi}_2, \bar{\phi}_3, \cdots, \bar{\eta}_1, \bar{\eta}_2, \bar{\eta}_3, \cdots$ in expansions (3.15) and (3.16), are functions of the slow modulation variables ϵx and ϵt. Furthermore, variables $\bar{\phi}_1, \bar{\phi}_2, \bar{\phi}_3, \cdots$ are depend on the basic vertical coordinate z, while we need to allow the appropriate scale for z be undecided for $\bar{\phi}_0$. This assumption is considered since we in the limit of deep water expect the appropriate scale to be modulation scale ϵz for induced-current potential $\bar{\phi}_0$, while for shallow water the scale will be limited by the actual depth (the depth being smaller than the modulation length). In addition, we are not going to let the depth be shallower than a wavelength, therefore the appropriate length scale is between ϵz and z. Accordingly, for zeroth harmonic we assume following scale for the horizontal coordinate

$$z_a = \epsilon^a z$$

where a is a scalar, and $a \in [0, 1]$ that the value 0 is for finite depth, and the value 1 is for deep water.

3.3 Exact solution of Laplace equation over uneven bathymetry

A study has been carried out by Kundu et al. (2013) to derive nonlinear evolution equations in a situation of crossing sea state characterized by water waves having two different spectral peaks. They introduced an operator which was denoted by

$$\Delta_m = mk - i\epsilon \frac{\partial}{\partial x_1}$$

They explored a type of operator-form solutions of the Laplace equation via applying this operator. In this section, we have got inspiration from the study of Kundu et al. (2013) to find this type of solutions for our equations.

Upon substituting expansion (3.16) into the Laplace equation (3.11), and sorting har-

monics, we obtain the following equation

$$\begin{aligned} &E^0[\epsilon^{2a}\frac{\partial^2\bar{\phi}_0}{\partial z_a^2}+\epsilon^2\frac{\partial^2\bar{\phi}_0}{\partial x_1^2}]+E^1[\epsilon^0(\frac{\partial^2\bar{\phi}_1}{\partial z^2}-\Delta_1^2\bar{\phi}_1)] \\ &+E^2[\epsilon(\frac{\partial^2\bar{\phi}_2}{\partial z^2}-\Delta_2^2\bar{\phi}_2)]+E^3[\epsilon^2(\frac{\partial^2\bar{\phi}_3}{\partial z^2}-\Delta_3^2\bar{\phi}_3)]+\cdots=0 \qquad \text{at} \quad -h<z<0 \end{aligned} \tag{3.26}$$

where Δ_m is given by

$$\Delta_m = mk - i\epsilon\frac{\partial}{\partial x_1}$$

Separately satisfying the coefficients of $E^m, m=1,2,\cdots$ on both sides of equation (3.26), we get the following

$$\frac{\partial^2\bar{\phi}_m}{\partial z^2}-\Delta_m^2\bar{\phi}_m=0 \qquad \text{at} \quad -h<z<0$$

The exact solution of this equation can be written as

$$\bar{\phi}_m(x_1,z,t_1)=e^{z\Delta_m}A_m(x_1,t_1)+e^{-z\Delta_m}B_m(x_1,t_1) \tag{3.27}$$

We may rewrite A_m and B_m

$$A_m=\sum_{n=0}^{\infty}\epsilon^n A_{m,n} \tag{3.28}$$

$$B_m=\sum_{n=0}^{\infty}\epsilon^n B_{m,n} \tag{3.29}$$

In order to get equations valid for arbitrary depth, we do not consider any specified expansions for induced-current potential $\bar{\phi}_0$ and set-down $\bar{\eta}_0$. Whereas, the following expansion is employed for $\bar{\eta}_m$ where $m \geqslant 1$

$$\bar{\eta}_m=\sum_{n=0}^{\infty}\epsilon^n\bar{\eta}_{m,n} \tag{3.30}$$

Since our interest is primarily in the surface elevation η, our strategy will be to express A_m, B_m and the final evolution equation in terms of $\bar{\eta}_{1,0}$. One advantage of this could be that while A_m and B_m are functions of z, $\bar{\eta}_{1,0}$ is not. Therefore, perturbation analysis has been done with the constraint that

$$\bar{\eta}_{1,n}=0 \tag{3.31}$$

for $n>0$, and it implies that $\bar{\eta}_1=\bar{\eta}_{1,0}$. Note that this constraint is not employed for $\bar{\eta}_{m,n}$ for $m>1$.

3.4 Rewriting boundary conditions in terms of Δ_m

The next step is rewriting our boundary conditions in term of Δ_m, and in this stage we need to know what the answer of following question is.

3.4.1 Question: What is $\frac{\partial}{\partial z}e^{z(f(x)+\frac{\partial}{\partial x})}$?

Write as series expansion

$$e^{z(f(x)+\frac{\partial}{\partial x})} = \sum_{n=0}^{\infty} \frac{z^n}{n!} \left(f(x) + \frac{\partial}{\partial x} \right)^n \tag{3.32}$$

Taking the derivative, we may factor out the common factor to the left

$$\begin{aligned} \frac{\partial}{\partial z}e^{z(f(x)+\frac{\partial}{\partial x})} &= \sum_{n=1}^{\infty} \frac{z^{n-1}}{(n-1)!} \left(f(x) + \frac{\partial}{\partial x} \right)^n \\ &= \left(f(x) + \frac{\partial}{\partial x} \right) \sum_{n=0}^{\infty} \frac{z^n}{n!} \left(f(x) + \frac{\partial}{\partial x} \right)^n \end{aligned} \tag{3.33}$$

or to the right

$$\begin{aligned} \frac{\partial}{\partial z}e^{z(f(x)+\frac{\partial}{\partial x})} &= \sum_{n=1}^{\infty} \frac{z^{n-1}}{(n-1)!} \left(f(x) + \frac{\partial}{\partial x} \right)^n \\ &= \sum_{n=0}^{\infty} \frac{z^n}{n!} \left(f(x) + \frac{\partial}{\partial x} \right)^n \left(f(x) + \frac{\partial}{\partial x} \right) \end{aligned} \tag{3.34}$$

Clearly, it does not matter if the common factor $\left(f(x) + \frac{\partial}{\partial x}\right)$ is factored out to the left or to the right, therefore we arrive at the result

$$\begin{aligned} \frac{\partial}{\partial z}e^{z(f(x)+\frac{\partial}{\partial x})} &= \left(f(x) + \frac{\partial}{\partial x} \right) e^{z(f(x)+\frac{\partial}{\partial x})} \\ &= e^{z(f(x)+\frac{\partial}{\partial x})} \left(f(x) + \frac{\partial}{\partial x} \right) \end{aligned} \tag{3.35}$$

This fact is applied to derive following equations for bottom and surface conditions.

3.4.2 Bottom condition in terms of Δ_m

By substituting harmonic expansions (3.15) and (3.16) in equation (3.14), we get the following boundary condition in terms of Δ_m along the bottom

$$\begin{aligned}&[\epsilon^a \frac{\partial \bar{\phi}_0}{\partial z_a} + \sum_{m=1}^{\infty} \epsilon^{m-1} (\frac{\partial \bar{\phi}_m}{\partial z} E^m + c.c.)] \\ &+ \epsilon^2 \frac{\partial h}{\partial x_1} [\epsilon^0 \frac{\partial \bar{\phi}_0}{\partial x_1} + \sum_{m=1}^{\infty} i\epsilon^{m-2} (\Delta_m \bar{\phi}_m E^m + c.c.)] = 0 \qquad \text{at} \quad z = -h(x_1)\end{aligned} \tag{3.36}$$

Equating coefficients of $E^m, m = 1, 2, \cdots$ on both sides of obtained equation, we achieve the following

$$\left\{1 + i\epsilon \frac{\partial h}{\partial x_1}\right\} e^{z\Delta_m} \Delta_m A_m + \left\{-1 + i\epsilon \frac{\partial h}{\partial x_1}\right\} e^{-z\Delta_m} \Delta_m B_m = 0 \qquad \text{at} \quad z = -h(x_1) \tag{3.37}$$

Extracting the leading order contribution from this equation, we get for each $m = 1, 2, \cdots$

$$e^{-mk(x_1)h(x_1)} mk(x_1) A_{m,0} - e^{mk(x_1)h(x_1)} mk(x_1) B_{m,0} = 0 \tag{3.38}$$

thus

$$A_{m,0} = e^{2mk(x_1)h(x_1)} B_{m,0} \tag{3.39}$$

3.4.3 Surface conditions in terms of Δ_m

After applying harmonic expansions (3.15) and (3.16) into kinematic surface condition (3.12) and dynamic surface condition (3.13), results could be expressed by following equations.

Kinematic Surface condition

$$
\begin{aligned}
&\epsilon[\epsilon\frac{\partial\bar{\eta}_0}{\partial t_1}-\sum_{m=1}^{\infty}i\epsilon^{m-2}(W_m\bar{\eta}_m E^m+c.c.)]\\
&+\epsilon^3[\epsilon^0\frac{\partial\bar{\phi}_0}{\partial x_1}+\sum_{m=1}^{\infty}i\epsilon^{m-2}(\Delta_m\bar{\phi}_m E^m+c.c.)][\epsilon\frac{\partial\bar{\eta}_0}{\partial x_1}+\sum_{m=1}^{\infty}i\epsilon^{m-2}(\Delta_m\bar{\eta}_m E^m+c.c.)]\\
&+\epsilon^4[\epsilon\bar{\eta}_0+\sum_{m=1}^{\infty}\epsilon^{m-1}(\bar{\eta}_m E^m+c.c.)][\epsilon^a\frac{\partial^2\bar{\phi}_0}{\partial z_a\partial x_1}+\sum_{m=1}^{\infty}i\epsilon^{m-2}(\frac{\partial}{\partial z}(\Delta_m\bar{\phi}_m)E^m+c.c.)]\\
&[\epsilon\frac{\partial\bar{\eta}_0}{\partial x_1}+\sum_{m=1}^{\infty}i\epsilon^{m-2}(\Delta_m\bar{\eta}_m E^m+c.c.)]=[\epsilon^a\frac{\partial\bar{\phi}_0}{\partial z_a}+\sum_{m=1}^{\infty}\epsilon^{m-1}(\frac{\partial\bar{\phi}_m}{\partial z}E^m+c.c.)]\\
&+\epsilon[\epsilon\bar{\eta}_0+\sum_{m=1}^{\infty}\epsilon^{m-1}(\bar{\eta}_m E^m+c.c.)][\epsilon^{2a}\frac{\partial^2\bar{\phi}_0}{\partial z_a^2}+\sum_{m=1}^{\infty}\epsilon^{m-1}(\frac{\partial^2\bar{\phi}_m}{\partial z^2}E^m+c.c.)]\\
&+\frac{1}{2}\epsilon^2[\epsilon\bar{\eta}_0+\sum_{m=1}^{\infty}\epsilon^{m-1}(\bar{\eta}_m E^m+c.c.)]^2[\epsilon^{3a}\frac{\partial^3\bar{\phi}_0}{\partial z_a^3}+\sum_{m=1}^{\infty}\epsilon^{m-1}(\frac{\partial^3\bar{\phi}_m}{\partial z^3}E^m+c.c.)]\qquad\text{at}\quad z=0
\end{aligned}
\tag{3.40}
$$

Dynamic Surface condition

$$
\begin{aligned}
&\epsilon[\epsilon^0\frac{\partial\bar{\phi}_0}{\partial t_1}-\sum_{m=1}^{\infty}i\epsilon^{m-2}(W_m\bar{\phi}_m E^m+c.c.)]\\
&+\epsilon^2[\epsilon\bar{\eta}_0+\sum_{m=1}^{\infty}\epsilon^{m-1}(\bar{\eta}_m E^m+c.c.)][\epsilon^a\frac{\partial^2\bar{\phi}_0}{\partial z_a\partial t_1}-\sum_{m=1}^{\infty}i\epsilon^{m-2}(\frac{\partial}{\partial z}(W_m\bar{\phi}_m)E^m+c.c.)]\\
&+\frac{1}{2}\epsilon^3[\epsilon\bar{\eta}_0+\sum_{m=1}^{\infty}\epsilon^{m-1}(\bar{\eta}_m E^m+c.c.)]^2[\epsilon^{2a}\frac{\partial^3\bar{\phi}_0}{\partial z_a^2\partial t_1}-\sum_{m=1}^{\infty}i\epsilon^{m-2}(\frac{\partial^2}{\partial z^2}(W_m\bar{\phi}_m)E^m+c.c.)]\\
&+[\epsilon\bar{\eta}_0+\sum_{m=1}^{\infty}\epsilon^{m-1}(\bar{\eta}_m E^m+c.c.)]+\frac{1}{2}\epsilon^3[\epsilon^0\frac{\partial\bar{\phi}_0}{\partial x_1}+\sum_{m=1}^{\infty}i\epsilon^{m-2}(\Delta_m\bar{\phi}_m E^m+c.c.)]^2\\
&+\epsilon^4[\epsilon\bar{\eta}_0+\sum_{m=1}^{\infty}\epsilon^{m-1}(\bar{\eta}_m E^m+c.c.)][\epsilon^0\frac{\partial\bar{\phi}_0}{\partial x_1}+\sum_{m=1}^{\infty}i\epsilon^{m-2}(\Delta_m\bar{\phi}_m E^m+c.c.)]\\
&[\epsilon^a\frac{\partial^2\bar{\phi}_0}{\partial x_1\partial z_a}+\sum_{m=1}^{\infty}i\epsilon^{m-2}(\frac{\partial}{\partial z}(\Delta_m\bar{\phi}_m)E^m+c.c.)]+\frac{1}{2}\epsilon[\epsilon^a\frac{\partial\bar{\phi}_0}{\partial z_a}+\sum_{m=1}^{\infty}\epsilon^{m-1}(\frac{\partial\bar{\phi}_m}{\partial z}E^m+c.c.)]^2\\
&+\epsilon^2[\epsilon\bar{\eta}_0+\sum_{m=1}^{\infty}\epsilon^{m-1}(\bar{\eta}_m E^m+c.c.)][\epsilon^a\frac{\partial\bar{\phi}_0}{\partial z_a}+\sum_{m=1}^{\infty}\epsilon^{m-1}(\frac{\partial\bar{\phi}_m}{\partial z}E^m+c.c.)]\\
&[\epsilon^{2a}\frac{\partial^2\bar{\phi}_0}{\partial z_a^2}+\sum_{m=1}^{\infty}\epsilon^{m-1}(\frac{\partial^2\bar{\phi}_m}{\partial z^2}E^m+c.c.)]=0\qquad\text{at}\quad z=0
\end{aligned}
\tag{3.41}
$$

where W_m is the operator

$$W_m=m+i\epsilon\frac{\partial}{\partial t_1}$$

3.5 Derivation of equations for different harmonics

For deriving equations from the bottom condition (3.36) for different harmonics, we introduce the following series expansion for $m = 1, 2, \cdots$

$$e^{z\Delta_m} = \sum_{n=0}^{\infty} \epsilon^n a_n \tag{3.42}$$

where

$$a_n = \frac{1}{n!} \frac{\partial^n}{\partial \epsilon^n} (e^{z\Delta_m}) \Big|_{\epsilon=0} \tag{3.43}$$

We evaluate (3.43) at $z = -h(x_1)$ after all differentiation, such that $h(x_1)$ is not subject to differentiation due to the differential operator Δ_m.

By calculating a_n, following expansion is achieved

$$e^{z\Delta_m} = e^{-mkh} + \frac{1}{1!}\epsilon ihe^{-mkh}\frac{\partial}{\partial x_1} + \frac{1}{2!}\epsilon^2(-1)h^2e^{-mkh}\frac{\partial^2}{\partial x_1^2} + \cdots \tag{3.44}$$

We will use this expansion to derive equations along the bottom for different harmonics.

3.5.1 Equations for first harmonic (E^1)

By substituting $m = 1$ in the equation (3.27), the solution of Laplace equation for the first harmonic can be represented by

$$\bar{\phi}_1 = e^{z\Delta_1} A_1(x_1, t_1) + e^{-z\Delta_1} B_1(x_1, t_1) \tag{3.45}$$

3.5.1.1 Zeroth order problem ($O(\epsilon^0)E^1$)

The equation corresponding to the boundary condition along the bottom is obtained by substituting (3.45) in the bottom condition (3.36) for $m = 1$, and extracting the leading order contribution

$$e^{-kh}A_{1,0} - e^{kh}B_{1,0} = 0$$

In addition, we get the following equations for free surface conditions from equations (3.40) and (3.41)

$$-kA_{1,0} + kB_{1,0} - i\bar{\eta}_1 = 0$$

$$-iA_{1,0} - iB_{1,0} + \bar{\eta}_1 = 0$$

where our unknowns are $A_{1,0}$, $B_{1,0}$, $\bar{\eta}_1$.

As we aim to express the evolution equation in term of the first harmonic and the zeroth order amplitude of the surface displacement, we represent our unknowns in the forms

$$A_{1,0} = -ie^{2hk}(1 + e^{2hk})^{-1}\bar{\eta}_1 \tag{3.46}$$

$$B_{1,0} = -i(1 + e^{2kh})^{-1}\bar{\eta}_1 \tag{3.47}$$

Note that we have assumed $\bar{\eta}_1 = \bar{\eta}_{1,0}$.

3.5.1.2 First order problem ($O(\epsilon)E^1$)

At this order after some simplifications, following three equations are achieved for the bottom condition and free surface conditions

- Bottom condition
$$\epsilon k e^{-kh} A_{1,1} - \epsilon k e^{kh} B_{1,1} = F_{1,1}$$

- Kinematic surface condition
$$-\epsilon k A_{1,1} + \epsilon k B_{1,1} - i\epsilon\bar{\eta}_{1,1} = G_{1,1}$$

- Dynamic surface condition
$$-i\epsilon A_{1,1} - i\epsilon B_{1,1} + \epsilon\bar{\eta}_{1,1} = H_{1,1}$$

where

$$\begin{aligned} F_{1,1} = \epsilon\{&i[1 - kh]e^{-kh}\frac{\partial A_{1,0}}{\partial x_1} - i[1 + kh]e^{kh}\frac{\partial B_{1,0}}{\partial x_1} - ik[e^{-kh}A_{1,0} + e^{kh}B_{1,0}]\frac{\partial h}{\partial x_1} \\ &- ih[e^{-kh}A_{1,0} + e^{kh}B_{1,0}]\frac{\partial k}{\partial x_1}\} \end{aligned} \tag{3.48}$$

$$G_{1,1} = -\epsilon\frac{\partial\bar{\eta}_1}{\partial t_1} - i\epsilon\frac{\partial A_{1,0}}{\partial x_1} + i\epsilon\frac{\partial B_{1,0}}{\partial x_1} + \epsilon^{1+2a}\frac{\partial^2\bar{\phi}_0}{\partial z_a^2}\bar{\eta}_1 \tag{3.49}$$

Clearly, the Laplace equation (3.26) for the zeroth harmonic suggests that

$$\epsilon^{2a}\frac{\partial^2\bar{\phi}_0}{\partial z_a^2} = O(\epsilon^2) \tag{3.50}$$

for all value of z. Since this term appears in the equation (3.49), we conclude that the very last term in the equation(3.49) is of order ϵ^3, and it can be neglected.

$H_{1,1}$ can be expressed by

$$H_{1,1} = -\epsilon\frac{\partial A_{1,0}}{\partial t_1} - \epsilon\frac{\partial B_{1,0}}{\partial t_1} + i\epsilon^{1+a}\frac{\partial \bar{\phi}_0}{\partial z_a}\bar{\eta}_1 \tag{3.51}$$

The kinematic surface condition (3.40) for the zeroth harmonic suggests

$$\epsilon^a\frac{\partial \bar{\phi}_0}{\partial z_a} = O(\epsilon^2) \tag{3.52}$$

at the surface. Therefore, the last term in $H_{1,1}$ is of order ϵ^3, and it does not belong to this order. Achieved equations can be represented in the following matrix form

$$Mx = b$$

where

$$M = \begin{pmatrix} ke^{-kh} & -ke^{kh} & 0 \\ -k & k & -i \\ -i & -i & 1 \end{pmatrix}$$

$$x = \begin{pmatrix} \epsilon A_{1,1} \\ \epsilon B_{1,1} \\ \epsilon\bar{\eta}_{1,1} \end{pmatrix} \quad , \quad b = \begin{pmatrix} F_{1,1} \\ G_{1,1} \\ H_{1,1} \end{pmatrix}$$

Simply, we can verify that $det(M) = 0$, and it means that we get a singularity. In order to remove the singularity, we can use the Fredholm's alternative theorem.

Fredholm's alternative theorem:

For any $A \in \mathbb{C}^{m\times n}, b \in \mathbb{C}^n$, one and only one of the following systems has a solution

$$(1) \quad Ax = b, \qquad (2) \quad A^*y = 0, y^*b \neq 0$$

In other words, $Ax = b$ has a solution if and only if

$$(b, ker((\bar{A})^T)) = 0$$

This is called *Fredholm's alternative* (Lyche, 2014).

By applying this theorem for our case, following equation which is called the solvability condition should be satisfied for removing the singularity

$$\frac{2i}{k(e^{-kh}-e^{kh})}F_{1,1} - iG_{1,1} + H_{1,1} = 0 \tag{3.53}$$

Considering expressions for $F_{1,1}$, $G_{1,1}$ and $H_{1,1}$ from (3.48), (3.49) and (3.51) in the equation (3.53), gives

$$i\epsilon\mu\frac{\partial h}{\partial x_1}\bar{\eta}_1 + i\epsilon(\frac{\partial\bar{\eta}_1}{\partial x_1} + \frac{1}{c_g}\frac{\partial\bar{\eta}_1}{\partial t_1}) = 0 \tag{3.54}$$

where c_g is given by the expression (3.25), and

$$\mu = \frac{(1-h)(k^2-1)}{4k^2c_g^2} \tag{3.55}$$

This result has also been reported by Djordjević and Redekopp (1978) and Zeng and Trulsen (2012).

At this stage, we aim to find unknowns $A_{1,1}$ and $B_{1,1}$ by solving the system, $Mx = b$. Simply, it can be verified that M is singular. Following section follows that the generalized inverse can be used as one of the methods to find the solution of this system.

Generalized inverse

Theorem:
consider linear system $Ax = b$ of m equations in n unknowns. The following is equivalent:

1. x is a least square solution,
2. $x = A^\dagger b + z$ for some $z \in \mathbb{C}^n$ with $Az = 0$,
3. $A^*Ax = A^*b$.

$A^\dagger$ is called the *generalized inverse* or *pseudo inverse* of A, and it defines by

$$A^\dagger = V_1\Sigma_1^{-1}U_1^*$$

for any singular value factorization $U_1\Sigma_1V_1^*$ of A (Lyche, 2014). Mentioned matrices U_1, Σ_1 and V_1 can be found by applying the following theorem.

Theorem (Existence of SVD):
Suppose for $m, n, r \in \mathbb{N}$ that $A \in \mathbb{C}^{m\times n}$ has rank r, and that $(\lambda_j, \vec{\nu}_j)$ are orthonormal eigenpairs for A^*A with $\lambda_1 \geq \ldots \lambda_r > 0 = \lambda_{r+1} = \ldots = \lambda_n$. Define

1. $V = [\vec{\nu}_1, \ldots, \vec{\nu}_n] \in \mathbb{C}^{n\times n}$,

2. $\Sigma \in \mathbb{R}^{m\times n}$ is a diagonal matrix with diagonal elements $\sigma_j = \sqrt{\lambda_j}$ for $j = 1, \ldots, min(m, n)$,

3. $U = [\vec{u}_1, \ldots, \vec{u}_m] \in \mathbb{C}^{m\times m}$,where $\vec{u}_j = \sigma_j^{-1}\overrightarrow{(A\nu_j)}$ for $j = 1, \ldots, r$, and $\vec{u}_{r+1}, \ldots, \vec{u}_m$ is an extension of $\vec{u}_1, \ldots, \vec{u}_r$ to an orthonormal basis $\vec{u}_1, \ldots, \vec{u}_m$ for $\mathbb{C}^m$.

Then $A = U\Sigma V^*$ is an ordered *singular value decomposition* of A (Lyche, 2014).

Singular value factorization is a decomposition of A such as

$$A = U_1\Sigma_1 V_1^*$$

where

$$\Sigma_1 = diag(\sigma_1, \ldots, \sigma_r) \in \mathbb{R}^{r\times r}$$

$$U_1 = [\vec{u}_1, \ldots, \vec{u}_r] \in \mathbb{C}^{m\times r}$$

$$V_1 = [\vec{\nu}_1, \ldots, \vec{\nu}_r] \in \mathbb{C}^{n\times r}$$

By applying this method, we can compute the generalized inverse of the singular matrix M, and unknowns can be found by computing $x = M^{\dagger}b + z$ for some $z \in \mathbb{C}^n$ with $Mz = 0$. Since this matrix appears for different harmonics, if someone try to solve this system for different harmonic, it can be useful to apply this method.

This method is not used in our thesis since we aim to solve this system once. Therefore, in order to find the unknowns, the Gaussian elimination method is employed, which is more convenient for our case.

Gaussian elimination method

In order to find $A_{1,1}$, $B_{1,1}$ and $\bar{\eta}_{1,1}$ from the matrix system, $Mx = b$, the Gaussian elimination method is applied. We convert the matrix M to an upper triangular matrix and same arithmetic operations should be applied on b. Then, via backward substitution, unknowns in the given system can be found. Applying this technique for our system yields an upper triangular system

$$Nx = d$$

where

$$N = \begin{pmatrix} ke^{-kh} & -ke^{kh} & 0 \\ 0 & k(1-e^{2kh}) & -i \\ 0 & 0 & \frac{(1+e^{2kh})}{k(1-e^{2kh})} + 1 \end{pmatrix}$$

$$d = \begin{pmatrix} F_{1,1} \\ e^{kh}F_{1,1} + G_{1,1} \\ \frac{i(1+e^{2kh})}{k(1-e^{2kh})}(e^{kh}F_{1,1} + G_{1,1}) + \frac{i}{k}e^{kh}F_{1,1} + H_{1,1} \end{pmatrix}$$

We define

$$\sigma = \tanh kh = \frac{e^{2kh} - 1}{e^{2kh} + 1}$$

Since $k\sigma = 1$, it follows that

$$N_{3,3} = \frac{(1 + e^{2kh})}{k(1 - e^{2kh})} + 1 = 0$$

Simply, we can verify that $d_{3,1}$ is equal to the right hand side of the solvability condition (3.53). Therefore, we conclude

$$d_{3,1} = 0$$

Hence, following simplified system of equations is obtained

$$\begin{pmatrix} ke^{-kh} & -ke^{kh} & 0 \\ 0 & k(1 - e^{2kh}) & -i \\ 0 & 0 & 0 \end{pmatrix} \begin{pmatrix} \epsilon A_{1,1} \\ \epsilon B_{1,1} \\ \epsilon \bar{\eta}_{1,1} \end{pmatrix} = \begin{pmatrix} F_{1,1} \\ e^{kh} F_{1,1} + G_{1,1} \\ 0 \end{pmatrix}.$$

From (3.31), we have assumed $\bar{\eta}_{1,1} = 0$, and according to this assumption, $A_{1,1}$ and $B_{1,1}$ can be written as

$$A_{1,1} = \frac{\epsilon^{-1} e^{kh}}{k} F_{1,1} + e^{2kh} B_{1,1} \tag{3.56}$$

$$B_{1,1} = \frac{\epsilon^{-1}}{k(1 - e^{2kh})} [e^{kh} F_{1,1} + G_{1,1}] \tag{3.57}$$

Substituting $F_{1,1}$ from (3.48) and $G_{1,1}$ from (3.49) and applying equation (3.54) for substituting $\frac{\partial \bar{\eta}_{1,0}}{\partial x_1}$, yield

$$\begin{aligned} A_{1,1} = &[\frac{h(k^2 - 1)}{8k^3 c_g^2}(h^2k^3 + k^2h^2 + (-h^2 + h + 1)k - h^2 + h)] \frac{\partial h}{\partial x_1} \bar{\eta}_1 \\ &+ [\frac{(k + 1)}{4k^2 c_g}(2kh - k^2h - h - 1)] \frac{\partial \bar{\eta}_1}{\partial t_1} \end{aligned} \tag{3.58}$$

$$B_{1,1} = [\frac{h(1 - k^2)}{8k^2 c_g^2}] \frac{\partial h}{\partial x_1} \bar{\eta}_1 + [\frac{1 - k}{4k^2 c_g}(hk^2 + 2kh + h + 1)] \frac{\partial \bar{\eta}_1}{\partial t_1} \tag{3.59}$$

3.5.2 Zeroth harmonic (E^0): Induced mean flow and set-down

Since the induced mean flow appears in the NLS equation to lower order on the finite depth than on the deep water, and we aim to derive the NLS equation in a general form which can apply for both finite and infinite depth, in this harmonic we do not consider any expansions for the induced-current potential $\bar{\phi}_0$ and the set-down $\bar{\eta}_0$. By including all first and second order terms in the Laplace equation, the bottom condition and boundary surface conditions for zeroth harmonic, the following set of differential equations is achieved.

$$\epsilon^2 \frac{\partial^2 \bar{\phi}_0}{\partial x_1^2} + \epsilon^{2a} \frac{\partial^2 \bar{\phi}_0}{\partial z_a^2} = 0 \qquad \text{at} \quad -\epsilon^a h < z_a < 0 \tag{3.60}$$

$$\epsilon^a \frac{\partial \bar{\phi}_0}{\partial z_a} + \epsilon^2 \frac{\partial h}{\partial x_1} \frac{\partial \bar{\phi}_0}{\partial x_1} = 0 \qquad \text{at} \quad z_a = -\epsilon^a h(x_1) \tag{3.61}$$

$$\epsilon^2 \frac{\partial \bar{\eta}_0}{\partial t_1} - \epsilon^a \frac{\partial \bar{\phi}_0}{\partial z_a} = \epsilon^2 [-2k \frac{\partial \mid \bar{\eta}_1 \mid^2}{\partial x_1} - \frac{(1-k^2)}{c_g} \mid \bar{\eta}_1 \mid^2 \frac{\partial h}{\partial x_1}] \qquad \text{at} \quad z_a = 0 \tag{3.62}$$

$$\epsilon \frac{\partial \bar{\phi}_0}{\partial t_1} + \epsilon \bar{\eta}_0 = \epsilon (1-k^2) \mid \bar{\eta}_1 \mid^2 \qquad \text{at} \quad z_a = 0 \tag{3.63}$$

In previous studies by Djordjević and Redekopp (1978) and Liu and Dingemans (1989), following perturbation expansions were employed for $\bar{\phi}_0$ and $\bar{\eta}_0$

$$\bar{\phi}_0 = \epsilon \bar{\phi}_{0,1} + \epsilon^2 \bar{\phi}_{0,2} + \epsilon^3 \bar{\phi}_{0,3} + \cdots$$

$$\bar{\eta}_0 = \epsilon \bar{\eta}_{0,1} + \epsilon^2 \bar{\eta}_{0,2} + \epsilon^3 \bar{\eta}_{0,3} + \cdots$$

Perturbation expansions applied in the study of Zeng and Trulsen (2012) were

$$\bar{\phi}_0 = \bar{\phi}_{0,1} + \epsilon \bar{\phi}_{0,2} + \epsilon^2 \bar{\phi}_{0,3} + \cdots$$

$$\bar{\eta}_0 = \bar{\eta}_{0,1} + \epsilon \bar{\eta}_{0,2} + \epsilon^2 \bar{\eta}_{0,3} + \cdots$$

By applying these expansions, they have implicitly assumed the depth is small, limited from above, and $kh = O(1)$, such that the vertical scale for $\bar{\phi}_0$ would be determined by the actual depth. Accordingly, their solution for $\bar{\phi}_0$ is not valid for greater depth when $\bar{\phi}_0$ will have vertical scale determined by the horizontal modulation of the wave $z_1 = \epsilon z$. Therefore, reported results by Djordjević and Redekopp (1978), Liu and Dingemans (1989) and Zeng and Trulsen (2012) are of limited validity because they have made such restricting assumptions of limiting depth from above. For this reason, we do not consider any specified expansions for the induced-current potential $\bar{\phi}_0$ and the set-down $\bar{\eta}_0$ in order to allow our depth, $(kh)^{-1} = O(1)$, limited from above.

3.5.3 Equations for second harmonic (E^2)

From (3.27) for $m = 2$, solution for the Laplace equation can be presented by

$$\bar{\phi}_2 = e^{z\Delta_2} A_2(x_1, t_1) + e^{-z\Delta_2} B_2(x_1, t_1) \tag{3.64}$$

3.5.3.1 Zeroth order ($O(\epsilon^0)E^2$)

- Bottom condition
  The bottom condition for this harmonic at this order yields

$$A_{2,0} = e^{4kh} B_{2,0} \tag{3.65}$$

- Kinematic and dynamic surface conditions
  we do not get any contribution from kinematic and dynamic conditions on the free surface for the second harmonic at the zeroth order.

3.5.3.2 First order ($O(\epsilon^1)E^2$)

- Bottom condition
  The equation from the bottom condition (3.36) for the second harmonic at the first order can be expressed as

$$\begin{aligned} 2ke^{-2kh} A_{2,1} - 2ke^{2kh} B_{2,1} = {} & i(1-2kh)e^{-2kh}\frac{\partial A_{2,0}}{\partial x_1} - i(1+2kh)e^{2kh}\frac{\partial B_{2,0}}{\partial x_1} \\ & - 2ik(e^{-2kh} A_{2,0} + e^{2hk} B_{2,0})\frac{\partial h}{\partial x_1} \\ & - 2ih(e^{-2kh} A_{2,0} + e^{2hk} B_{2,0})\frac{\partial k}{\partial x_1} \end{aligned} \tag{3.66}$$

- Kinematic surface condition
  The kinematic condition on the free surface for this case requires

$$-2i\bar{\eta}_{2,0} = 2k^2(A_{1,0} + B_{1,0})\bar{\eta}_1 + 2k(A_{2,0} - B_{2,0}) \tag{3.67}$$

  By substituting $A_{1,0}$ from the expression (3.46) and $B_{1,0}$ from the expression (3.47) and applying the expression(3.65), we end up with

$$\bar{\eta}_{2,0} = k^2\bar{\eta}_1^2 + ik(e^{4kh} - 1)B_{2,0} \tag{3.68}$$

- Dynamic surface condition
  The following equation is the contribution from dynamic surface condition for the

second harmonic at the first order

$$-2i(A_{2,0}+B_{2,0})+\bar{\eta}_{2,0}=ik(A_{1,0}-B_{1,0})\bar{\eta}_1-\frac{1}{2}k^2(A_{1,0}-B_{1,0})^2-\frac{1}{2}k^2(A_{1,0}+B_{1,0})^2 \tag{3.69}$$

After some simplifications, we get

$$B_{2,0}=\frac{(k-1)^2(k^2-3)}{8i(k^2+1)}\bar{\eta}_1^2+\frac{(k-1)^2}{4i(k^2+1)}\bar{\eta}_{2,0} \tag{3.70}$$

By substituting $B_{2,0}$ from the expression (3.70) in the equation (3.68), we get the second harmonic amplitude $\bar{\eta}_{2,0}$ of the surface displacement as below

$$\bar{\eta}_{2,0}=\frac{k^2(3k^2-1)}{2}\bar{\eta}_1^2 \tag{3.71}$$

which is consistent with the result of Zeng and Trulsen (2012).

3.5.4 Equations for first harmonic at second order ($O(\epsilon^2)E^1$)

Following equations are achieved for the first harmonic at the second order.

- Boundary condition along the bottom

$$\epsilon^2 k e^{-kh}A_{1,2}-\epsilon^2 k e^{kh}B_{1,2}=F_{1,2}$$

- Kinematic surface condition

$$-\epsilon^2 kA_{1,2}+\epsilon^2 kB_{1,2}-i\epsilon^2\bar{\eta}_{1,2}=G_{1,2}$$

- Dynamic surface condition

$$-i\epsilon^2 A_{1,2}-i\epsilon^2 B_{1,2}+\epsilon^2\bar{\eta}_{1,2}=H_{1,2}$$

where

$$
\begin{aligned}
F_{1,2} = \epsilon^2\{&\frac{1}{2}(kh-2)he^{-kh}\frac{\partial^2 A_{1,0}}{\partial x_1^2} + h^2e^{-kh}\frac{\partial k}{\partial x_1}\frac{\partial A_{1,0}}{\partial x_1} + \frac{1}{2}h^2e^{-kh}\frac{\partial^2 k}{\partial x_1^2}A_{1,0} \\
&+ i(1-kh)e^{-kh}\frac{\partial A_{1,1}}{\partial x_1} - ihe^{-kh}\frac{\partial k}{\partial x_1}A_{1,1} - \frac{1}{2}(kh+2)he^{kh}\frac{\partial^2 B_{1,0}}{\partial x_1^2} \\
&- h^2e^{kh}\frac{\partial k}{\partial x_1}\frac{\partial B_{1,0}}{\partial x_1} - \frac{1}{2}h^2e^{kh}\frac{\partial^2 k}{\partial x_1^2}B_{1,0} - i(1+kh)e^{kh}\frac{\partial B_{1,1}}{\partial x_1} \\
&- ihe^{kh}\frac{\partial k}{\partial x_1}B_{1,1} - i\frac{\partial h}{\partial x_1}[-i(1-kh)e^{-kh}\frac{\partial A_{1,0}}{\partial x_1} + ihe^{-kh}\frac{\partial k}{\partial x_1}A_{1,0} \\
&+ ke^{-kh}A_{1,1} - i(1+kh)e^{kh}\frac{\partial B_{1,0}}{\partial x_1} - ihe^{kh}\frac{\partial k}{\partial x_1}B_{1,0} + ke^{kh}B_{1,1}]\}
\end{aligned}
\tag{3.72}
$$

$$
\begin{aligned}
G_{1,2} = \epsilon^2\{&2k^2(A_{2,0}+B_{2,0})\bar{\eta}_1^* - k^2(A_{1,0}^*+B_{1,0}^*)\bar{\eta}_{2,0} + i(\frac{\partial B_{1,1}}{\partial x_1} - \frac{\partial A_{1,1}}{\partial x_1}) \\
&+ k^3(A_{1,0}-B_{1,0}) \mid \bar{\eta}_1 \mid^2 - \frac{1}{2}k^3(A_{1,0}^*-B_{1,0}^*)\bar{\eta}_1^2 - ik\frac{\partial \bar{\phi}_0}{\partial x_1}\bar{\eta}_1 + k^2(A_{1,0}+B_{1,0})\bar{\eta}_0\}
\end{aligned}
\tag{3.73}
$$

$$
\begin{aligned}
H_{1,2} = \epsilon^2\{&-(\frac{\partial A_{1,1}}{\partial t_1} + \frac{\partial B_{1,1}}{\partial t_1}) - ik(A_{1,0}^*-B_{1,0}^*)\bar{\eta}_{2,0} + 4ik(A_{2,0}-B_{2,0})\bar{\eta}_1^* \\
&- \frac{1}{2}ik^2(A_{1,0}^*+B_{1,0}^*)\bar{\eta}_{1,0}^2 + ik^2(A_{1,0}+B_{1,0}) \mid \bar{\eta}_1 \mid^2 - 2k^2(A_{1,0}^*+B_{1,0}^*)(A_{2,0}+B_{2,0}) \\
&- 2k^2(A_{1,0}^*-B_{1,0}^*)(A_{2,0}-B_{2,0}) - k^3(A_{1,0}^2-B_{1,0}^2)\bar{\eta}_1^* - k^3(A_{1,0}-B_{1,0})(A_{1,0}^*+B_{1,0}^*)\bar{\eta}_1 \\
&+ k^3(A_{1,0}^2-B_{1,0}^2)\bar{\eta}_1^* - k^3[(A_{1,0}-B_{1,0})(A_{1,0}^*+B_{1,0}^*) + (A_{1,0}+B_{1,0})(A_{1,0}^*-B_{1,0}^*)]\bar{\eta}_1 \\
&- k^3(A_{1,0}+B_{1,0})(A_{1,0}^*-B_{1,0}^*)\bar{\eta}_1 + ik(A_{1,0}-B_{1,0})\bar{\eta}_0 - ik(A_{1,0}+B_{1,0})\frac{\partial \bar{\phi}_0}{\partial x_1}\}
\end{aligned}
\tag{3.74}
$$

Note that all terms which get contribution from $\epsilon^a\frac{\partial \bar{\phi}_0}{\partial z_a}$ and $\epsilon^{2a}\frac{\partial^2 \bar{\phi}_0}{\partial z_a^2}$ in the expressions (3.73) and (3.74), are so small that they are neglected due to (3.50) and (3.52).

Matrix form of the equations can be expressed as

$$Mx = b$$

where

$$
M = \begin{pmatrix} ke^{-kh} & -ke^{kh} & 0 \\ -k & k & -i \\ -i & -i & 1 \end{pmatrix}
$$

$$x = \begin{pmatrix} \epsilon^2 A_{1,2} \\ \epsilon^2 B_{1,2} \\ \epsilon^2 \bar{\eta}_{1,2} \end{pmatrix} \quad , \quad b = \begin{pmatrix} F_{1,2} \\ G_{1,2} \\ H_{1,2} \end{pmatrix}$$

Since M is singular, the Fredholm's alternative theorem is applied to find the solvability condition. It implies the following condition

$$\frac{2i}{k(e^{-kh} - e^{kh})} F_{1,2} - iG_{1,2} + H_{1,2} = 0 \tag{3.75}$$

Substituting the expressions for $F_{1,2}$, $G_{1,2}$ and $H_{1,2}$ from (3.72), (3.73) and (3.74) into the solvability condition (3.75), after some algebra we obtain

$$\begin{aligned} \epsilon^2 \{ \bar{\lambda} \frac{\partial^2 \bar{\eta}_1}{\partial t_1^2} + \bar{\alpha} (\frac{\partial h}{\partial x_1})^2 \bar{\eta}_1 + \bar{\beta} \frac{\partial^2 h}{\partial x_1^2} \bar{\eta}_1 + \bar{\gamma} \frac{\partial h}{\partial x_1} \frac{\partial \bar{\eta}_1}{\partial t_1} + \bar{\nu} \bar{\eta}_1 \mid \bar{\eta}_1 \mid^2 \\ + \bar{\theta_1} \frac{\partial \bar{\phi}_0}{\partial x_1} \bar{\eta}_1 + \bar{\theta_2} \bar{\eta}_0 \bar{\eta}_1 \} = 0 \qquad \text{at} \quad z = 0 \end{aligned} \tag{3.76}$$

where the coefficients are given by

$$c_g = \frac{1}{2k}[1 + h(k^2 - 1)]$$

$$\bar{\nu} = \frac{-k^2}{2}[9k^4 - 10k^2 + 9]$$

$$\bar{\lambda} = \frac{-1}{4k^2 c_g^2}[-3h^2 + 2h + 1 + d(-2k) + d^2(k^2 + 2)]$$

$$\bar{\beta} = \frac{-1}{8k^2 c_g^2}[h^3 + h^2 - 2h + d(2k) + d^2(-2h - 1) + d^3(k)]$$

$$\bar{\alpha} = \frac{-1}{16k^4 c_g^4}[k^2 - h^4 + 2h^2 - 1 + d(3k - 3k^3) + d^2(k^4 + k^2 + 3h^2 - 3h - 4) + d^3(6k - 3k^3) + d^4(k^2 - 3)]$$

$$\begin{aligned} \bar{\gamma} = \frac{1}{8k^4 c_g^3}[-2k^2 + h^4 - 3h^3 + 5h^2 - 5h + 2 + d(3k^3 + 2k) + d^2(-4k^4 + 9k^2 \\ - 4h^2 + 14h - 10) + d^3(-k^5 + 10k^3 - 20k) + d^4(k^4 - 4k^2 + 6)] \end{aligned}$$

$$\bar{\theta_1} = -2k$$

$$\bar{\theta_2} = 1 - k^2$$

and $d = kh$. Note that in this case all of the mentioned coefficients are the functions of x_1.

Since we aim to derive both space and time evolution equations in terms of $\bar{\eta}_1$, we change all the first and second derivatives with respect to t_1 to the first and second derivatives with respect to x_1 in the equation (3.76). The time and space derivatives are related to each other based on the following expression which is achieved from the equation (3.54)

$$\epsilon \frac{\partial \bar{\eta}_1}{\partial t_1} = -\epsilon c_g \frac{\partial \bar{\eta}_1}{\partial x_1} - \epsilon c_g \mu \frac{\partial h}{\partial x_1} \bar{\eta}_1 \tag{3.77}$$

and consequently

$$\begin{aligned} \epsilon \frac{\partial^2 \bar{\eta}_1}{\partial t_1^2} &= \frac{\partial}{\partial t_1}[-\epsilon c_g \frac{\partial \bar{\eta}_1}{\partial x_1} - \epsilon c_g \mu \frac{\partial h}{\partial x_1} \bar{\eta}_1] \\ &= \epsilon\{c_g \frac{\partial c_g}{\partial x_1} \frac{\partial \bar{\eta}_1}{\partial x_1} + c_g^2 \frac{\partial^2 \bar{\eta}_1}{\partial x_1^2} + c_g \frac{\partial (c_g \mu)}{\partial x_1} \frac{\partial h}{\partial x_1} \bar{\eta}_1 \\ &\quad + c_g^2 \mu \frac{\partial^2 h}{\partial x_1^2} \bar{\eta}_1 + 2 c_g^2 \mu \frac{\partial h}{\partial x_1} \frac{\partial \bar{\eta}_1}{\partial x_1} + c_g^2 \mu^2 (\frac{\partial h}{\partial x_1})^2 \bar{\eta}_1\} \end{aligned} \tag{3.78}$$

By inserting into the equation (3.76), after some calculations and simplifications we get

$$\begin{aligned} &\epsilon^2\{\bar{\Lambda} \frac{\partial^2 \bar{\eta}_1}{\partial x_1^2} + \bar{\Psi} (\frac{\partial h}{\partial x_1})^2 \bar{\eta}_1 + \bar{\Upsilon} \frac{\partial^2 h}{\partial x_1^2} \bar{\eta}_1 + \bar{\Gamma} \frac{\partial h}{\partial x_1} \frac{\partial \bar{\eta}_1}{\partial x_1} + \bar{\vartheta} \bar{\eta}_1 \mid \bar{\eta}_1 \mid^2 \\ &+ \bar{\theta_3} \frac{\partial \bar{\phi}_0}{\partial x_1} \bar{\eta}_1 + \bar{\theta_4} \bar{\eta}_0 \bar{\eta}_1\} = 0 \qquad \text{at} \quad z = 0 \end{aligned} \tag{3.79}$$

where

$$c_g = \frac{1}{2k}[1 + h(k^2 - 1)]$$

$$\bar{\vartheta} = \frac{-k^2}{2}[9k^4 - 10k^2 + 9]$$

$$\bar{\Lambda} = \frac{-1}{4k^2}[-3h^2 + 2h + 1 + d(-2k) + d^2(k^2 + 2)]$$

$$\bar{\Upsilon} = -\frac{1}{16k^4 c_g^2}[k^2 - 3h^3 + 5h^2 - h - 1 + d(2k^3 - k) + d^2(k^4 + k^2 + 7h - 7) + d^3(k^3 - 5k)]$$

$$\bar{\Psi} = \frac{1}{64k^8c_g^4}[k^6 - 3k^4 + 2k^2 + d(4k^7 - 12k^5 + 22k^3 - 14k) + d^2(5k^8 - 24k^6 + 61k^4 - 74k^2 - 2h^3 + 14h^2 - 32h + 32) + d^3(2k^9 - 18k^7 + 70k^5 - 126k^3 + 104k) + d^4(-3k^8 + 26k^6 - 74k^4 + 96k^2 + 10h - 59) + d^5(2k^7 - 10k^5 + 20k^3 - 20k)]$$

$$\bar{\Gamma} = \frac{1}{8k^4c_g^2}[-h^4 + 9h^3 - 15h^2 + 7h + d(k^3 - 8k) + d^2(2k^4 - 15k^2 + 4h^2 - 24h + 28) + d^3(k^5 - 8k^3 + 22k) + d^4(-k^4 + 4k^2 - 6)]$$

$$\bar{\theta_3} = -2k$$

$$\bar{\theta_4} = 1 - k^2$$

and $d = kh$. These coefficients are also the functions of x_1.

3.6 Modified nonlinear Schrödinger model

NLS-type equations can be formulated in different forms suitable for describing the time evolution of a spatial field or the space evolution of a temporal field (Toffoli et al., 2010). In this thesis, the nonlinear Schrödinger equation is represented in both space evolution and time evolution equations.

3.6.1 Space evolution in terms of surface elevation

The nonlinear Schrödinger equation with variable coefficients and shoaling terms for uneven bottom is derived from (3.54) and (3.76)

$$\begin{aligned}\epsilon\{i\frac{\partial\bar{\eta}_1}{\partial x_1} + \frac{i}{c_g}\frac{\partial\bar{\eta}_1}{\partial t_1} + i\mu\frac{\partial h}{\partial x_1}\bar{\eta}_1\} + \epsilon^2\{\lambda\frac{\partial^2\bar{\eta}_1}{\partial t_1^2} + \alpha(\frac{\partial h}{\partial x_1})^2\bar{\eta}_1 + \beta\frac{\partial^2 h}{\partial x_1^2}\bar{\eta}_1 \\ + \gamma\frac{\partial h}{\partial x_1}\frac{\partial\bar{\eta}_1}{\partial t_1} + \nu\bar{\eta}_1 \mid \bar{\eta}_1 \mid^2 + \theta_1\frac{\partial\bar{\phi}_0}{\partial x_1}\bar{\eta}_1 + \theta_2\bar{\eta}_0\bar{\eta}_1\} = 0 \qquad \text{at} \quad z_a = 0\end{aligned} \tag{3.80}$$

where

$$c_g = \frac{1}{2k}[1 + h(k^2 - 1)]$$

$$\mu = \frac{(1-h)(k^2-1)}{4k^2c_g^2} \tag{3.81}$$

$$\nu = \frac{-k^2}{4c_g}[9k^4 - 10k^2 + 9]$$

$$\lambda = \frac{-1}{8k^2c_g^3}[-3h^2 + 2h + 1 + d(-2k) + d^2(k^2+2)] \tag{3.82}$$

$$\beta = \frac{-1}{16k^2c_g^3}[h^3 + h^2 - 2h + d(2k) + d^2(-2h-1) + d^3(k)]$$

$$\alpha = \frac{-1}{32k^4c_g^5}[k^2 - h^4 + 2h^2 - 1 + d(3k - 3k^3) + d^2(k^4 + k^2 + 3h^2 - 3h - 4) + d^3(6k - 3k^3) + d^4(k^2 - 3)]$$

$$\gamma = \frac{1}{16k^4c_g^4}[-2k^2 + h^4 - 3h^3 + 5h^2 - 5h + 2 + d(3k^3 + 2k) + d^2(-4k^4 + 9k^2 - 4h^2 + 14h - 10) + d^3(-k^5 + 10k^3 - 20k) + d^4(k^4 - 4k^2 + 6)]$$

$$\theta_1 = \frac{-k}{c_g}$$

$$\theta_2 = \frac{1-k^2}{2c_g}$$

Note that since we are interested in the space evolution in terms of the surface elevation, all of the coefficients of the equation (3.76) have been divided by $2c_g$. The coefficients μ and λ have also been reported in the studies by Djordjević and Redekopp (1978) and Zeng and Trulsen (2012).

Since the induced-current potential $\bar{\phi}_0$ and the set-down $\bar{\eta}_0$ appear in the equation (3.80), the evolution equation is coupled with the equations from the zeroth harmonic

$$\epsilon^2 \frac{\partial^2 \bar{\phi}_0}{\partial x_1^2} + \epsilon^{2a} \frac{\partial^2 \bar{\phi}_0}{\partial z_a^2} = 0 \qquad \text{at} \quad -\epsilon^a h < z_a < 0 \tag{3.83}$$

$$\epsilon^a \frac{\partial \bar{\phi}_0}{\partial z_a} + \epsilon^2 \frac{\partial h}{\partial x_1} \frac{\partial \bar{\phi}_0}{\partial x_1} = 0 \qquad \text{at} \quad z_a = -\epsilon^a h(x_1) \tag{3.84}$$

$$\epsilon^2 \frac{\partial \bar{\eta}_0}{\partial t_1} - \epsilon^a \frac{\partial \bar{\phi}_0}{\partial z_a} = \epsilon^2 [-2k \frac{\partial \mid \bar{\eta}_1 \mid^2}{\partial x_1} - \frac{(1-k^2)}{c_g} \mid \bar{\eta}_1 \mid^2 \frac{\partial h}{\partial x_1}] \qquad \text{at} \quad z_a = 0 \tag{3.85}$$

$$\epsilon \frac{\partial \bar{\phi}_0}{\partial t_1} + \epsilon \bar{\eta}_0 = \epsilon (1-k^2) \mid \bar{\eta}_1 \mid^2 \qquad \text{at} \quad z_a = 0 \tag{3.86}$$

Clearly, the equation (3.86) suggests that

$$\bar{\eta}_0 = -\frac{\partial \bar{\phi}_0}{\partial t_1}\bigg|_{z_a=0} + (1-k^2) \mid \bar{\eta}_1 \mid^2 \tag{3.87}$$

By inserting into the kinematic surface condition (3.85), we achieve

$$\epsilon^2 \frac{\partial^2 \bar{\phi}_0}{\partial t_1^2} + \epsilon^a \frac{\partial \bar{\phi}_0}{\partial z_a} = \epsilon^2 [(1-k^2) \frac{\partial \mid \bar{\eta}_1 \mid^2}{\partial t_1} + 2k \frac{\partial \mid \bar{\eta}_1 \mid^2}{\partial x_1} + \frac{(1-k^2)}{c_g} \mid \bar{\eta}_1 \mid^2 \frac{\partial h}{\partial x_1}] \qquad \text{at} \quad z_a = 0 \tag{3.88}$$

Following plot demonstrates behavior of the coefficients as a function of dimensionless depth kh on the interval $[0, 10]$.

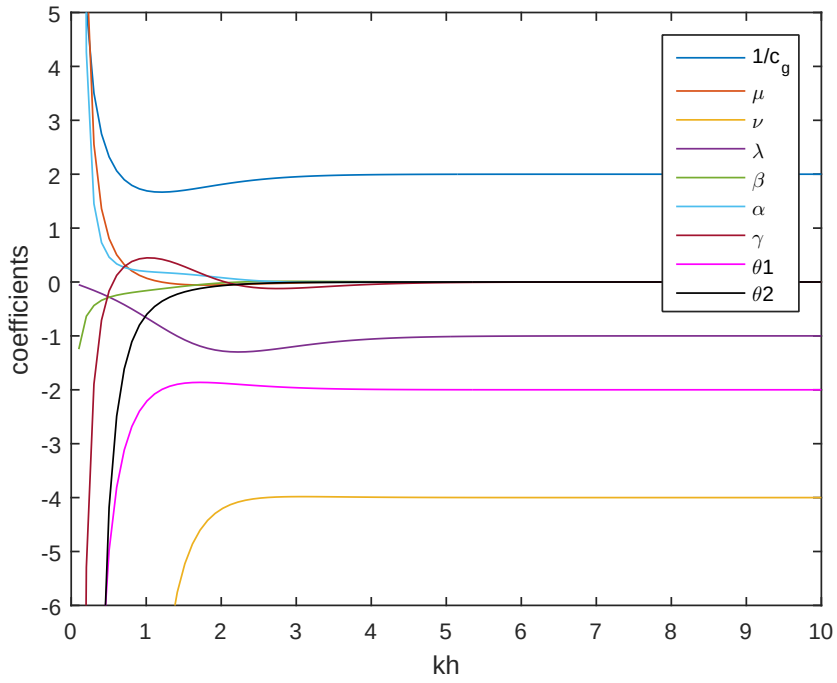

Figure 3.4: Coefficients of space evolution equations with respect to dimensionless depth kh.

3.6.2 Time evolution in terms of surface elevation

By considering both equations (3.54) and (3.79), the time evolution equations can be expressed by

$$\begin{aligned}\epsilon\{i\frac{\partial\bar{\eta}_1}{\partial t_1}+ic_g\frac{\partial\bar{\eta}_1}{\partial x_1}+i\mu_1\frac{\partial h}{\partial x_1}\bar{\eta}_1\}+\epsilon^2\{\Lambda\frac{\partial^2\bar{\eta}_1}{\partial x_1^2}+\Psi(\frac{\partial h}{\partial x_1})^2\bar{\eta}_1+\Upsilon\frac{\partial^2 h}{\partial x_1^2}\bar{\eta}_1\\ +\Gamma\frac{\partial h}{\partial x_1}\frac{\partial\bar{\eta}_1}{\partial x_1}+\vartheta\bar{\eta}_1\mid\bar{\eta}_1\mid^2+\theta_3\frac{\partial\bar{\phi}_0}{\partial x_1}\bar{\eta}_1+\theta_4\bar{\eta}_0\bar{\eta}_1\}=0 \qquad \text{at} \quad z_a=0\end{aligned} \tag{3.89}$$

where coefficients are given by

$$c_g=\frac{1}{2k}[1+h(k^2-1)]$$

$$\mu_1=\frac{(1-h)(k^2-1)}{4k^2c_g}$$

$$\vartheta=\frac{-k^2}{4}[9k^4-10k^2+9]$$

$$\Lambda=\frac{-1}{8k^2}[-3h^2+2h+1+d(-2k)+d^2(k^2+2)]$$

$$\Upsilon=-\frac{1}{32k^4c_g^2}[k^2-3h^3+5h^2-h-1+d(2k^3-k)+d^2(k^4+k^2+7h-7)+d^3(k^3-5k)]$$

$$\begin{aligned}\Psi=\frac{1}{128k^8c_g^4}[&k^6-3k^4+2k^2+d(4k^7-12k^5+22k^3-14k)+d^2(5k^8-24k^6+61k^4\\ &-74k^2-2h^3+14h^2-32h+32)+d^3(2k^9-18k^7+70k^5-126k^3+104k)\\ &+d^4(-3k^8+26k^6-74k^4+96k^2+10h-59)+d^5(2k^7-10k^5+20k^3-20k)]\end{aligned}$$

$$\begin{aligned}\Gamma=\frac{1}{16k^4c_g^2}[&-h^4+9h^3-15h^2+7h+d(k^3-8k)+d^2(2k^4-15k^2+4h^2-24h+28)\\ &+d^3(k^5-8k^3+22k)+d^4(-k^4+4k^2-6)]\end{aligned}$$

$$\theta_3=-k$$

$$\theta_4 = \frac{1-k^2}{2}$$

The induced mean flow $\bar{\phi}_0$ is governed by

$$\epsilon^2 \frac{\partial^2 \bar{\phi}_0}{\partial x_1^2} + \epsilon^{2a} \frac{\partial^2 \bar{\phi}_0}{\partial z_a^2} = 0 \qquad \text{at} \quad -\epsilon^a h < z_a < 0 \tag{3.90}$$

$$\epsilon^a \frac{\partial \bar{\phi}_0}{\partial z_a} + \epsilon^2 \frac{\partial h}{\partial x_1} \frac{\partial \bar{\phi}_0}{\partial x_1} = 0 \qquad \text{at} \quad z_a = -\epsilon^a h(x_1) \tag{3.91}$$

$$\epsilon^2 \frac{\partial^2 \bar{\phi}_0}{\partial t_1^2} + \epsilon^a \frac{\partial \bar{\phi}_0}{\partial z_a} = \epsilon^2 [(1-k^2) \frac{\partial \mid \bar{\eta}_1 \mid^2}{\partial t_1} + 2k \frac{\partial \mid \bar{\eta}_1 \mid^2}{\partial x_1} + \frac{(1-k^2)}{c_g} \mid \bar{\eta}_1 \mid^2 \frac{\partial h}{\partial x_1}] \qquad \text{at} \quad z_a = 0 \tag{3.92}$$

and the set-down $\bar{\eta}_0$ can be achieved from

$$\bar{\eta}_0 = -\frac{\partial \bar{\phi}_0}{\partial t_1}\bigg|_{z_a=0} + (1-k^2) \mid \bar{\eta}_1 \mid^2 \tag{3.93}$$

Note that we tried to derive the time evolution in terms of the surface elevation in the equation (3.89), therefore all coefficients of (3.79) have been divided by 2. The behavior of the coefficients with respect to dimensionless depth kh on interval $[0, 10]$ is described by figure 3.5.

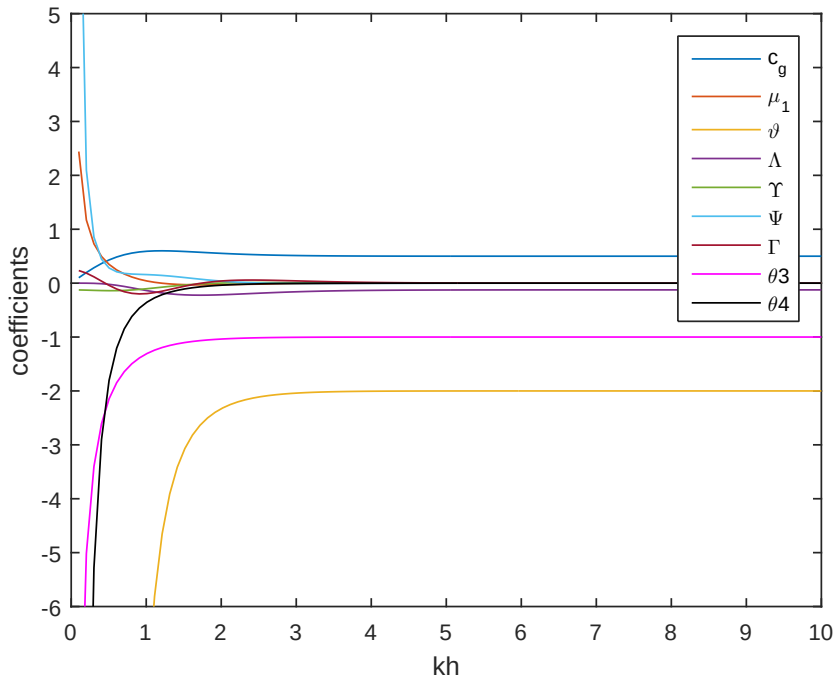

Figure 3.5: Coefficients of time evolution equations with respect to dimensionless depth kh.

Chapter 4

Special cases

In this chapter the Green's law is investigated for space evolution equation as a special case. Furthermore, this chapter includes space and time evolution equations in the limit of flat bottom for both deep water and finite depth. Analytical solutions of induced mean flow $\bar{\phi_0}$ and set-down $\bar{\eta}_0$ are also presented. We aim to use the equations derived in this chapter to study the stability of uniform Stokes waves in chapter 5.

4.1 Green's law

Our expectation for the amplitude of a wave field, changes in relation to the depth when the waves move from deeper to the shallower water, can be found by Green's law. The Green's law states that as a consequence of the conservation of energy flux, the amplitude $\bar{\eta}_1$ should vary proportional to the depth h to the power $-\frac{1}{4}$ in the limit h becomes small (Lamb, 1932). In the following, we purpose to recover the Green's law in our case. By removing all nonlinear terms and terms which contain temporal derivatives in the equation (3.80), following equation is achieved

$$i\frac{\partial\bar{\eta}_1}{\partial x_1} + i\mu\frac{\partial h}{\partial x_1}\bar{\eta}_1 + \epsilon[\alpha(\frac{\partial h}{\partial x_1})^2\bar{\eta}_1 + \beta\frac{\partial^2 h}{\partial x_1^2}\bar{\eta}_1] = 0 \tag{4.1}$$

Since the Green's law is valid for the region of gradual shoaling, h is considered to be small. By considering this assumption for h and applying the dominant balance technique, we get

$$\frac{\partial\bar{\eta}_1}{\partial x_1} + \mu\frac{\partial h}{\partial x_1}\bar{\eta}_1 = 0 \tag{4.2}$$

We consider S as an arbitrary function of h and $S(h)\bar{\eta}_1$ is constant, therefore we get

$$\begin{aligned} 0 &= \frac{\partial}{\partial x_1}[S(h)\bar{\eta}_1] \\ &= S(h)\frac{\partial \bar{\eta}_1}{\partial x_1} + S'(h)\frac{\partial h}{\partial x_1}\bar{\eta}_1 \\ &= S(h)[\frac{\partial \bar{\eta}_1}{\partial x_1} + \frac{S'(h)}{S(h)}\frac{\partial h}{\partial x_1}\bar{\eta}_1] \end{aligned} \tag{4.3}$$

This leads to

$$\frac{\partial \bar{\eta}_1}{\partial x_1} + \frac{S'(h)}{S(h)}\frac{\partial h}{\partial x_1}\bar{\eta}_1 = 0 \tag{4.4}$$

In addition, since $S(h)$ is an arbitrary function of h, we suppose $S(h) = h^{\frac{1}{4}}$. In this case, our assumption that $S(h)\bar{\eta}_1$ is constant, gives us

$$\bar{\eta}_1 \propto h^{-\frac{1}{4}} \tag{4.5}$$

Comparing equations (4.4) and (4.2) reveals that if μ is proportional to $\frac{S'(h)}{S(h)}$, we can claim that the Green's law can be recovered in our case. Therefore, we need to show that

$$\mu \propto \frac{S'(h)}{S(h)} = \frac{1}{4}h^{-1}$$

where μ is given by

$$\mu = \frac{(1-h)(k^2-1)}{4k^2c_g^2}$$

In the limit of very shallow water, the dispersion relation is given by $\omega = k\sqrt{gh}$. This implies that

$$c_g = \sqrt{gh}$$

Therefore, k and c_g are proportional to $h^{-\frac{1}{2}}$ and $h^{\frac{1}{2}}$ respectively, and this leads to the desired asymptotic behavior of μ

$$\mu \propto \frac{1}{4}h^{-1}$$

4.2 Space evolution equations in the limit of flat bottom

Flat bottom assumption implies that h is constant and $\frac{\partial h}{\partial x_1} = 0$. By applying this assumption in the equation (3.80), simplified space evolution equation is expressed as

$$\epsilon[i\frac{\partial \bar{\eta}_1}{\partial x_1} + \frac{i}{c_g}\frac{\partial \bar{\eta}_1}{\partial t_1}] + \epsilon^2[\lambda\frac{\partial^2 \bar{\eta}_1}{\partial t_1^2} + \nu\bar{\eta}_1 \mid \bar{\eta}_1 \mid^2 + \theta_1\frac{\partial \bar{\phi}_0}{\partial x_1}\bar{\eta}_1 + \theta_2\bar{\eta}_0\bar{\eta}_1] = 0 \qquad \text{at} \quad z_a = 0 \tag{4.6}$$

which is coupled with

$$\epsilon^2 \frac{\partial^2 \bar{\phi}_0}{\partial x_1^2} + \epsilon^{2a} \frac{\partial^2 \bar{\phi}_0}{\partial z_a^2} = 0 \qquad \text{at} \quad -\epsilon^a h < z_a < 0 \tag{4.7}$$

$$\epsilon^a \frac{\partial \bar{\phi}_0}{\partial z_a} = 0 \qquad \text{at} \quad z_a = -\epsilon^a h \tag{4.8}$$

$$\epsilon^2 \frac{\partial^2 \bar{\phi}_0}{\partial t_1^2} + \epsilon^a \frac{\partial \bar{\phi}_0}{\partial z_a} = \epsilon^2 [(1-k^2) \frac{\partial \mid \bar{\eta}_1 \mid^2}{\partial t_1} + 2k \frac{\partial \mid \bar{\eta}_1 \mid^2}{\partial x_1}] \qquad \text{at} \quad z_a = 0 \tag{4.9}$$

Furthermore, the set-down $\bar{\eta}_0$ is given by

$$\bar{\eta}_0 = -\frac{\partial \bar{\phi}_0}{\partial t_1}\bigg|_{z_a=0} + (1-k^2) \mid \bar{\eta}_1 \mid^2 \tag{4.10}$$

Note that all coefficients are constant since h and k are not functions of x_1 in the flat bottom limit.

At this step, we aim to solve the general auxiliary system for the induced flow. This set of equations has two types of solutions, a forced (inhomogeneous) solution which will be locked to the modulation of the short wave, and a free (homogeneous) solution which obeys its own dispersion relation for very shallow wave. We are interested in the forced solution only, and we do not want a free-wave solution for the induced flow which is a very long and shallow free wave. In order to find the analytical forced solution of this system, we will apply flat bottom assumption on the first order Schrödinger equation (3.54). We get

$$\frac{\partial \bar{\eta}_1}{\partial t_1} + c_g \frac{\partial \bar{\eta}_1}{\partial x_1} = 0 \tag{4.11}$$

and consequently

$$\frac{\partial \bar{\phi}_0}{\partial x_1} = -\frac{1}{c_g} \frac{\partial \bar{\phi}_0}{\partial t_1} \qquad \text{and} \qquad \frac{\partial^2 \bar{\phi}_0}{\partial x_1^2} = \frac{1}{c_g^2} \frac{\partial^2 \bar{\phi}_0}{\partial t_1^2} \tag{4.12}$$

By considering these expressions, the general auxiliary system for the induced flow can be simplified as

$$\frac{\epsilon^2}{c_g^2} \frac{\partial^2 \bar{\phi}_0}{\partial t_1^2} + \epsilon^{2a} \frac{\partial^2 \bar{\phi}_0}{\partial z_a^2} = 0 \qquad \text{at} \quad -\epsilon^a h < z_a < 0 \tag{4.13}$$

$$\epsilon^a \frac{\partial \bar{\phi}_0}{\partial z_a} = 0 \qquad \text{at} \quad z_a = -\epsilon^a h \tag{4.14}$$

$$\epsilon^2 \frac{\partial^2 \bar{\phi}_0}{\partial t_1^2} + \epsilon^a \frac{\partial \bar{\phi}_0}{\partial z_a} = \epsilon^2 [\frac{-2k}{c_g} + (1-k^2)] \frac{\partial \mid \bar{\eta}_1 \mid^2}{\partial t_1} \qquad \text{at} \quad z_a = 0 \tag{4.15}$$

Following temporal Fourier transform pair is used to solve this system of equations

$$\hat{\bar{\phi}}_0(x_1, z_a, \omega) = \frac{1}{2\pi} \int_{-\infty}^{\infty} \bar{\phi}_0(x_1, z_a, t_1) e^{i\omega t_1} dt_1 \tag{4.16}$$

$$\bar{\phi}_0(x_1, z_a, t_1) = \int_{-\infty}^{\infty} \hat{\bar{\phi}}_0(x_1, z_a, \omega) e^{-i\omega t_1} d\omega \tag{4.17}$$

We take the Fourier transform of our system in time by considering this fact that

$$\mathcal{F}_{t_1}(\frac{\partial^n \bar{\phi}_0}{\partial t_1^n}) = (-i\omega)^n \mathcal{F}_{t_1}(\bar{\phi}_0)$$

where $\mathcal{F}_{t_1}$ is the temporal Fourier transform operator.

The system can be expressed by

$$-\epsilon^2 \frac{\omega^2}{c_g^2} \hat{\bar{\phi}}_0 + \epsilon^{2a} \frac{\partial^2 \hat{\bar{\phi}}_0}{\partial z_a^2} = 0 \qquad \text{at} \quad -\epsilon^a h < z_a < 0 \tag{4.18}$$

$$\epsilon^a \frac{\partial \hat{\bar{\phi}}_0}{\partial z_a} = 0 \qquad \text{at} \quad z_a = -\epsilon^a h \tag{4.19}$$

$$-\epsilon^2 \omega^2 \hat{\bar{\phi}}_0 + \epsilon^a \frac{\partial \hat{\bar{\phi}}_0}{\partial z_a} = \epsilon^2 (-i\omega)[\frac{-2k}{c_g} + (1-k^2)] \mathcal{F}_{t_1}(\mid \bar{\eta}_1 \mid^2) \qquad \text{at} \quad z_a = 0 \tag{4.20}$$

This is a standard second order ODE with constant coefficients with two mixed boundary conditions. The solution of this system after considering the boundary conditions, can be express by

$$\hat{\bar{\phi}}_0(x_1, z_a, \omega) = C(x_1, \omega) \cosh(\frac{\omega}{c_g} \epsilon^{(1-a)} (z_a + \epsilon^a h)) \tag{4.21}$$

where

$$C(x_1, \omega) = \frac{-i\epsilon[\frac{-2k}{c_g} + (1-k^2)] \mathcal{F}_{t_1}(\mid \bar{\eta}_1 \mid^2)}{-\epsilon\omega \cosh(\frac{\epsilon\omega h}{c_g}) + \frac{1}{c_g} \sinh(\frac{\epsilon\omega h}{c_g})} \tag{4.22}$$

Now we take the inverse Fourier transform to represent the solution for $\bar{\phi}_0$ in integral form

$$\bar{\phi}_0(x_1, z_a, t_1) = \int_{-\infty}^{\infty} C(x_1, \omega) \cosh(\frac{\omega}{c_g} \epsilon^{(1-a)} (z_a + \epsilon^a h)) e^{-i\omega t_1} d\omega \tag{4.23}$$

where $C(x_1, \omega)$ is given by (4.22). Moreover, the surface elevation for the zeroth harmonic can be computed from

$$\bar{\eta}_0 = -\frac{\partial \bar{\phi}_0}{\partial t_1}\bigg|_{z_a=0} + (1-k^2) \mid \bar{\eta}_1 \mid^2 \tag{4.24}$$

Since derivatives of $\bar{\phi}_0$ with respect to the horizontal coordinate x_1 and time t_1 appear in (4.6) and (4.24) respectively, we compute them in the following way

$$\frac{\partial \bar{\phi}_0}{\partial x_1}\bigg|_{z_a=0} = -i\epsilon[-\frac{2k}{c_g} + (1-k^2)] \int_{-\infty}^{\infty} \frac{\frac{\partial}{\partial x_1}(\mathcal{F}_{t_1}(\mid \bar{\eta}_1 \mid^2))}{-\epsilon\omega + \frac{1}{c_g} \tanh(\frac{\epsilon\omega h}{c_g})} e^{-i\omega t_1} d\omega \tag{4.25}$$

$$\left.\frac{\partial\bar{\phi}_0}{\partial t_1}\right|_{z_a=0} = -\epsilon[-\frac{2k}{c_g} + (1-k^2)]\int_{-\infty}^{\infty}\frac{\mathcal{F}_{t_1}(\mid\bar{\eta}_1\mid^2)}{-\epsilon + \frac{1}{\omega c_g}\tanh(\frac{\epsilon\omega h}{c_g})}e^{-i\omega t_1}d\omega \tag{4.26}$$

Therefore, the set-down $\bar{\eta}_0$ can be represented by

$$\begin{aligned}\bar{\eta}_0 &= -\left.\frac{\partial\bar{\phi}_0}{\partial t_1}\right|_{z_a=0} + (1-k^2)\mid\bar{\eta}_1\mid^2 \\ &= \epsilon[-\frac{2k}{c_g} + (1-k^2)]\int_{-\infty}^{\infty}\frac{\mathcal{F}_{t_1}(\mid\bar{\eta}_1\mid^2)}{-\epsilon + \frac{1}{\omega c_g}\tanh(\frac{\epsilon\omega h}{c_g})}e^{-i\omega t_1}d\omega + (1-k^2)\mid\bar{\eta}_1\mid^2\end{aligned} \tag{4.27}$$

4.2.1 Deep water

In the case of deep water, the induced-current potential $\bar{\phi}_0$ depends on the slow vertical coordinate ϵz. Hence, we assume $a \to 1$ which gives

$$z_1 = \epsilon z$$

In the sense of deep water assumption ($h \to \infty$), we also obtain

$$c_g \to \frac{1}{2}$$

$$k \to 1$$

$$\lambda \to -1$$

$$\nu \to -4$$

$$\theta_1 \to -2$$

$$\theta_2 \to 0$$

So the space evolution equation can be simplified in the following way

$$\epsilon[i\frac{\partial\bar{\eta}_1}{\partial x_1} + 2i\frac{\partial\bar{\eta}_1}{\partial t_1}] - \epsilon^2[\frac{\partial^2\bar{\eta}_1}{\partial t_1^2} + 4\bar{\eta}_1\mid\bar{\eta}_1\mid^2 + 2\frac{\partial\bar{\phi}_0}{\partial x_1}\bar{\eta}_1] = 0 \qquad \text{at} \quad z_1 = 0 \tag{4.28}$$

The deep water limit, $h \to \infty$, implies $\tanh(\infty) \to 1$. Therefore, $\frac{\partial\bar{\phi}_0}{\partial x_1}$ from (4.25) can be expressed as

$$\left.\frac{\partial\bar{\phi}_0}{\partial x_1}\right|_{z_1=0} = 2i\epsilon\int_{-\infty}^{\infty}\frac{\partial}{\partial x_1}(\mathcal{F}_{t_1}(\mid\bar{\eta}_1\mid^2))e^{-i\omega t_1}d\omega \tag{4.29}$$

After inserting into the equation (4.28), the deep water limit of the space evolution equation is

$$\begin{aligned}&\epsilon[i\frac{\partial\bar{\eta}_1}{\partial x_1}+2i\frac{\partial\bar{\eta}_1}{\partial t_1}]-\epsilon^2[\frac{\partial^2\bar{\eta}_1}{\partial t_1^2}+4\bar{\eta}_1\mid\bar{\eta}_1\mid^2]\\&-4i\epsilon^3[\int_{-\infty}^{\infty}\frac{\partial}{\partial x_1}(\mathcal{F}_{t_1}(\mid\bar{\eta}_1\mid^2))e^{-i\omega t_1}d\omega]\bar{\eta}_1=0\qquad\text{at}\quad z_1=0\end{aligned}\tag{4.30}$$

Since we are interested in the first and second order terms, the last term in the equation (4.30) can be neglected. Therefore, the deep water space evolution equation becomes

$$\frac{\partial\bar{\eta}_1}{\partial x_1}+2\frac{\partial\bar{\eta}_1}{\partial t_1}+i\epsilon[\frac{\partial^2\bar{\eta}_1}{\partial t_1^2}+4\bar{\eta}_1\mid\bar{\eta}_1\mid^2]=0\tag{4.31}$$

This equation is completely in agreement with the deep water space evolution equation reported by Trulsen (2006).

4.2.2 Finite depth

In the limit of flat bathymetry, we assume $\frac{\partial h}{\partial x_1}=0$. Moreover, the finite depth assumption suggests that $a\to 0$, and it implies that the appropriate scale for the horizontal coordinate of the induced mean flow becomes $z_0=z$. By applying these assumptions in the equation (3.80), following space evolution equation with constant coefficients is achieved

$$\epsilon[i\frac{\partial\bar{\eta}_1}{\partial x_1}+\frac{i}{c_g}\frac{\partial\bar{\eta}_1}{\partial t_1}]+\epsilon^2[\lambda\frac{\partial^2\bar{\eta}_1}{\partial t_1^2}+\nu\bar{\eta}_1\mid\bar{\eta}_1\mid^2+\theta_1\frac{\partial\bar{\phi}_0}{\partial x_1}\bar{\eta}_1+\theta_2\bar{\eta}_0\bar{\eta}_1]=0\qquad\text{at}\quad z=0\tag{4.32}$$

Substituting $\frac{\partial\bar{\phi}_0}{\partial x_1}$ and the set-down $\bar{\eta}_0$ from the expressions (4.12) and (4.27), we get

$$\epsilon[i\frac{\partial\bar{\eta}_1}{\partial x_1}+\frac{i}{c_g}\frac{\partial\bar{\eta}_1}{\partial t_1}]+\epsilon^2[\lambda\frac{\partial^2\bar{\eta}_1}{\partial t_1^2}+(\nu+\theta_2(1-k^2))\bar{\eta}_1\mid\bar{\eta}_1\mid^2-(\frac{\theta_1}{c_g}+\theta_2)\frac{\partial\bar{\phi}_0}{\partial t_1}\bar{\eta}_1]=0\qquad\text{at}\quad z=0\tag{4.33}$$

Finite depth assumption which means that the uniform depth h is small, allows us to approximate $\tanh(\frac{\epsilon\omega h}{c_g})$ with the first term of the Taylor expansion around zero. Therefore, $\frac{\partial\bar{\phi}_0}{\partial t_1}$ from the equation (4.26) can be simplified

$$\begin{aligned}\frac{\partial\bar{\phi}_0}{\partial t_1}\Big|_{z_a=0}&=-\frac{[-\frac{2k}{c_g}+(1-k^2)]}{[-1+\frac{h}{c_g^2}]}\int_{-\infty}^{\infty}\mathcal{F}_{t_1}(\mid\bar{\eta}_1\mid^2)e^{-i\omega t_1}d\omega\\&=-\frac{[-\frac{2k}{c_g}+(1-k^2)]}{[-1+\frac{h}{c_g^2}]}\mid\bar{\eta}_1\mid^2\end{aligned}\tag{4.34}$$

Inserting into the evolution equation (4.33) leads to

$$\begin{aligned}&\epsilon[i\frac{\partial\bar{\eta}_1}{\partial x_1}+\frac{i}{c_g}\frac{\partial\bar{\eta}_1}{\partial t_1}]+\epsilon^2[\lambda\frac{\partial^2\bar{\eta}_1}{\partial t_1^2}+(\nu+\theta_2(1-k^2)\\&+(\frac{\theta_1}{c_g}+\theta_2)\frac{[-\frac{2k}{c_g}+(1-k^2)]}{[-1+\frac{h}{c_g^2}]})\bar{\eta}_1\mid\bar{\eta}_1\mid^2]=0\qquad\text{at}\quad z=0\end{aligned}\tag{4.35}$$

4.3 Time evolution equations in the limit of flat bottom

By neglecting all shoaling terms in the time evolution equation (3.89) in the sense of flat bottom assumption, following simplified nonlinear Schrödinger equation with constant coefficients is obtained

$$\epsilon[i\frac{\partial\bar{\eta}_1}{\partial t_1}+ic_g\frac{\partial\bar{\eta}_1}{\partial x_1}]+\epsilon^2[\Lambda\frac{\partial^2\bar{\eta}_1}{\partial x_1^2}+\vartheta\bar{\eta}_1\mid\bar{\eta}_1\mid^2+\theta_3\frac{\partial\bar{\phi}_0}{\partial x_1}\bar{\eta}_1+\theta_4\bar{\eta}_0\bar{\eta}_1]=0\qquad\text{at}\quad z_a=0\tag{4.36}$$

which is coupled with

$$\epsilon^2\frac{\partial^2\bar{\phi}_0}{\partial x_1^2}+\epsilon^{2a}\frac{\partial^2\bar{\phi}_0}{\partial z_a^2}=0\qquad\text{at}\quad -\epsilon^a h<z_a<0\tag{4.37}$$

$$\epsilon^a\frac{\partial\bar{\phi}_0}{\partial z_a}=0\qquad\text{at}\quad z_a=-\epsilon^a h\tag{4.38}$$

$$\epsilon^2\frac{\partial^2\bar{\phi}_0}{\partial t_1^2}+\epsilon^a\frac{\partial\bar{\phi}_0}{\partial z_a}=\epsilon^2[(1-k^2)\frac{\partial\mid\bar{\eta}_1\mid^2}{\partial t_1}+2k\frac{\partial\mid\bar{\eta}_1\mid^2}{\partial x_1}]\qquad\text{at}\quad z_a=0\tag{4.39}$$

In addition, the set-down $\bar{\eta}_0$ is given by

$$\bar{\eta}_0=-\frac{\partial\bar{\phi}_0}{\partial t_1}\bigg|_{z_a=0}+(1-k^2)\mid\bar{\eta}_1\mid^2\tag{4.40}$$

This set of equations has two types of solutions, a forced (inhomogeneous) solution which will be locked to the modulation of the short wave, and a free (homogeneous) solution which obeys its own dispersion relation for very shallow wave. The forced solution is the solution which we are interested in, and we do not want a free-wave solution for the induced flow which is a very long and shallow free wave. In order to find the analytical forced solution of $\bar{\phi}_0$ from the auxiliary system, the flat bottom assumption is applied to

the first order Schrödinger equation (3.54). This leads to

$$\frac{\partial \bar{\eta}_1}{\partial t_1} + c_g \frac{\partial \bar{\eta}_1}{\partial x_1} = 0 \tag{4.41}$$

and consequently

$$\frac{\partial \bar{\phi}_0}{\partial t_1} = -c_g \frac{\partial \bar{\phi}_0}{\partial x_1} \qquad \text{and} \qquad \frac{\partial^2 \bar{\phi}_0}{\partial t_1^2} = c_g^2 \frac{\partial^2 \bar{\phi}_0}{\partial x_1^2} \tag{4.42}$$

Inserting into the auxiliary system gives

$$\epsilon^2 \frac{\partial^2 \bar{\phi}_0}{\partial x_1^2} + \epsilon^{2a} \frac{\partial^2 \bar{\phi}_0}{\partial z_a^2} = 0 \qquad \text{at} \quad -\epsilon^a h < z_a < 0 \tag{4.43}$$

$$\epsilon^a \frac{\partial \bar{\phi}_0}{\partial z_a} = 0 \qquad \text{at} \quad z_a = -\epsilon^a h \tag{4.44}$$

$$\epsilon^2 c_g^2 \frac{\partial^2 \bar{\phi}_0}{\partial x_1^2} + \epsilon^a \frac{\partial \bar{\phi}_0}{\partial z_a} = \epsilon^2 [2k - (1-k^2) c_g] \frac{\partial \mid \bar{\eta}_1 \mid^2}{\partial x_1} \qquad \text{at} \quad z_a = 0 \tag{4.45}$$

and $\bar{\eta}_0$ is given by

$$\bar{\eta}_0 = c_g \left. \frac{\partial \bar{\phi}_0}{\partial x_1} \right|_{z_a=0} + (1-k^2) \mid \bar{\eta}_1 \mid^2$$

To solve this system of equations, following spatial Fourier transform pair is applied

$$\hat{\bar{\phi}}_0(\kappa, z_a, t_1) = \int_{-\infty}^{\infty} \bar{\phi}_0(x_1, z_a, t_1) e^{-i\kappa x_1} dx_1 \tag{4.46}$$

$$\bar{\phi}_0(x_1, z_a, t_1) = \frac{1}{2\pi} \int_{-\infty}^{\infty} \hat{\bar{\phi}}_0(\kappa, z_a, t_1) e^{i\kappa x_1} d\kappa \tag{4.47}$$

We take the Fourier transform of our system in space by considering this fact that

$$\mathcal{F}_{x_1}\left(\frac{\partial^n \bar{\phi}_0}{\partial x_1^n}\right) = (i\kappa)^n \mathcal{F}_{x_1}(\bar{\phi}_0)$$

where $\mathcal{F}_{x_1}$ is the spatial Fourier transform operator.

Therefore, a standard second order ODE with two mixed boundary conditions is achieved

$$-\epsilon^2 \kappa^2 \hat{\bar{\phi}}_0 + \epsilon^{2a} \frac{\partial^2 \hat{\bar{\phi}}_0}{\partial z_a^2} = 0 \qquad \text{at} \quad -\epsilon^a h < z_a < 0 \tag{4.48}$$

$$\epsilon^a \frac{\partial \hat{\bar{\phi}}_0}{\partial z_a} = 0 \qquad \text{at} \quad z_a = -\epsilon^a h \tag{4.49}$$

$$-\epsilon^2\kappa^2 c_g^2\hat{\bar{\phi}}_0 + \epsilon^a \frac{\partial\hat{\bar{\phi}}_0}{\partial z_a} = \epsilon^2(i\kappa)[2k-(1-k^2)c_g]\mathcal{F}_{x_1}(\mid \bar{\eta}_1 \mid^2) \qquad \text{at} \quad z_a = 0 \tag{4.50}$$

Simply, it can be verified that the solution of this system is

$$\hat{\bar{\phi}}_0(\kappa, z_a, t_1) = D(\kappa, t_1)\cosh(\epsilon^{(1-a)}\kappa(z_a + \epsilon^a h)) \tag{4.51}$$

where

$$D(\kappa, t_1) = \frac{-i\epsilon[(1-k^2)c_g - 2k]\mathcal{F}_{x_1}(\mid \bar{\eta}_1 \mid^2)}{-\epsilon\kappa c_g^2\cosh(\epsilon\kappa h) + \sinh(\epsilon\kappa h)} \tag{4.52}$$

By taking the inverse Fourier transform, the solution for $\bar{\phi}_0$ in integral form can be represented by

$$\bar{\phi}_0(x_1, z_a, t_1) = \frac{1}{2\pi}\int_{-\infty}^{\infty} D(\kappa, t_1)\cosh(\epsilon^{(1-a)}\kappa(z_a + \epsilon^a h))e^{i\kappa x_1}d\kappa \tag{4.53}$$

where $D(\kappa, t_1)$ is given by (4.52). Furthermore, $\bar{\eta}_0$ can be expressed by

$$\bar{\eta}_0 = c_g \left.\frac{\partial\bar{\phi}_0}{\partial x_1}\right|_{z_a=0} + (1-k^2) \mid \bar{\eta}_1 \mid^2$$

Derivative of $\bar{\phi}_0$ with respect to x_1 should be calculated in order to obtain the simplified time evolution equation. This calculation yields

$$\left.\frac{\partial\bar{\phi}_0}{\partial x_1}\right|_{z_a=0} = \frac{\epsilon}{2\pi}[(1-k^2)c_g - 2k]\int_{-\infty}^{\infty}\frac{\mathcal{F}_{x_1}(\mid \bar{\eta}_1 \mid^2)}{-\epsilon c_g^2 + \frac{1}{\kappa}\tanh(\epsilon\kappa h)}e^{i\kappa x_1}d\kappa \tag{4.54}$$

This gives following expression to describe the set-down

$$\begin{aligned}\bar{\eta}_0 &= c_g \left.\frac{\partial\bar{\phi}_0}{\partial x_1}\right|_{z_a=0} + (1-k^2) \mid \bar{\eta}_1 \mid^2 \\ &= \epsilon\frac{c_g}{2\pi}[(1-k^2)c_g - 2k]\int_{-\infty}^{\infty}\frac{\mathcal{F}_{x_1}(\mid \bar{\eta}_1 \mid^2)}{-\epsilon c_g^2 + \frac{1}{\kappa}\tanh(\epsilon\kappa h)}e^{i\kappa x_1}d\kappa + (1-k^2) \mid \bar{\eta}_1 \mid^2\end{aligned} \tag{4.55}$$

4.3.1 Deep-water limit

If the water depth is sufficiently large, the induced-current depends on the slow vertical coordinate ϵz. This implies that $a \to 1$, and consequently

$$z_1 = \epsilon z$$

Therefore, the time evolution equation simplifies greatly in the limit of infinite depth, and this is obtained by letting $h \to \infty$. We get

$$c_g \to \frac{1}{2}$$

$$k \to 1$$

$$\Lambda \to -\frac{1}{8}$$

$$\vartheta \to -2$$

$$\theta_3 \to -1$$

$$\theta_4 \to 0$$

Hence, the deep-water limit of (4.36) is

$$\epsilon[i\frac{\partial\bar{\eta}_1}{\partial t_1} + \frac{i}{2}\frac{\partial\bar{\eta}_1}{\partial x_1}] + \epsilon^2[-\frac{1}{8}\frac{\partial^2\bar{\eta}_1}{\partial x_1^2} - 2\bar{\eta}_1 \mid \bar{\eta}_1 \mid^2 - \frac{\partial\bar{\phi}_0}{\partial x_1}\bar{\eta}_1] = 0 \qquad \text{at} \quad z_1 = 0 \tag{4.56}$$

The deep water assumption, $h \to \infty$, leads to $\tanh(\infty) \to 1$, and this implies that

$$\left.\frac{\partial\bar{\phi}_0}{\partial x_1}\right|_{z_1=0} = \frac{\epsilon}{2\pi}[(1-k^2)c_g - 2k]\int_{-\infty}^{\infty}\kappa\mathcal{F}_{x_1}(\mid \bar{\eta}_1 \mid^2)e^{i\kappa x_1}d\kappa \tag{4.57}$$

This simply suggests to ignore the last term in equation (4.56) as this term is of order ϵ^3. Therefore, the time evolution equation in the limit of deep water is

$$\frac{\partial\bar{\eta}_1}{\partial t_1} + \frac{1}{2}\frac{\partial\bar{\eta}_1}{\partial x_1} + i\epsilon[\frac{1}{8}\frac{\partial^2\bar{\eta}_1}{\partial x_1^2} + 2\bar{\eta}_1 \mid \bar{\eta}_1 \mid^2] = 0 \qquad \text{at} \quad z_1 = 0 \tag{4.58}$$

This result is in agreement with the results reported by Trulsen (2006) and Gramstad and Trulsen (2011) for the deep water time evolution equations.

4.3.2 Finite depth

Finite depth assumption allows us to apply $a \to 0$ which means that the induced-current $\bar{\phi}_0$ depends on the original horizontal coordinate z. Furthermore, by applying expressions (4.41) and (4.55) in the time evolution equation (4.36), we get

$$\epsilon[i\frac{\partial\bar{\eta}_1}{\partial t_1} + ic_g\frac{\partial\bar{\eta}_1}{\partial x_1}] + \epsilon^2[\Lambda\frac{\partial^2\bar{\eta}_1}{\partial x_1^2} + (\vartheta + \theta_4(1-k^2))\bar{\eta}_1 \mid \bar{\eta}_1 \mid^2 + (\theta_3 + c_g\theta_4)\frac{\partial\bar{\phi}_0}{\partial x_1}\bar{\eta}_1] = 0 \qquad \text{at} \quad z = 0 \tag{4.59}$$

Since we considered the finite depth assumption which means that the uniform depth h is small, we are allowed to use the first term of the Taylor expansion of $\tanh(\epsilon\kappa h)$ to

calculate $\frac{\partial\bar{\phi}_0}{\partial x_1}$ from the expression (4.54). Hence, we obtain

$$\begin{aligned}\left.\frac{\partial\bar{\phi}_0}{\partial x_1}\right|_{z_a=0} &= \frac{[c_g(1-k^2)-2k]}{2\pi[h-c_g^2]}\int_{-\infty}^{\infty}\mathcal{F}_{x_1}(\mid\bar{\eta}_1\mid^2)e^{i\kappa x_1}d\kappa \\ &= \frac{[c_g(1-k^2)-2k]}{[h-c_g^2]}\mid\bar{\eta}_1\mid^2\end{aligned} \tag{4.60}$$

Inserting into the evolution equation (4.59) yields following time evolution equation in the limit of finite depth and flat bottom

$$\begin{aligned}&\epsilon[i\frac{\partial\bar{\eta}_1}{\partial t_1}+ic_g\frac{\partial\bar{\eta}_1}{\partial x_1}]+\epsilon^2[\Lambda\frac{\partial^2\bar{\eta}_1}{\partial x_1^2}+(\vartheta+\theta_4(1-k^2) \\ &+(\theta_3+c_g\theta_4)\frac{[c_g(1-k^2)-2k]}{[h-c_g^2]})\bar{\eta}_1\mid\bar{\eta}_1\mid^2]=0 \qquad \text{at} \quad z=0\end{aligned} \tag{4.61}$$

The equations derived in this chapter will be employed to study the stability of the uniform Stokes wave trains in the next chapter.

Chapter 5

Modulational instability of Stokes waves on flat bottom

It is natural to associate appearance of freak waves with the modulation instability of Stokes waves (Zakharov et al., 2006). The exponential growth of unstable perturbations such that a Stokes wave is broken, is known as modulational instability, and this phenomenon can create extreme waves. Modulational instability has been a topic of interest for scientists for several decades, and for the first time T. Brooke Benjamin and Jim E. Feir explored it, for surface gravity waves on deep water. Due to this, it is also known as the Benjamin-Feir instability.

In this chapter, the stability analysis for Stokes waves for both deep water and finite depth on flat bottom has been investigated via applying space and time evolution equations from the previous chapter. Furthermore, growth rates for perturbation of Stokes waves are studied for both cases.

5.1 Space evolution equations

5.1.1 Deep water

In the limit of deep water, the space evolution equation is

$$\frac{\partial \bar{\eta}_1}{\partial x_1} + 2\frac{\partial \bar{\eta}_1}{\partial t_1} + i\epsilon[\frac{\partial^2 \bar{\eta}_1}{\partial t_1^2} + 4\bar{\eta}_1 \mid \bar{\eta}_1 \mid^2] = 0 \tag{5.1}$$

We are looking for a uniform solution, by considering that the solution $\bar{\eta}_1$ is independent of time. This leads to

$$\frac{\partial \bar{\eta}_1}{\partial x_1} + 4i\epsilon\bar{\eta}_1 \mid \bar{\eta}_1 \mid^2 = 0$$

This equation has a particularly simple exact wave solution known as the Stokes wave. The solution is given by

$$\bar{\eta}_1 = B_0 e^{-4i\epsilon|B_0|^2 x_1}$$

where B_0 is a constant.

The stability of Stokes wave can be found by perturbing it in amplitude and phase. We set

$$\bar{\eta}_1 = B_0(1 + \alpha_1 + i\beta_1)e^{-4i\epsilon|B_0|^2 x_1} \tag{5.2}$$

where α_1 and β_1 are infinitesimal and real.

By inserting into the equation (5.1) and after linearization, we get

$$\frac{\partial \alpha_1}{\partial x_1} + i\frac{\partial \beta_1}{\partial x_1} + 2\frac{\partial \alpha_1}{\partial t_1} + 2i\frac{\partial \beta_1}{\partial t_1} + i\epsilon\frac{\partial^2 \alpha_1}{\partial t_1^2} - \epsilon\frac{\partial^2 \beta_1}{\partial t_1^2} + 8i\epsilon \mid B_0 \mid^2 \alpha_1 = 0$$

Following pair of equations is achieved by splitting up this equation into real and imaginary parts

$$\frac{\partial \alpha_1}{\partial x_1} + 2\frac{\partial \alpha_1}{\partial t_1} - \epsilon\frac{\partial^2 \beta_1}{\partial t_1^2} = 0 \tag{5.3}$$

$$\frac{\partial \beta_1}{\partial x_1} + 2\frac{\partial \beta_1}{\partial t_1} + \epsilon\frac{\partial^2 \alpha_1}{\partial t_1^2} + 8\epsilon \mid B_0 \mid^2 \alpha_1 = 0 \tag{5.4}$$

Assume plane-wave solutions

$$\begin{pmatrix} \alpha_1 \\ \beta_1 \end{pmatrix} = \begin{pmatrix} \hat{\alpha}_1 \\ \hat{\beta}_1 \end{pmatrix} e^{i(Kx_1 - \Omega t_1)} + c.c.$$

By inserting into equations for real and imaginary parts, we obtain

$$iK\hat{\alpha}_1 - 2i\Omega\hat{\alpha}_1 + \epsilon\Omega^2\hat{\beta}_1 = 0 \tag{5.5}$$

$$iK\hat{\beta}_1 - 2i\Omega\hat{\beta}_1 - \epsilon\Omega^2\hat{\alpha}_1 + 8\epsilon \mid B_0 \mid^2 \hat{\alpha}_1 = 0 \tag{5.6}$$

System of equations is written in the matrix form

$$\begin{pmatrix} i(K - 2\Omega) & \epsilon\Omega^2 \\ -\epsilon\Omega^2 + 8\epsilon \mid B_0 \mid^2 & i(K - 2\Omega) \end{pmatrix} \begin{pmatrix} \hat{\alpha}_1 \\ \hat{\beta}_1 \end{pmatrix} = \begin{pmatrix} 0 \\ 0 \end{pmatrix}$$

Since we are looking for a nontrivial solution, the determinant of the coefficient matrix has to be zero. Hence, it is found that the perturbation behaves according to the dispersion relation

$$K = 2\Omega \pm \sqrt{\epsilon^2\Omega^2(\Omega^2 - 8 \mid B_0 \mid^2)} \tag{5.7}$$

A perturbation is unstable if the modulational wavenumber K has a nonzero imaginary part. Therefore, the unstable region is given by

$$| \Omega | < 2\sqrt{2} \mid B_0 \mid \tag{5.8}$$

The growth rate of the instability is defined as

$$| Im(K) | = \sqrt{\epsilon^2 \Omega^2 (8 \mid B_0 \mid^2 - \Omega^2)} \tag{5.9}$$

This result is consistent with the study of Trulsen (2006). Figure 5.1 shows the growth rate for perturbation of Stokes wave.

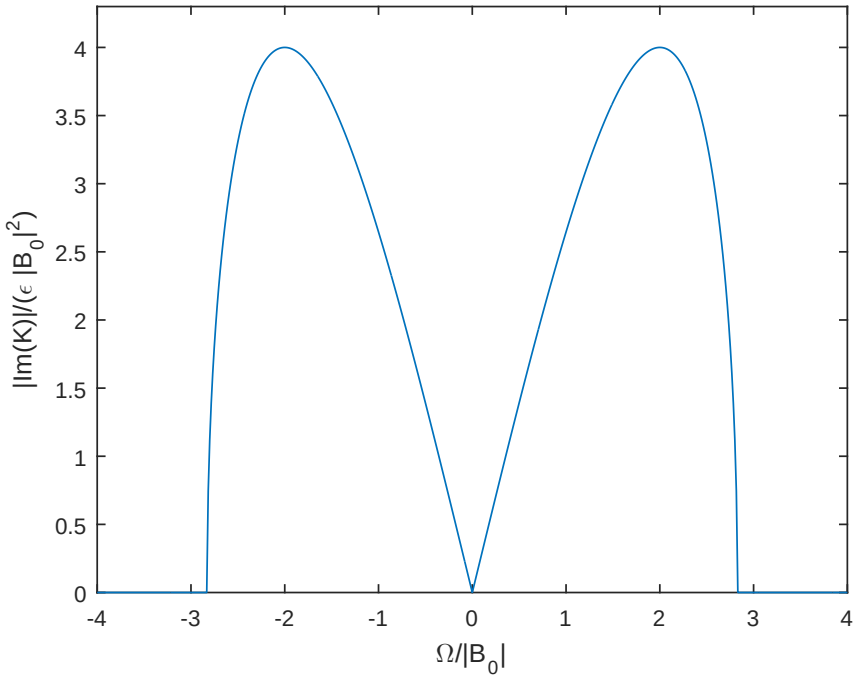

Figure 5.1: Growth rate for perturbation of Stokes wave for the space evolution equation in the deep-water limit.

5.1.2 Finite depth

By applying the uniform and finite depth assumptions, the space evolution equation can be expressed by

$$\begin{aligned}&\epsilon[i\frac{\partial\bar{\eta}_1}{\partial x_1}+\frac{i}{c_g}\frac{\partial\bar{\eta}_1}{\partial t_1}]+\epsilon^2[\lambda\frac{\partial^2\bar{\eta}_1}{\partial t_1^2}+(\nu+\theta_2(1-k^2)\\&+(\frac{\theta_1}{c_g}+\theta_2)\frac{[-\frac{2k}{c_g}+(1-k^2)]}{[-1+\frac{h}{c_g^2}]})\bar{\eta}_1\mid\bar{\eta}_1\mid^2]=0\qquad\text{at}\quad z=0\end{aligned}\tag{5.10}$$

We aim to find the uniform solution, by assuming that the solution $\bar{\eta}_1$ of the equation does not vary in time. This leads to the simplified equation

$$\begin{aligned}&\frac{\partial\bar{\eta}_1}{\partial x_1}-i\epsilon[\nu+\theta_2(1-k^2)\\&+(\frac{\theta_1}{c_g}+\theta_2)\frac{[-\frac{2k}{c_g}+(1-k^2)]}{[-1+\frac{h}{c_g^2}]}]\bar{\eta}_1\mid\bar{\eta}_1\mid^2=0\qquad\text{at}\quad z=0\end{aligned}\tag{5.11}$$

The exact uniform wave solution of this equation is given by the following equation known as the Stokes wave

$$\bar{\eta}_1=B_0e^{i\epsilon\{\nu+\theta_2(1-k^2)+(\frac{\theta_1}{c_g}+\theta_2)\frac{[-\frac{2k}{c_g}+1-k^2]}{[-1+\frac{h}{c_g^2}]}\}|B_0|^2x_1}\tag{5.12}$$

where B_0 is a constant.

In order to investigate the stability of the Stokes wave, it is perturbed in amplitude and phase. We suppose

$$\bar{\eta}_1=B_0(1+\alpha_1+i\beta_1)e^{i\epsilon\{\nu+\theta_2(1-k^2)+(\frac{\theta_1}{c_g}+\theta_2)\frac{[-\frac{2k}{c_g}+1-k^2]}{[-1+\frac{h}{c_g^2}]}\}|B_0|^2x_1}\tag{5.13}$$

where α_1 and β_1 are infinitesimal and real.

We aim to substitute the perturbed Stokes wave (5.13) in the equation (5.10). Therefore, following computations are carried out and after linearization with respect to α_1 and β_1, we obtain

$$\mid\bar{\eta}_1\mid^2=\mid B_0\mid^2(1+2\alpha_1)$$

$$\bar{\eta}_1\mid\bar{\eta}_1\mid^2=B_0\mid B_0\mid^2(1+3\alpha_1+i\beta_1)e^{i\epsilon\{\nu+\theta_2(1-k^2)+(\frac{\theta_1}{c_g}+\theta_2)\frac{[-\frac{2k}{c_g}+1-k^2]}{[-1+\frac{h}{c_g^2}]}\}|B_0|^2x_1}$$

$$\frac{\partial\bar{\eta}_1}{\partial x_1} = \{i\epsilon[\nu+\theta_2(1-k^2)+(\frac{\theta_1}{c_g}+\theta_2)\frac{[-\frac{2k}{c_g}+1-k^2]}{[-1+\frac{h}{c_g^2}]} \mid B_0 \mid^2 B_0(1+\alpha_1+i\beta_1) + B_0(\frac{\partial\alpha_1}{\partial x_1}+i\frac{\partial\beta_1}{\partial x_1})\}e^{i\epsilon\{\nu+\theta_2(1-k^2)+(\frac{\theta_1}{c_g}+\theta_2)\frac{[-\frac{2k}{c_g}+1-k^2]}{[-1+\frac{h}{c_g^2}]}\}|B_0|^2x_1}$$

$$\frac{\partial\bar{\eta}_1}{\partial t_1} = B_0(\frac{\partial\alpha_1}{\partial t_1}+i\frac{\partial\beta_1}{\partial t_1})e^{i\epsilon\{\nu+\theta_2(1-k^2)+(\frac{\theta_1}{c_g}+\theta_2)\frac{[-\frac{2k}{c_g}+1-k^2]}{[-1+\frac{h}{c_g^2}]}\}|B_0|^2x_1}$$

$$\frac{\partial^2\bar{\eta}_1}{\partial t_1^2} = B_0(\frac{\partial^2\alpha_1}{\partial t_1^2}+i\frac{\partial^2\beta_1}{\partial t_1^2})e^{i\epsilon\{\nu+\theta_2(1-k^2)+(\frac{\theta_1}{c_g}+\theta_2)\frac{[-\frac{2k}{c_g}+1-k^2]}{[-1+\frac{h}{c_g^2}]}\}|B_0|^2x_1}$$

Inserting into the equation (5.10) and simplifying, lead to the following equation

$$\begin{aligned} &i\epsilon\frac{\partial\alpha_1}{\partial x_1}-\epsilon\frac{\partial\beta_1}{\partial x_1}+\frac{i\epsilon}{c_g}\frac{\partial\alpha_1}{\partial t_1}-\frac{\epsilon}{c_g}\frac{\partial\beta_1}{\partial t_1}+\epsilon^2\lambda\frac{\partial^2\alpha_1}{\partial t_1^2}+i\epsilon^2\lambda\frac{\partial^2\beta_1}{\partial t_1^2} \\ &+2\epsilon^2[\nu+\theta_2(1-k^2)+(\frac{\theta_1}{c_g}+\theta_2)\frac{[-\frac{2k}{c_g}+1-k^2]}{[-1+\frac{h}{c_g^2}]} \mid B_0 \mid^2 \alpha_1 = 0 \end{aligned} \tag{5.14}$$

This equation is split up into real and imaginary parts, and following equations are achieved

$$\begin{aligned} &-\epsilon\frac{\partial\beta_1}{\partial x_1}-\frac{\epsilon}{c_g}\frac{\partial\beta_1}{\partial t_1}+\epsilon^2\lambda\frac{\partial^2\alpha_1}{\partial t_1^2}+2\epsilon^2[\nu+\theta_2(1-k^2) \\ &+(\frac{\theta_1}{c_g}+\theta_2)\frac{[-\frac{2k}{c_g}+1-k^2]}{[-1+\frac{h}{c_g^2}]} \mid B_0 \mid^2 \alpha_1 = 0 \end{aligned} \tag{5.15}$$

$$\epsilon\frac{\partial\alpha_1}{\partial x_1}+\frac{\epsilon}{c_g}\frac{\partial\alpha_1}{\partial t_1}+\epsilon^2\lambda\frac{\partial^2\beta_1}{\partial t_1^2} = 0 \tag{5.16}$$

The perturbations α_1 and β_1 are supposed to take the following form

$$\begin{pmatrix}\alpha_1\\ \beta_1\end{pmatrix} = \begin{pmatrix}\hat{\alpha}_1\\ \hat{\beta}_1\end{pmatrix}e^{i(Kx_1-\Omega t_1)}+c.c.$$

By inserting into equations for real and imaginary parts, we get the following pair of

equations

$$\{-\epsilon^2\lambda\Omega^2 + 2\epsilon^2[\nu + \theta_2(1-k^2) + (\frac{\theta_1}{c_g} + \theta_2)\frac{[-\frac{2k}{c_g} + 1 - k^2]}{[-1 + \frac{h}{c_g^2}]} \mid B_0 \mid^2\}\hat{\alpha}_1 + \{-i\epsilon(K - \frac{\Omega}{c_g})\}\hat{\beta}_1 = 0 \tag{5.17}$$

$$\{i\epsilon(K - \frac{\Omega}{c_g})\}\hat{\alpha}_1 - \{\epsilon^2\lambda\Omega^2\}\hat{\beta}_1 = 0 \tag{5.18}$$

These equations can be represented in the matrix form

$$\begin{pmatrix} -\epsilon^2\lambda\Omega^2 + 2\epsilon^2\Theta|B_0|^2 & -i\epsilon(K - \frac{\Omega}{c_g}) \\ i\epsilon(K - \frac{\Omega}{c_g}) & -\epsilon^2\lambda\Omega^2 \end{pmatrix} \begin{pmatrix} \hat{\alpha}_1 \\ \hat{\beta}_1 \end{pmatrix} = \begin{pmatrix} 0 \\ 0 \end{pmatrix}$$

where

$$\Theta = \nu + \theta_2(1-k^2) + (\frac{\theta_1}{c_g} + \theta_2)\frac{[-\frac{2k}{c_g} + 1 - k^2]}{[-1 + \frac{h}{c_g^2}]}$$

By substituting ν, θ_1 and θ_2, we obtain

$$\Theta = -\frac{k^2}{4c_g}[9k^4 - 10k^2 + 9] + \frac{1}{2c_g(h - c_g^2)}[h - 2kd + k^3d + 4k^2 - 4kc_g + 4k^3c_g] \tag{5.19}$$

where $d = kh$.

The determinant of the coefficient matrix has to be zero due to the condition for a non-trivial solution for this system. This leads to the following dispersion relation

$$K = \frac{\Omega}{c_g} \pm \sqrt{\epsilon^2\Omega^2(\lambda^2\Omega^2 - 2\lambda\Theta \mid B_0 \mid^2)} \tag{5.20}$$

If the modulational wavenumber K has a nonzero imaginary part, the perturbation is unstable. Hence, the unstable region can be expressed as

$$\mid \Omega \mid < \sqrt{\frac{2\Theta}{\lambda}} \mid B_0 \mid \tag{5.21}$$

where

$$\lambda = \frac{-1}{8k^2c_g^3}[-3h^2 + 2h + 1 + d(-2k) + d^2(k^2 + 2)]$$

$$\Theta = -\frac{k^2}{4c_g}[9k^4 - 10k^2 + 9] + \frac{1}{2c_g(h - c_g^2)}[h - 2kd + k^3d + 4k^2 - 4kc_g + 4k^3c_g]$$

We can simply verify that λ takes always negative sign, whereas Θ changes its sign from negative to positive across $kh \approx 1.363$ as kh decreases, and this behavior is demonstrated by the figure 5.2. This means that our solution is stable to relatively small disturbances only if $\frac{\Theta}{\lambda} > 0$ which leads to $kh < 1.363$.

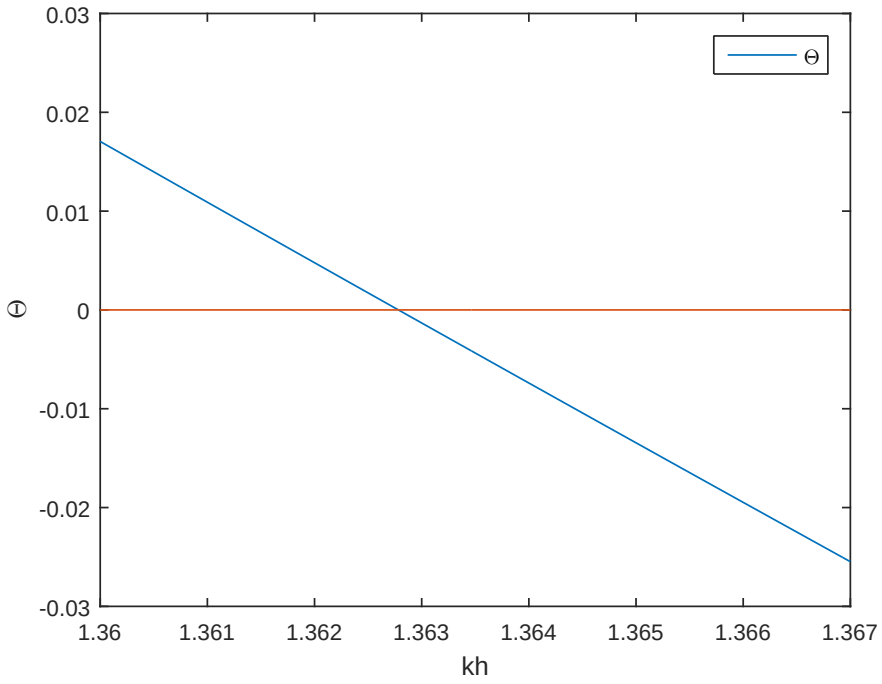

Figure 5.2: Behavior of Θ as a function of dimensionless depth kh.

We find also the initial growth rate of the perturbation in the form

$$\mid Im(K) \mid = \sqrt{\epsilon^2\Omega^2(2\lambda\Theta \mid B_0 \mid^2 - \lambda^2\Omega^2)} \tag{5.22}$$

The behavior of the growth rate demonstrated in figure 5.3 is completely in agreement with our expectation that for $kh < 1.363$ we do not have instability.

By supposing that the depth becomes infinitely large, $h \to \infty$, we obtain

$$c_g \to \frac{1}{2}$$

$$\lambda \to -1$$

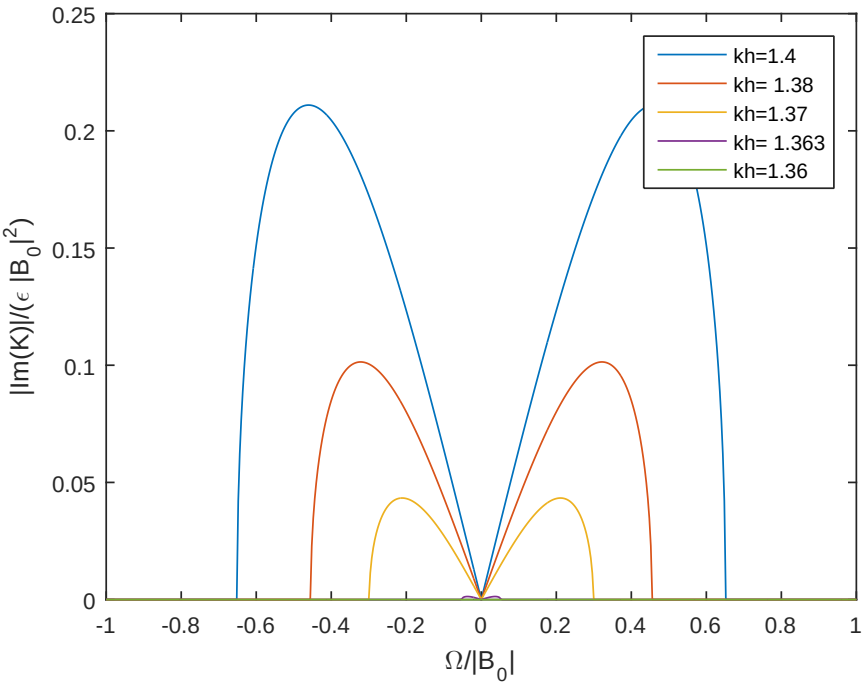

Figure 5.3: Growth rate for perturbation of Stokes wave for the space evolution equation in the limit of uniform and finite depth by assuming different magnitudes of kh.

$$\Theta \to -4$$

By inserting into (5.21) and (5.22), the unstable region and the growth rate can be expressed by

$$\mid \Omega \mid < 2\sqrt{2} \mid B_0 \mid \tag{5.23}$$

$$\mid Im(K) \mid = \sqrt{\epsilon^2\Omega^2(8 \mid B_0 \mid^2 - \Omega^2)} \tag{5.24}$$

These results are in good agreement with the results achieved for deep-water limit presented in the previous section. This shows that the limit of the finite-depth results when the depth becomes infinitely large are in fact equal to the deep-water results.

5.2 Time evolution equations

5.2.1 Deep water

The time evolution equation in the deep-water limit is

$$\frac{\partial \bar{\eta}_1}{\partial t_1} + \frac{1}{2}\frac{\partial \bar{\eta}_1}{\partial x_1} + i\epsilon[\frac{1}{8}\frac{\partial^2 \bar{\eta}_1}{\partial x_1^2} + 2\bar{\eta}_1 \mid \bar{\eta}_1 \mid^2] = 0 \tag{5.25}$$

An equilibrium solution can be found, by assuming that the solution $\bar{\eta}_0$ does not vary in space. This leads to the equation

$$\frac{\partial \bar{\eta}_1}{\partial t_1} + 2i\epsilon\bar{\eta}_1 \mid \bar{\eta}_1 \mid^2 = 0$$

A solution of the following form which is known as the Stokes wave, is assumed

$$\bar{\eta}_1 = B_0 e^{-2i\epsilon|B_0|^2 t_1}$$

where B_0 is a constant.

Our goal is to consider the modulational instability of the Stokes wave in the horizontal coordinate x_1. Therefore, the stability of the Stokes wave is investigated by assuming small perturbations of the form

$$\bar{\eta}_1 = B_0(1 + \alpha_1 + i\beta_1)e^{-2i\epsilon|B_0|^2 t_1}$$

where α_1 and β_1 are infinitesimal and real.

We now insert the perturbed equilibrium solution into the simplified nonlinear Schrödinger equation (5.25), and linearize with respect to α_1 and β_1. We obtain

$$\frac{\partial \alpha_1}{\partial t_1} + i\frac{\partial \beta_1}{\partial t_1} + \frac{1}{2}\frac{\partial \alpha_1}{\partial x_1} + \frac{i}{2}\frac{\partial \beta_1}{\partial x_1} + \frac{i\epsilon}{8}\frac{\partial^2 \alpha_1}{\partial x_1^2} - \frac{\epsilon}{8}\frac{\partial^2 \beta_1}{\partial x_1^2} + 4i\epsilon \mid B_0 \mid^2 \alpha_1 = 0$$

Splitting up this equation into real and imaginary parts gives us following pair of equations

$$\frac{\partial \alpha_1}{\partial t_1} + \frac{1}{2}\frac{\partial \alpha_1}{\partial x_1} - \frac{\epsilon}{8}\frac{\partial^2 \beta_1}{\partial x_1^2} = 0 \tag{5.26}$$

$$\frac{\partial \beta_1}{\partial t_1} + \frac{1}{2}\frac{\partial \beta_1}{\partial x_1} + \frac{\epsilon}{8}\frac{\partial^2 \alpha_1}{\partial x_1^2} + 4\epsilon \mid B_0 \mid^2 \alpha_1 = 0 \tag{5.27}$$

We assume plane-wave solutions for α_1 and β_1 in the following forms

$$\begin{pmatrix} \alpha_1 \\ \beta_1 \end{pmatrix} = \begin{pmatrix} \hat{\alpha}_1 \\ \hat{\beta}_1 \end{pmatrix} e^{i(Kx_1 - \Omega t_1)} + c.c.$$

Inserting into equations for real and imaginary parts gives a set of two linear equations

$$-i\Omega\hat{\alpha}_1 + \frac{iK}{2}\hat{\alpha}_1 + \frac{\epsilon K^2}{8}\hat{\beta}_1 = 0 \tag{5.28}$$

$$-i\Omega\hat{\beta}_1 + \frac{iK}{2}\hat{\beta}_1 - \frac{\epsilon K^2}{8}\hat{\alpha}_1 + 4\epsilon \mid B_0 \mid^2 \hat{\alpha}_1 = 0 \tag{5.29}$$

Matrix form of these equations can be expressed by

$$\begin{pmatrix} -i(\Omega - \frac{K}{2}) & \frac{\epsilon K^2}{8} \\ -\frac{\epsilon K^2}{8} + 4\epsilon \mid B_0 \mid^2 & -i(\Omega - \frac{K}{2}) \end{pmatrix} \begin{pmatrix} \hat{\alpha}_1 \\ \hat{\beta}_1 \end{pmatrix} = \begin{pmatrix} 0 \\ 0 \end{pmatrix}.$$

In order to get a nontrivial solution of this system, the determinant of the coefficient matrix has to be zero. This condition leads to the dispersion relation

$$\Omega = \frac{K}{2} \pm \sqrt{\frac{\epsilon^2 K^2}{8}(\frac{K^2}{8} - 4 \mid B_0 \mid^2)}. \tag{5.30}$$

If the perturbation frequency Ω has a nonzero imaginary part, the perturbations α_1 and β_1 will grow unboundedly. Therefore, the system is unstable if

$$\mid K \mid < 4\sqrt{2} \mid B_0 \mid \tag{5.31}$$

Moreover, the growth rate of the perturbations is in the form

$$\mid Im(\Omega) \mid = \sqrt{\frac{\epsilon^2 K^2}{8}(4 \mid B_0 \mid^2 - \frac{K^2}{8})} \tag{5.32}$$

This result is in good agreement with the study by Trulsen (2006). The growth rate for perturbation of Stokes wave is plotted in figure 5.4.

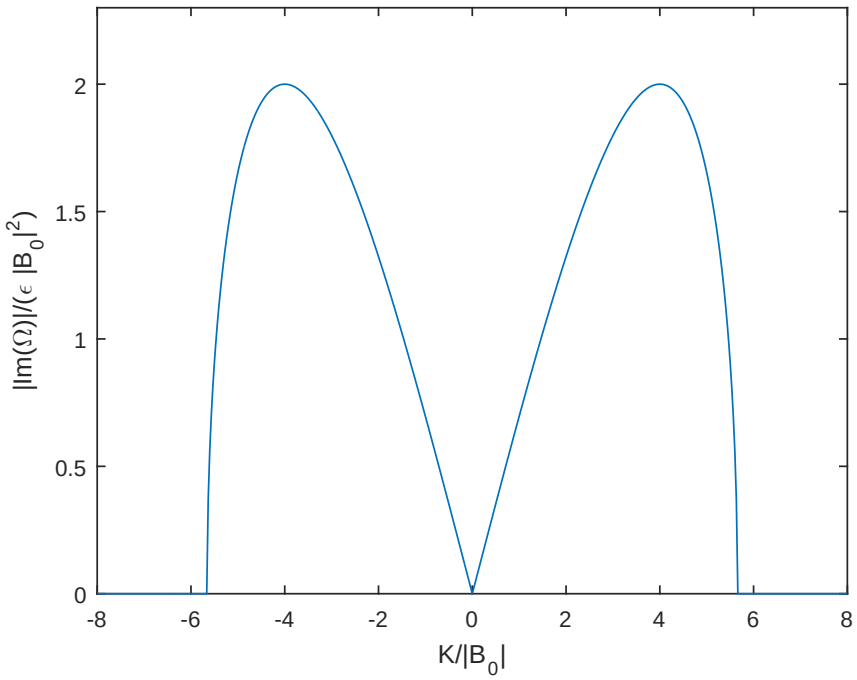

Figure 5.4: Growth rate for perturbation of Stokes wave for the time evolution equation in the deep-water limit.

5.2.2 Finite depth

The nonlinear Schrödinger equation which describes the time evolution for finite depth and flat bottom is

$$\begin{aligned}&\epsilon[i\frac{\partial\bar{\eta}_1}{\partial t_1}+ic_g\frac{\partial\bar{\eta}_1}{\partial x_1}]+\epsilon^2[\Lambda\frac{\partial^2\bar{\eta}_1}{\partial x_1^2}+(\vartheta+\theta_4(1-k^2)\\&+(\theta_3+c_g\theta_4)\frac{[c_g(1-k^2)-2k]}{[h-c_g^2]})\bar{\eta}_1\mid\bar{\eta}_1\mid^2]=0\qquad\text{at}\quad z_1=0\end{aligned}\tag{5.33}$$

We are interested in a uniform solution of this equation, by assuming that the solution $\bar{\eta}_1$ is independent of space. This suggests

$$\begin{aligned}&\frac{\partial\bar{\eta}_1}{\partial t_1}-i\epsilon[\vartheta+\theta_4(1-k^2)\\&+(\theta_3+c_g\theta_4)\frac{[c_g(1-k^2)-2k]}{[h-c_g^2]}]\bar{\eta}_1\mid\bar{\eta}_1\mid^2=0\qquad\text{at}\quad z_1=0\end{aligned}$$

A uniform Stokes wave solution of this equation is given by

$$\bar{\eta}_1=B_0e^{i\epsilon\{\vartheta+\theta_4(1-k^2)+(\theta_3+c_g\theta_4)\frac{[c_g(1-k^2)-2k]}{[h-c_g^2]}\}|B_0|^2t_1}\tag{5.34}$$

where B_0 is a constant.

The stability of Stokes wave is investigated by perturbing it in amplitude and phase. We set

$$\bar{\eta}_1=B_0(1+\alpha_1+i\beta_1)e^{i\epsilon\{\vartheta+\theta_4(1-k^2)+(\theta_3+c_g\theta_4)\frac{[c_g(1-k^2)-2k]}{[h-c_g^2]}\}|B_0|^2t_1}\tag{5.35}$$

where α_1 and β_1 are infinitesimal and real.

Since we purpose to insert this solution into the equation (5.33), following computations are performed and after linearizing with respect to α_1 and β_1, we achieve

$$\mid\bar{\eta}_1\mid^2=\mid B_0\mid^2(1+2\alpha_1)$$

$$\bar{\eta}_1\mid\bar{\eta}_1\mid^2=B_0\mid B_0\mid^2(1+3\alpha_1+i\beta_1)e^{i\epsilon\{\vartheta+\theta_4(1-k^2)+(\theta_3+c_g\theta_4)\frac{[c_g(1-k^2)-2k]}{[h-c_g^2]}\}|B_0|^2t_1}$$

$$\begin{aligned}\frac{\partial\bar{\eta}_1}{\partial t_1}&=\{i\epsilon\{\vartheta+\theta_4(1-k^2)+(\theta_3+c_g\theta_4)\frac{[c_g(1-k^2)-2k]}{[h-c_g^2]}\}\mid B_0\mid^2B_0(1+\alpha_1+i\beta_1)\\&+B_0(\frac{\partial\alpha_1}{\partial t_1}+i\frac{\partial\beta_1}{\partial t_1})\}e^{i\epsilon\{\vartheta+\theta_4(1-k^2)+(\theta_3+c_g\theta_4)\frac{[c_g(1-k^2)-2k]}{[h-c_g^2]}\}|B_0|^2t_1}\end{aligned}$$

$$\frac{\partial \bar{\eta}_1}{\partial x_1} = B_0(\frac{\partial \alpha_1}{\partial x_1} + i\frac{\partial \beta_1}{\partial x_1})e^{i\epsilon\{\vartheta+\theta_4(1-k^2)+(\theta_3+c_g\theta_4)\frac{[c_g(1-k^2)-2k]}{[h-c_g^2]}\}|B_0|^2 t_1}$$

$$\frac{\partial^2 \bar{\eta}_1}{\partial x_1^2} = B_0(\frac{\partial^2 \alpha_1}{\partial x_1^2} + i\frac{\partial^2 \beta_1}{\partial x_1^2})e^{i\epsilon\{\vartheta+\theta_4(1-k^2)+(\theta_3+c_g\theta_4)\frac{[c_g(1-k^2)-2k]}{[h-c_g^2]}\}|B_0|^2 t_1}$$

The perturbed uniform solution (5.35) is inserted into the time evolution equation (5.33) and after some simplification, we obtain

$$\begin{aligned} &i\epsilon\frac{\partial \alpha_1}{\partial t_1} - \epsilon\frac{\partial \beta_1}{\partial t_1} + i\epsilon c_g\frac{\partial \alpha_1}{\partial x_1} - \epsilon c_g\frac{\partial \beta_1}{\partial x_1} + \epsilon^2\Lambda\frac{\partial^2 \alpha_1}{\partial x_1^2} + i\epsilon^2\Lambda\frac{\partial^2 \beta_1}{\partial x_1^2} \\ &+ 2\epsilon^2[\vartheta + \theta_4(1-k^2) + (\theta_3 + c_g\theta_4)\frac{[c_g(1-k^2)-2k]}{[h-c_g^2]}] \mid B_0 \mid^2 \alpha_1 = 0 \end{aligned} \tag{5.36}$$

Splitting up this equation into real and imaginary parts yields

$$\begin{aligned} &-\epsilon\frac{\partial \beta_1}{\partial t_1} - \epsilon c_g\frac{\partial \beta_1}{\partial x_1} + \epsilon^2\Lambda\frac{\partial^2 \alpha_1}{\partial x_1^2} + 2\epsilon^2[\vartheta + \theta_4(1-k^2) \\ &+ (\theta_3 + c_g\theta_4)\frac{[c_g(1-k^2)-2k]}{[h-c_g^2]}] \mid B_0 \mid^2 \alpha_1 = 0 \end{aligned} \tag{5.37}$$

$$\epsilon\frac{\partial \alpha_1}{\partial t_1} + \epsilon c_g\frac{\partial \alpha_1}{\partial x_1} + \epsilon^2\Lambda\frac{\partial^2 \beta_1}{\partial x_1^2} = 0 \tag{5.38}$$

Finally we assume that the perturbations α_1 and β_1 take the following form

$$\begin{pmatrix} \alpha_1 \\ \beta_1 \end{pmatrix} = \begin{pmatrix} \hat{\alpha}_1 \\ \hat{\beta}_1 \end{pmatrix} e^{i(Kx_1 - \Omega t_1)} + c.c.$$

Inserting into real and imaginary parts gives following system of equations

$$\begin{aligned} &\{-\epsilon^2\Lambda K^2 + 2\epsilon^2[\vartheta + \theta_4(1-k^2) + (\theta_3 + c_g\theta_4)\frac{[c_g(1-k^2)-2k]}{[h-c_g^2]}] \mid B_0 \mid^2\}\hat{\alpha}_1 \\ &+ \{i\epsilon(\Omega - c_g K)\}\hat{\beta}_1 = 0 \end{aligned} \tag{5.39}$$

$$\{-i\epsilon(\Omega - c_g K)\}\hat{\alpha}_1 - \{\epsilon^2\Lambda K^2\}\hat{\beta}_1 = 0 \tag{5.40}$$

Matrix form of this system is given by

$$\begin{pmatrix} -\epsilon^2\Lambda K^2+2\epsilon^2\varphi|B_0|^2 & i\epsilon(\Omega-c_gK) \\ -i\epsilon(\Omega-c_gK) & -\epsilon^2\Lambda K^2 \end{pmatrix} \begin{pmatrix} \hat{\alpha}_1 \\ \hat{\beta}_1 \end{pmatrix} = \begin{pmatrix} 0 \\ 0 \end{pmatrix}$$

where

$$\varphi = \vartheta + \theta_4(1-k^2) + (\theta_3 + c_g\theta_4)\frac{[c_g(1-k^2)-2k]}{[h-c_g^2]}$$

By substituting ϑ, θ_3 and θ_4, we get

$$\varphi = -\frac{k^2}{4}[9k^4 - 10k^2 + 9] + \frac{1}{2(h-c_g^2)}[h - 2kd + k^3d + 4k^2 - 4kc_g + 4k^3c_g] \tag{5.41}$$

where $d = kh$.

We are looking for a nontrivial solution for this system, and this forced us to consider the determinant of the coefficient matrix equals to zero. Hence, we achieve the following dispersion relation

$$\Omega = c_gK \pm \sqrt{\epsilon^2K^2(\Lambda^2K^2 - 2\Lambda\varphi \mid B_0 \mid^2)} \tag{5.42}$$

The unstable region is found by considering that the perturbation frequency Ω has a nonzero imaginary part

$$\mid K \mid < \sqrt{\frac{2\varphi}{\Lambda}} \mid B_0 \mid \tag{5.43}$$

where

$$\Lambda = \frac{-1}{8k^2}[-3h^2 + 2h + 1 + d(-2k) + d^2(k^2+2)]$$

$$\varphi = -\frac{k^2}{4}[9k^4 - 10k^2 + 9] + \frac{1}{2(h-c_g^2)}[h - 2kd + k^3d + 4k^2 - 4kc_g + 4k^3c_g]$$

As is seen, Λ is always negative, whereas the sign of φ changes from negative to positive across $kh \approx 1.363$ as kh decrease, and this feature is described by figure 5.5. This result is in agreement with the result reported by Hasimoto and Ono (1972) and $-\varphi$ is identical with $X(k)$ represented by equation (30) in Benjamin's paper (Benjamin, 1967).

The initial growth rate is also found

$$\mid Im(\Omega) \mid = \sqrt{\epsilon^2K^2(2\Lambda\varphi \mid B_0 \mid^2 - \Lambda^2K^2)} \tag{5.44}$$

In figure 5.6, it is shown that wave trains on water of uniform depth h are unstable if the

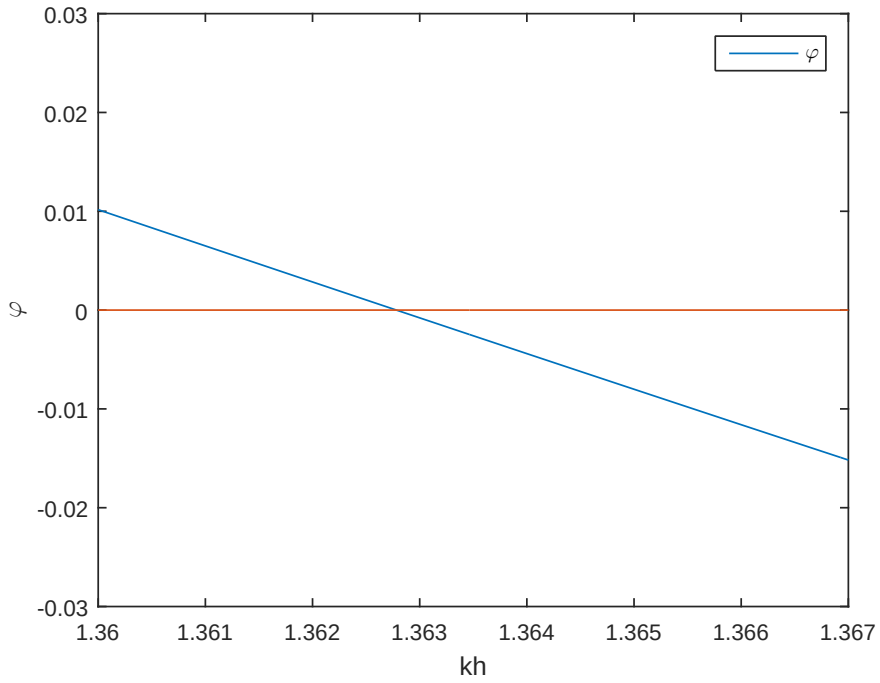

Figure 5.5: Behavior of φ with respect to dimensionless depth kh.

wavenumber k satisfies $kh > 1.363$, but they are otherwise stable. This stability criterion is identical with that derived by Benjamin (1967).

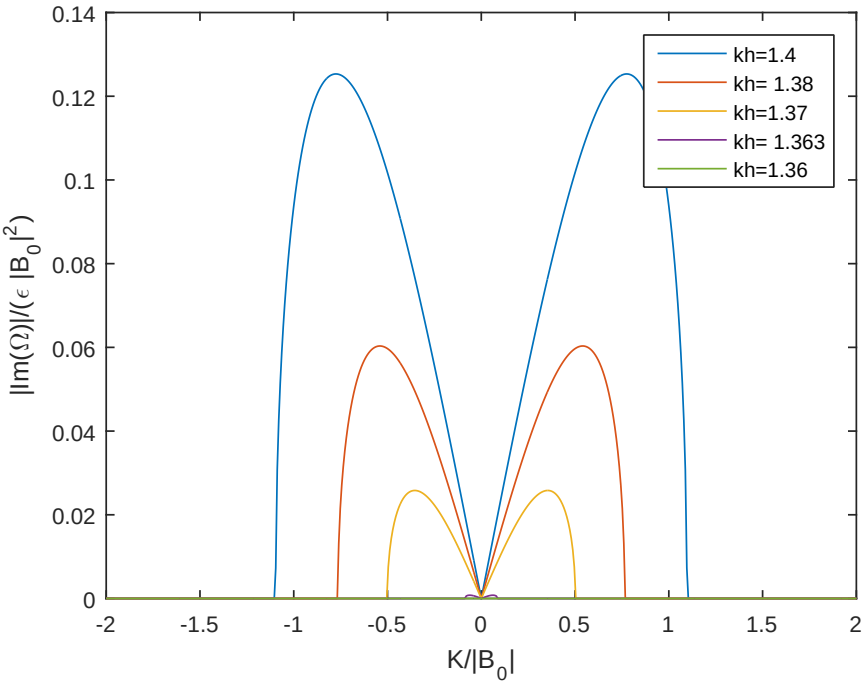

Figure 5.6: Growth rate for perturbation of Stokes wave for the time evolution equation in the limit of uniform and finite depth by assuming different magnitudes of kh.

Let us to allow that the depth h becomes infinitely large, we get

$$c_g \to \frac{1}{2}$$

$$\varphi \to -2$$

$$\Lambda \to -\frac{1}{8}$$

substituting in (5.43) and (5.44), the unstable region and the growth rate are expressed as

$$\mid K \mid < 4\sqrt{2} \mid B_0 \mid \tag{5.45}$$

$$\mid Im(\Omega) \mid = \sqrt{\frac{\epsilon^2 K^2}{8}(4 \mid B_0 \mid^2 - \frac{K^2}{8})} \tag{5.46}$$

These results are consistent with the results reported for deep-water limit in the previous section. This demonstrates that when the depth becomes infinitely large, the limit of the finite-depth results for the time evolution equation reproduce the deep-water results.

Chapter 6

Discussion and further work

In this chapter the results presented in chapters 3, 4 and 5 are discussed. First, we present a discussion how the space and time evolution equations derived in this thesis are connected with previous experimental and theoretical works and whether these can be compared. Furthermore, the results for modulational instability of Stokes wave presented in the previous chapter are discussed. The final section is dedicated to some future works that will be a continuation of the work and the results of this thesis.

6.1 Modified nonlinear Schrödinger equation discussed with previous studies

In this thesis, we aim to improve previous NLS equations for nonuniform depth in order to better represent abrupt bathymetry of arbitrary depth. As we know the nonlinear Schrödinger equation with variable coefficients and a shoaling term for slowly varying depth is the first and simplest model for water of finite depth derived by Djordjević and Redekopp (1978). By slowly varying depth they meant that the depth varied with the slope bottom of order ϵ^2 which simply suggested $\frac{\partial h}{\partial x} = O(\epsilon^2)$. The NLS equation derived in their study was in the form of space evolution in terms of velocity potential, and the method of derivation used by them was the multiple scale method. In the derivation process the induced mean flow $\bar{\phi}_0$ and the set-down $\bar{\eta}_0$ were expanded in the power series of ϵ. By employing these expansions they limited their model small depth bounded from above and $kh = O(1)$, and this restricted assumption caused that their result can not be reliable for greater depth. In fact their model is appropriate to describe the behavior of the waves propagate over a nonuniform bathymetry with a bottom variation of order ϵ^2 for shallow water. Our assumption regarding the bottom variation is $\frac{\partial h}{\partial x} = O(\epsilon)$, and this distinguishes our study from the study by Djordjević and Redekopp (1978). Furthermore, since we do not employ any special expansions for $\bar{\phi}_0$ and $\bar{\eta}_0$, we do not restrict our model to small depth assumption, and our equations can be used as a model for arbitrary depth. In addition, in our work both space and time evolution equations are presented in terms of the surface elevation instead of the velocity potential, and this choice is more attractive

for practical applications. Despite of these differences, some of the coefficients such as μ and λ represented by the equations (3.81) and (3.82) in our study, are essentially identical to μ and λ defined by the equations (2.15) and (2.16) in the paper by Djordjević and Redekopp (1978).

In the study by Liu and Dingemans (1989), a third-order evolution equation for the envelope of a modulated wave train propagating over an uneven bottom and the associated long-wave equation were derived by assuming bottom variation of order ϵ so that $\frac{\partial h}{\partial x} = O(\epsilon)$. The bottom topography consisted of two components h_0 and h_1, and they assumed that h_0 varied on the scale of ϵ so that $h_0 = h_0(\epsilon x)$, whereas h_1 was assumed to be small, $O(kh_1) = O(\epsilon^2)$, depended on actual horizontal coordinate x. These assumptions suggested to present depth by $h = h_0(x_1) + \epsilon h_1(x_1)$ where $x_1 = \epsilon x$. The bottom topography we describe in this thesis is different from their bathymetry since we assume h_1 is zero for our case consistent with the experiment of Raustøl (2014). They got a contribution of h_1 in their NLS equation as shoaling terms, whereas these terms do not appear in our NLS equation. On the other hand by expanding the velocity potential and the free surface displacement in terms of the small parameter ϵ and applying the same expansions for the induced mean flow $\bar{\phi}_0$ and the set-down $\bar{\eta}_0$, it seems their model is also restricted to shallow water assumption, $kh = O(1)$, and it is valid when maximum depth is sufficiently small. Whereas, we present a model which can be applied for both finite and infinite depth. We also mention that they derived a space evolution equation in terms of velocity potential, and this representation of the NLS equation can be useful for analytical consideration, while our representation of the NLS equation is in terms of the surface elevation, more convenient for most practical applications.

The nonlinear Schrödinger equation with variable coefficients by Zeng and Trulsen (2012) as a model to describe waves passing over uneven bottom, is simpler than the NLS equation derived in this study. They assumed that the depth h was slowly varying, $\frac{\partial h}{\partial x} = O(\epsilon^2)$, and this led to only one shoaling term for uneven bottom in their NLS equation. Moreover, the same method of derivation as used by Djordjević and Redekopp (1978) and Liu and Dingemans (1989) was employed in their investigation, which means that their model is of limited validity because they have made such restricting assumption of limiting the depth from above. Although, there are differences between their research and our study, two of the coefficients that appear in the space evolution equation (3.80) are identical to the coefficients reported by Zeng and Trulsen (2012). Theses coefficients are μ and λ represented by (3.81) and (3.82), respectively, identical to the coefficients μ and λ reported by equations (11) and (12) in the study of Zeng and Trulsen (2012).

With this review of previous mathematical models, it seems that none of them are appropriate for describing the experimental observations by Raustøl (2014), since all of these models assumed slower variation of the bottom topography than that one used by Raustøl (2014), or they limited their model to shallow water. The NLS equation derived in this study is more general since it can be used for arbitrary depth which covers both finite and infinite depth. Moreover, our mathematical model seems to be more appropriate for the previous experimental studies reported in table 1.1, and more attractive for practical applications.

6.2 Stability analysis discussion

In this study, a stability analysis is performed for the case of gravity waves on water of both infinite and finite depth. As one of the dramatic discoveries in fluid mechanics, modulational instability of such wave trains has been proved theoretically by Whitham (1974) and Benjamin (1967). Analysis in study by Benjamin (1967) demonstrated that according as water deeper or shallower than the critical depth $kh \gtrless 1.363$, a uniform wave train is modulationally unstable or stable for infinitesimal two dimensional perturbations. The critical depth $kh \approx 1.363$ is a limiting depth for a uniform long-crested wave being stable or unstable to long-crested perturbations. A stability analysis presented by Benney and Roskes (1969) has been performed for the three dimensional case of gravity waves. It is shown that there are unstable short-crested or skewed perturbations on both sides of the limiting value $kh \approx 1.363$. By considering a two dimensional disturbance as a special case, they could reproduce the criteria reported by Benjamin (1967). These studies have been performed without using this fact that the evolution of such waves is governed by a simple equation of the form NLS equation. This fact has been used for the first time by Hasimoto and Ono (1972) by reducing the complicated system of two dimensional equations used by Benjamin (1967) to a simple NLS equation. They adopted the method of multiple scale for the equations which described gravity waves on the water layer with uniform depth, and derived the NLS equation in the form of time evolution equation in terms of velocity potential. In their research the important results by Whitham (1974) and Benjamin (1967) were reproduced by considering the remarkable fact that the solution of NLS equation corresponds to the Stokes wave. In the study of Davey and Stewartson (1974), a modulational instability investigation was carried out by employing NLS equation which described the evolution of a three dimensional wave-packet on water of finite depth. They made use of the method of multiple scales and derived time evolution equations in terms of velocity potential.

In chapter 5 of this thesis, the stability of a uniform wave train is investigated for a uniform depth by applying time and space evolution equations derived in chapter 4. By employing the NLS equation in the form of time evolution in the limit of finite depth, we obtain that the Stokes wave is stable to relatively small two dimensional disturbances only if $kh < 1.363$, and unstable if $kh > 1.363$. This result demonstrates a good agreement with previous studies of Benjamin (1967) and Hasimoto and Ono (1972). It seems that all the previous analyses have been performed for the NLS equation in the form of time evolution. In this study we employ the space evolution equation for the stability analysis of Stokes wave. Stability analysis for space evolution equation is carried out for both deep-water limit and finite depth. We conclude that the Stokes wave as the uniform solution of the space evolution equation in the limit of finite depth is unstable if $kh > 1.363$, and it is stable in water shallower than the critical depth $kh < 1.363$. This result is in excellent agreement with earlier studies which applied time evolution equations. Furthermore, the surprising fact brought to light was that by applying sufficiently deep water assumption on results for finite depth in both temporal and spatial models, the achieved results for deep water are reproduced for both cases.

6.3 Further work

As the next phase, one can pick up temporal and/or spatial model(s) derived in this thesis to carry out the numerical study in order to investigate if our model allows to account for previous experimental observations by (Raustøl, 2014).

Chapter 7

Conclusion

This work presents a theoretical study to develop a model to describe wave dynamics propagating over arbitrary nonuniform depth. By assuming bottom variation of order ϵ, we derive a nonlinear Schrödinger equation enhanced with shoaling terms and depth-dependent coefficients. The temporal and spatial models are described, and in both models the NLS equation is coupled with the equations for the induced mean flow and the set-down. The analytical solutions of integral forms are also presented for the induced mean flow and the set-down in the case of flat bottom. The NLS equation derived in this study is general since it can be applied for arbitrary depth which covers both finite and infinite depth. Furthermore, we employ the time and space evolution equations in the limit of deep water and finite and uniform depth to perform the stability analysis of uniform wave trains. In the finite depth assumption for both time and space evolution equations, it is found that a uniform wave train is modulationally unstable in water deeper than the critical depth $kh > 1.363$, while it becomes stable in water shallower than the critical depth $kh < 1.363$. Moreover, it is concluded that the limit of the finite-depth results when the depth becomes infinitely large, are in fact equal to the deep-water results for stability analysis.

Bibliography

Benjamin, T. B. (1967). Instability of periodic wavetrains in nonlinear dispersive systems. *Proc. Roy. Soc. Lond. A.*, 299:59–76.

Benney, D. J. and Roskes, G. J. (1969). Wave instabilities. *Studies in Applied Mathematics*, 48(4):377–385.

Bunnik, T. (2010). Benchmark workshop on numerical wave modeling–description of test cases. Technical report, Technical Report 700221RD, MARIN, The Netherlands, Wageningen, The Netherlands.

Davey, A. and Stewartson, K. (1974). On three-dimensional packets of surface waves. In *Proceedings of the Royal Society of London A: Mathematical, Physical and Engineering Sciences*, volume 338, pages 101–110. The Royal Society.

Djordjević, V. D. and Redekopp, L. G. (1978). On the development of packets of surface gravity waves moving over an uneven bottom. *Zeitschrift für angewandte Mathematik und Physik ZAMP*, 29(6):950–962.

Dysthe, K., Krogstad, H. E., and Müller, P. (2008). Oceanic rogue waves. *Annu. Rev. Fluid Mech.*, 40:287–310.

Gramstad, O. and Trulsen, K. (2011). Hamiltonian form of the modified nonlinear Schrödinger equation for gravity waves on arbitrary depth. *Journal of Fluid Mechanics*, 670:404–426.

Gramstad, O., Zeng, H., Trulsen, K., and Pedersen, G. K. (2013). Freak waves in weakly nonlinear unidirectional wave trains over a sloping bottom in shallow water. *Physics of Fluids*, 25(12):122103.

Hasimoto, H. and Ono, H. (1972). Nonlinear modulation of gravity waves. *Journal of the Physical Society of Japan*, 33(3):805–811.

Iusim, R. and Stiassnie, M. (1985). Shoaling of nonlinear wave-groups on water of slowly varying depth. *Zeitschrift für angewandte Mathematik und Physik ZAMP*, 36(5):680–698.

Kashima, H., Hirayama, K., and Mori, N. (2013). Numerical study of aftereffects of offshore generated freak waves shoaling to coast. In *7th International Conference on Coastal Dynamics*.

Kashima, H., Hirayama, K., and Mori, N. (2014). Estimation of freak wave occurrence from deep to shallow water regions. *Coastal Engineering Proceedings*, 1(34):36.

Kharif, C., Pelinovsky, E., and Slunyaev, A. (2009). *Rogue Waves in the Ocean. Advances in Geophysical and Environmental Mechanics and Mathematics*. Springer, Berlin.

Kundu, S., Debsarma, S., and Das, K. P. (2013). Modulational instability in crossing sea states over finite depth water. *Physics of Fluids*, 25(6):066605.

Lamb, H. (1932). *Hydrodynamics*. Cambridge university press.

Liu, P. L. F. and Dingemans, M. W. (1989). Derivation of the third-order evolution equations for weakly nonlinear water waves propagating over uneven bottoms. *Wave Motion*, 11(1):41–64.

Lyche, T. (2014). *Lecture Notes for MAT-INF 4130*. Department of Mathematics, University of Oslo.

Ma, Y., Dong, G., and Ma, X. (2014). Experimental study of statistics of random waves propagating over a bar. *Coastal Engineering Proceedings*, 1(34):30.

Madsen, P. A., Bingham, H. B., and Liu, H. (2002). A new Boussinesq method for fully nonlinear waves from shallow to deep water. *Journal of Fluid Mechanics*, 462:1–30.

Mori, N. and Janssen, P. A. E. M. (2006). On kurtosis and occurrence probability of freak waves. *Journal of Physical Oceanography*, 36(7):1471–1483.

Raustøl, A. (2014). Freake bølger over variabelt dyp. Master's thesis, University of Oslo.

Sergeeva, A., Pelinovsky, E., and Talipova, T. (2011). Nonlinear random wave field in shallow water: variable Korteweg–de Vries framework. *Nat. Haz. Earth Syst. Sci.*, 11:323–330.

Toffoli, A., Gramstad, O., Trulsen, K., Monbaliu, J., Bitner-Gregersen, E., and Onorato, M. (2010). Evolution of weakly nonlinear random directional waves: laboratory experiments and numerical simulations. *Journal of Fluid Mechanics*, 664:313–336.

Trulsen, K. (2006). *Tsunamis, rogue waves, internal waves and internal tides,chap. Weakly nonlinear and stochastic properties of ocean wave fields*. Springer Wien NewYork.

Trulsen, K. and Dysthe, K. (1997). Freak waves–a three-dimensional wave simulation. In *Proceedings of the 21st Symposium on naval Hydrodynamics*, volume 550, page 558. National Academy Press Washington, DC, USA.

Trulsen, K., Zeng, H., and Gramstad, O. (2012). Laboratory evidence of freak waves provoked by non-uniform bathymetry. *Physics of Fluids*, 24(9):097101.

Viotti, C. and Dias, F. (2014). Extreme waves induced by strong depth transitions: Fully nonlinear results. *Phys. Fluids*, 26:051705.

Whitham, G. B. (1974). Linear and nonlinear waves. *Wiley*.

Zakharov, V. E., Dyachenko, A. I., and Prokofiev, A. O. (2006). Freak waves as nonlinear stage of Stokes wave modulation instability. *European Journal of Mechanics-B/Fluids*, 25(5):677–692.

Zeng, H. and Trulsen, K. (2012). Evolution of skewness and kurtosis of weakly nonlinear unidirectional waves over a sloping bottom. *Natural Hazards and Earth System Science*, 12(3):631–638.

Zhao, M., Teng, B., and Cheng, L. (2004). A new form of generalized Boussinesq equations for varying water depth. *Ocean Eng.*, 31(16):2047–2072.